THE INFLUENCE OF RED BLOOD CELL SCATTERING IN OPTICAL PATHWAYS OF RETINAL VESSEL OXIMETRY

By

SERGE EMILE LEBLANC

Thesis submitted to the
Faculty of Graduate and Postdoctoral Studies
In partial fulfillment of the requirements
For the Doctoral Degree in Physics

Department of Physics
Faculty of Sciences
University of Ottawa

SUMMARY

The ability to measure the oxygen saturation, oximetry, of retinal blood both non-invasively and *in-vivo* has been a goal of eye research for years. Retinal oximetry can in principle be achieved from the measurement of the reflectance spectrum of the ocular fundus. Oximetry calculations are however complicated by the scattering of red blood cells, the different pathways of light through blood and the ocular tissues that light interacts with before exiting the eye. The goal of this thesis was to investigate the influence of red blood cell scattering for different light paths relevant to retinal oximetry. Results of *in-vitro* whole blood experiments found calculated oxygen saturation differences between blood samples measured under different retinal light paths, and these differences did not depend on the absorbance path length. We also showed that the calculated oxygen saturation value determined by a multiple linear regression Beer-Lambert absorbance model depended on the wavelength range chosen for analysis. The wavelength dependency on the calculated oxygen saturation value is due in part to the correlation that exists between the oxyhaemoglobin and deoxyhaemoglobin extinction coefficient spectra and to errors in the assumptions built into the Beer-Lambert absorbance model. A wavelength region with low correlation between the oxyhaemoglobin and deoxyhaemoglobin extinction coefficients was found that is hypothesized to be a good range to calculate oxygen saturation using a multiple linear regression approach.

ACKNOWLEDGEMENTS

I am very thankful to many people who supported me throughout the long journey of completing a Ph.D. I would first like to thank my supervisor Dr. Rejean Munger for his help, guidance and patience during this project, and for giving me the opportunity to pursue this degree. I would also like to thank my colleagues and the other students in the lab that helped me throughout this project: Monica Atanya , Michael Fancy, David Kahn, Dr. Michael Butler, Dr. Michael Dollin, Ashley Berry, Sylvie L'Heureux, Cynthia Clark, Melanie Lalonde, Gail Kayuk and a big thank you to Malcom Latorre. This Ph.D. would not have been possible without the support of my family and friends. I would like to thank my parents, Bernard and Charlotte, my cousin Dr. Alan Fraser and my brother Jean-Marc for your support and encouragement. A special thanks also goes to 2 close friends who were very supportive and helped me get through this process: Dave Babineau and Mathieu Boudreau. Finally, I would like to thank my very supportive and patient girlfriend Stephanie Hebert. I definitely couldn't have done this without you. Thank you for being understanding, and encouraging me when things got tough. I love you very much and look forward to start building a life with you now that my Ph.D. is finally over.

LIST OF PUBLICATIONS INCLUDED IN THESIS

This is a thesis by articles. It is based in part on work reported in the following two manuscripts:

1 S. E. LeBlanc, M. Atanya, K. Burns and R. Munger

Quantitative Impact of Small Angle Forward Scatter on Whole Blood Oximetry Using a Beer-Lambert Absorbance Model

Accepted in The Analyst (in print)

2 S. E. LeBlanc and R. Munger

Wavelength Dependence of Deviations to the Beer-Lambert Model for Different Light Paths in Retinal Oximetry

Submitted to The Analyst

TABLE OF CONTENTS

LIST OF FIGURES IN THESIS

LIST OF ABREVIATIONS & ACRONYMS IN THESIS

CT	Computed Tomography
MRI	Magnetic Resonance Imaging
SLO	Scanning Laser Ophthalmoscopy
OCT	Optical Coherence Tomography
Hb	Haemoglobin
RBC	Red Blood Cell
O_2Hb	Oxyhaemoglobin
HHb	Deoxyhaemoglobin
O_2	Oxygen Molecule
ABG	Arterial Blood Gas
LED	Light Emitting Diode
DC	Direct Current
FDA	Federal Drug Administration
MLR	Multiple Linear Regression
ANSI	American National Standards Institute
TH	Tungsten Halogen
CCD	Charge-Coupled Device
USB	Universal Serial Bus
GUI	Graphic User Interface
HeNe	Helium-Neon
FWHM	Full Width at Half Maximum
UV	Ultra Violet
NIR	Near Infrared
Vis	Visible
OHREB	Ottawa Hospital Research Ethics Board
COP	Cyclo-Olefin Polymer
DI	De-Ionized
ANOVA	Analysis of Variance
PCA	Principal Component Analysis
RPE	Retinal Pigment Epithelium
SEM	Standard Error of the Mean
SVD	Singular Value Decomposition

CHAPTER 1 - INTRODUCTION

In modern medicine, advances in science & technology have greatly improved not only the duration but also the quality of human life. Pharmaceutical products have been created to relieve almost every symptom imaginable caused by thousands of different diseases. Surgical procedures have been developed that restore everything from limb function to perfect vision. Imaging technologies such as X-ray computed tomography (CT scan) and nuclear magnetic resonance imaging (MRI) allow medical professionals to collect anatomical information from inside the human body non-invasively to better establish treatment protocols and improve disease prognosis. New innovations from both academia and the private sector continue to improve medicine's ability to treat diseases and improve the quality of life.

Among medical fields, ophthalmology has benefited greatly from these advances in science & technology. For example, multi-spectral retinal imaging, scanning laser ophthalmoscopy (SLO) and optical coherence tomography (OCT) technologies allow retinal specialists to collect anatomical data with micron-level precision that help to detect physical signs of disease, often before any functional symptoms are present. What is missing, however, is the ability to measure metabolic activity in the retina both reliably and non-invasively. The motivation to measure metabolic activity in the eye is to be able to detect diseases and identify patients at risk in the early stages of disease progression, before any clinical signs are present. Previous studies [1-3] have linked changes in metabolic activity, specifically use of oxygen, to ocular diseases. Non optimal oxygen delivery stresses cells in the tissue and as a result, the cells eventually start faltering and

their efficacy at performing their assigned task is reduced. This leads to more cells being stressed and eventually, symptoms develop and a disease is identified. However, if the rate at which oxygen is delivered to cells could be measured, any change in this rate could be an early warning sign of disease. After detection, early treatment and monitoring could begin, thus greatly improving prognosis. Consequently, numerous studies have been dedicated to the measurement of oxygen delivery to cells in the retina. This thesis is a contribution to those efforts.

In this thesis, we will present the design and development of an instrument to measure the oxygen saturation of retinal blood. A model to calculate the oxygen saturation of blood is presented, and *in-vitro* whole blood spectroscopy experiments are performed to analyze the effects that red blood cell scattering will have on different light paths in retinal oximetry. Finally, the stability of a multiple linear regression approach to oximetry is examined and the effect of the chosen fitting wavelength range on the calculated oxygen saturation value is determined.

1.1 The Need for Retinal Oximetry

As in every other tissue throughout the human body, oxygen is essential for normal retinal function. Several ocular diseases have been linked to oxygen delivery problems. Previous studies have suggested that oxygen is an important factor in the pathogenesis and treatment of retinal diseases such as retinal occlusions [4-11] (blockage of a blood vessel), retinal detachment [12-17], age-related macular degeneration (AMD) [2, 18, 19] and diabetic retinopathy [20-35]. Although glaucoma is mostly associated with an increase in intraocular pressure, poor regulation of blood flow, which results in

poor oxygen delivery, has been postulated as a mechanism of glaucomatous optic atrophy [36, 37] (degeneration of the nerve fibers). Also, animal studies have showed that both vitrectomy [5, 38-40] (removal of the vitreous humor from the eye) and laser photocoagulation [6, 7, 28, 38, 40-47] (laser used to cauterize ocular blood vessels) procedures increase the oxygen tension (oxygen partial pressure) in the retina. In addition, the retina is one of the most metabolically active tissues in the body, consuming oxygen more rapidly than many other tissues, including the brain [48-50]. Consequently, any alteration in circulation and oxygen delivery results in functional impairment and extensive retinal tissue damage [51]. Furthermore, the rate of oxygen consumption is not constant as a function of retinal depth. Oxygen tension is highest at the layers containing vessels / capillaries, which act as oxygen sources, and declines following diffusion principles, moving away from the source if no oxygen consumption is needed. Metabolically active centers such as the photoreceptors and the ganglion cell/nerve fiber layers act as sinks and increase the oxygen gradient between them and the source. Cringle *et al.* [52] measured intraretinal oxygen consumption in the rat and quantified how oxygen tension varied with retinal depth (figure 1.1)

Given the critical role that oxygen plays in retinal function and in the pathogenesis of retinal diseases, it is very important to be able to monitor or measure retinal oxygen accurately. Unfortunately, systemic measurements of oxygen, such as clinical blood gas measurements, CO-Oximeters and pulse oximeters, which measure the oxygen saturation of blood at specific locations in the body, cannot be used to obtain information from the retina because of its reliance upon an autoregulatory response from behind the blood-retina barrier [3]. The blood autoregulation of an organ is defined as the

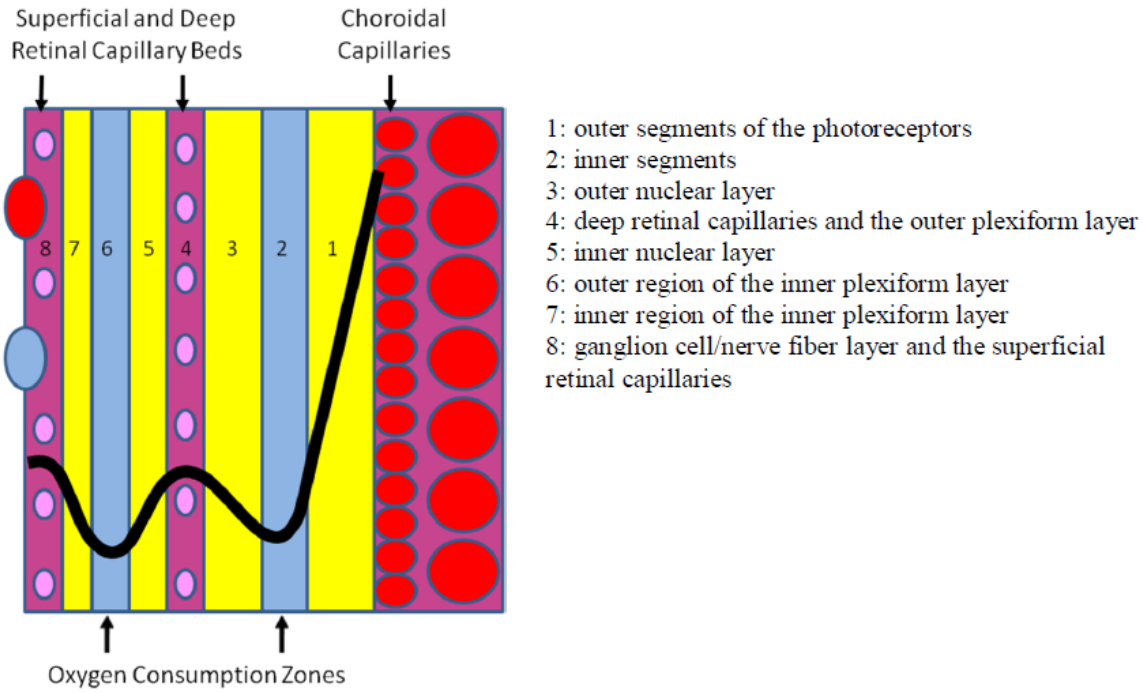

Figure 1.1: Schematic model of oxygen distribution across the eight layers of the retina. The black line represents oxygen tension and decreases from top to bottom. Recreated from Cringle et *al.* [52].

intrinsic tendency of an organ to maintain constant blood flow despite changes in perfusion pressure (blood pressure) to that organ [53]. Robinson *et al.* [54] showed that the retina is capable of efficiently autoregulating its blood flow under acute systemic hypertension, resulting from an average rise in mean systemic blood pressure of approximately 40% above resting levels [54]. Therefore, specific *in-vivo* retinal oximetry instruments and techniques need to be developed. A good starting point to achieve this objective is to build upon existing oxygen measurement technologies and adapt for ocular use.

1.2 Clinical Oximetry

1.2.1 Haemoglobin and Oxygen Saturation

The word oximetry is used in medical science to refer to the measurement of oxygen saturation of blood vessels. To understand the definition of oxygen saturation, it is important to know how oxygen is delivered to tissues throughout the human body. The transport of oxygen through the blood stream is performed by the haemoglobin (*Hb*) molecule, an iron-containing protein residing inside red blood cells (RBC). Each haemoglobin molecule has four oxygen binding sites (heme) that it uses to transport oxygen to tissues. In its fully oxygenated state (4 bound O_2 molecules), haemoglobin is referred to as oxyhaemoglobin (O_2Hb), and in its fully deoxygenated state (no bound O_2 molecules), it is referred to as deoxyhaemoglobin (*HHb*). The oxygen saturation of blood is a measurement of the percentage of occupied oxygen binding sites on the haemoglobin molecules within the volume measurement. It is a measure of the functional capacity of blood to deliver oxygen to tissue. The oxygen saturation (SO_2) can be represented mathematically by equation (1-1):

$$SO_2 = \frac{[O_2Hb]}{[O_2Hb]+[HHb]} \quad [55] \tag{1-1}$$

where [O_2Hb] and [*HHb*] represent the respective number of occupied and unoccupied oxygen binding sites on the haemoglobin molecules and is usually expressed as a percentage. For example, a blood sample that has an oxygen saturation of 95% indicates that 95% of all oxygen binding sites on the *Hb* molecules are occupied by oxygen. The

value of SO_2 represents an average of the percentage of occupied binding sites in the sample of blood being measured.

The number of O_2 molecules bound to haemoglobin depends mostly on the partial pressure of oxygen around the haemoglobin molecules, but is also dependent to a lesser extent on other factors such as blood pH and temperature. The relationship between the oxygen saturation of blood and the partial pressure of oxygen in the blood is represented by the oxyhaemoglobin dissociation curve (figure 1.2):

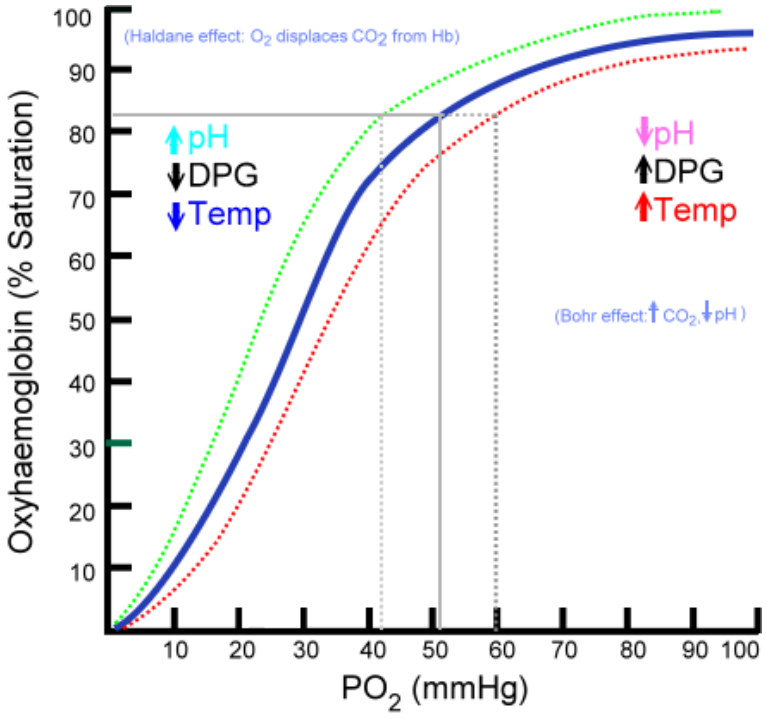

Figure 1.2: Oxyhaemoglobin dissociation curve showing the dependence of the oxygen saturation on the partial pressure of oxygen dissolved in blood and as a function of other parameters such as pH, temperature and DPG (www.ganfyd.org) [56].

where PO_2 is the partial pressure of oxygen in blood, CO_2 is carbon dioxide, *Temp* is the temperature of the blood and *DPG* is disphosphoglycerate. The O_2Hb dissociation curve

also shows how factors like pH and temperature can affect haemoglobin's affinity to oxygen. An increase or decrease in these factors causes a shift in the dissociation curve that has a positive impact for the transport of oxygen. For example, in the presence of carbon dioxide, the haemoglobin affinity to oxygen decreases, helping the release of oxygen as carbon dioxide accumulates through metabolism [57]. This is known as the Bohr effect and it facilitates oxygen transport by releasing O_2 in areas in most need of oxygen.

1.2.2 Measuring Oxygen Saturation of Blood

There are different types of instruments that have been developed to measure oxygen in blood (these instruments are referred to as oximeters). The three most commonly used in the hospital and clinical environment are the pulse oximeter, the blood gas analyzer and the CO-oximeter [55]. All three have different methods of determining the oxygen saturation of blood and will be briefly reviewed in this section.

Blood Gas Analyzer

As the name suggests, the blood gas analyzer is an instrument that measures dissolved gases in blood. Using electrodes, the blood gas analyzer obtains a direct measurement of the partial pressure of oxygen and carbon dioxide, the pH of the blood and the bicarbonate level. Many blood gas analyzers also report concentrations of several electrolytes as well as the oxygen saturation of blood. Blood gas analyzers are most commonly used to analyze arterial blood and the test is referred to as an arterial blood gas (ABG). A blood sample is extracted from a patient and taken to the lab for analysis.

In order to extract the oxygen saturation value from the blood sample, the blood gas analyzer uses the relationships between blood parameters from the dissociation curve (figure 1.1) to determine a calculated value of oxygen saturation. Each instrument has its own proprietary method of calculating the SO_2 value (examples shown below).

(1-2) $$SO_2 = \frac{100}{\left(1+10^{-\left(\log pO_2 + 0.48 \cdot pH - 0.0013 \cdot BE - 4.962\right)/0.369}\right)}\% \quad [58]$$

(1-3) $$SO_2 = \frac{Q}{(Q+1)}\%$$
$$\log Q = -4.14 + 1.66 \cdot \exp_{10}\left(-0.074 \cdot pO_2\right) + 2.9 \cdot \log pO_2 + \log\left(1+10^{pH-6.81}\right) - \log\left(1+10^{8.03-pH}\right) \quad [59]$$

where pO_2 is the partial pressure of oxygen in the blood and BE represents Base Excess, a measure of metabolic acidosis or alkalosis. While the blood gas analyzer uses electrodes to calculate the oxygen saturation of blood, the pulse oximeter and the CO-oximeter take advantage of the optical properties of haemoglobin to determine the SO_2 value of a blood sample. Therefore, a review of these optical properties is essential to understanding how they function.

Optical Properties of Haemoglobin

The optical properties of human haemoglobin have been studied extensively over the years [60-67]. When in solution, haemoglobin is non-scattering and has an absorption spectrum that depends on the number of occupied heme sites [55]. The absorption spectra of O_2Hb and HHb are shown in figure 1.3 below.

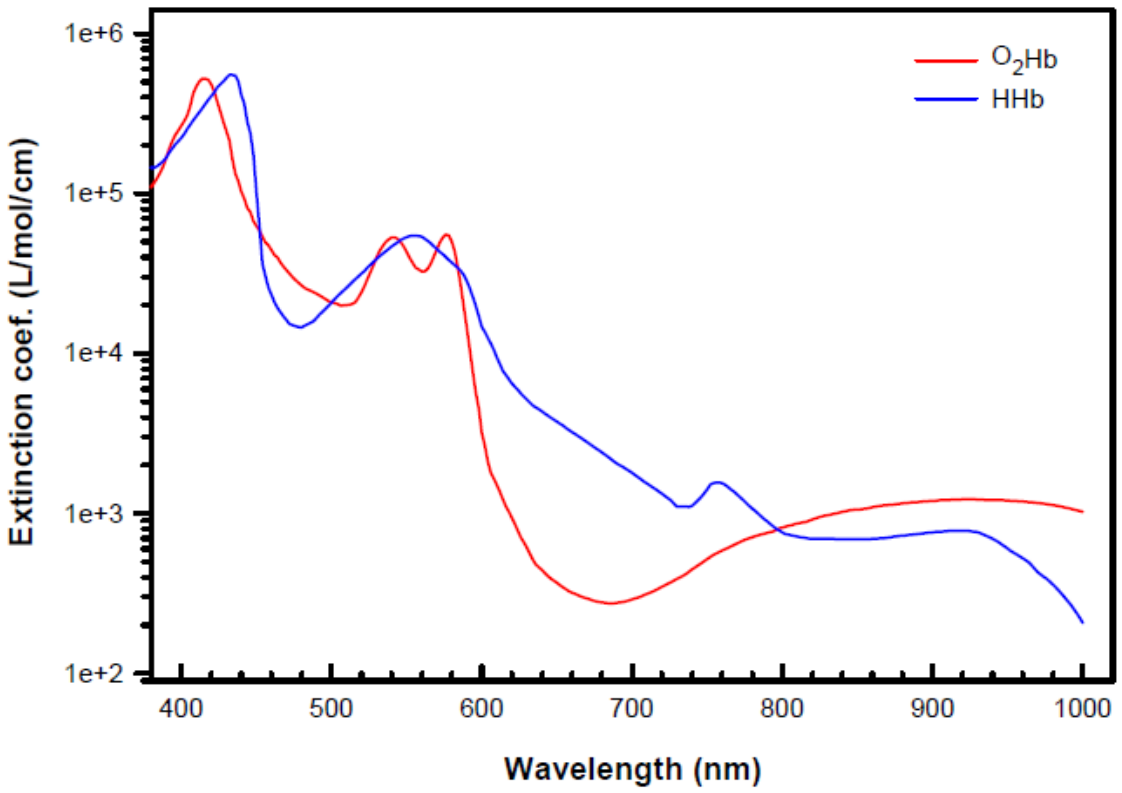

Figure 1.3: Spectral dependence of *O_2Hb* and *HHb* extinction coefficients on wavelength based on data by Prahl et *al.* [68]

The measurement of the oxygen saturation of a blood sample is made possible by the different optical properties of *O_2Hb* and *HHb* and the use of the Beer-Lambert law. It is not clear what the uncertainty in data points are from these curves, but these haemoglobin extinction coefficient values are the most quoted in the literature and are also used in CO-Oximetry measurements. It has been shown that using these curves allow *SO_2* measurements to better than 1% accuracy.

Beer-Lambert Law

The Beer-Lambert law relates the light absorption properties of a homogeneously absorbent sample to the properties of its light absorbing components. It is usually expressed using absorbance, *A(λ)*

(1-4) $A(\lambda) = -\log_{10}\left(\frac{I(\lambda)}{I_0(\lambda)}\right) = -\log_{10}(T(\lambda))$ [55]

where I_0 and I are the intensity of light incident and transmitted through the sample respectively, and T is the transmittance. The Beer-Lambert law relates the absorbance to the absorbers' efficacy at capturing photons, expressed as the molar extinction coefficient $\varepsilon(\lambda)$, l the path length of light through the sample and c the concentration of the light absorbing substance

(1-5) $A(\lambda) = \varepsilon(\lambda) \cdot l \cdot c$ [55]

The law implies that the absorbance is directly proportional to the concentration of the absorber in solution and the distance light must travel in the mixture, and implicitly implies that the intensity of light transmitted through the sample depends only on light absorption. When multiple light absorbing substances are present in a mixture, the Beer-Lambert law is expressed as a sum of the contribution of n known substances of concentrations c_n,

(1-6) $A(\lambda) = \sum_n \varepsilon_n(\lambda) \cdot c_n \cdot l$ [55]

For a mixture of known substances of unknown concentrations, the c_n are unknown but can be extracted by measuring the absorbance at multiple wavelengths and solving the system of linear equations for the various c_n. This approach to measuring substance concentration in a solution is a basic tool of most chemistry laboratories. This approach holds only if the Beer-Lambert law is obeyed, which implies a homogeneous and isotropic medium with negligible scattering, and no reaction between the different absorbents and/or the solvent (no molecular associations or dissociations), and no possibility of a photochemical reaction [55].

The Beer-Lambert law can be very useful in calculating the oxygen saturation of a blood sample. Not all instruments rely on the law to extract SO_2 however, as is the case in the pulse oximeter.

Pulse Oximeter

By far the most popular and commonly used oximeter is the pulse oximeter. This instrument, usually placed on the tip of the index finger or sometimes on the ear lobe, gives a real time measurement of the oxygen saturation of blood along with a measure of the heart rate as well. In fact, the pulse oximeter relies on the heart rate to extract oximetry from its measurements.

The pulse oximeter operates by measuring the light at two wavelengths (usually from light-emitting diodes (LEDs)) that is transmitted through the tissue. The LED wavelengths are usually 660 nm (red) and 905 nm (infrared) but other combinations are

possible [55]. The values are chosen to be in the wavelength regions where the extinction coefficients of O_2Hb and HHb differ significantly (see figure 1.3). The final measurement used to calculate oxygen saturation is the ratio of absorption between the two selected wavelengths. As the blood circulates through the arteries, the absorption cross-section of RBCs changes with the heart rate during systolic and diastolic pressure (they align themselves with the flow of serum during blood push, and relax into random orientation between heart beats). This results in an oscillating transmitted signal through the finger. By examining the oscillating part of the signal, the absorption caused by arteriole blood (oscillatory part) can be isolated and the part of the signal that is caused by the absorption and scattering of the rest of the biological tissues can be ignored (DC term).

First attempts at developing pulse oximeters tried to use the Beer-Lambert law to calculate the oxygen saturation. The scattering and absorption caused by the biological tissues as well as the scattering by the RBCs made the use of the Beer-Lambert law impractical. In modern pulse oximeters, the oxygen saturation values are calculated by the ratio from the transmission of red and infrared LEDs. The ratios have linear relationship with SO_2 and values are determined empirically by calibrating with a sample population of volunteers. Different oxygen gas mixtures are administered to volunteers and the ratios are then measured and put in a look-up table for use by the pulse oximeter. For these reasons, pulse oximeters are unreliable below 80% oxygen saturation because these values must be extrapolated, since it is considered unethical to subject volunteers to oxygen saturation levels below 80% which would put their health in danger. Even with their limited accuracy (2 – 5% error depending on SO_2 value), pulse oximeters are the instruments of choice for patient SO_2 monitoring because of their ease of use, real time

SO_2 determination and their ability to instantly show large changes in SO_2 values, which is usually clinically more important than determining the exact SO_2 value at very high accuracy.

CO-oximeter

The gold standard in oximetry is the CO-oximeter. The CO-oximeter requires a small sample of blood to be drawn from an artery or vein and measures oxygen saturation at the instant and location at which the blood sample was drawn. The sample is introduced into the CO-oximeter and is hemolysed (RBCs torn apart to form a haemoglobin solution) by ultrasound thus producing a pure haemoglobin mixture (solution is filtered to remove RBC residues). The absorbance at different wavelengths of monochromatic light are measured and the Beer-Lambert law is employed to calculate the concentration of the various blood components present in the solution. The wavelengths of light in the CO-oximeter are usually in the visible range (taking advantage of the different spectral dependencies of O_2Hb and HHb in the 500 to 600 nm range) and some CO-oximeters use up to 17 wavelengths to determine the concentration of absorbing elements in the blood sample [55]. The higher the number of wavelengths used, the more accurate the calibration of the instrument will be. In addition to O_2Hb and HHb, the CO-oximeter is able to measure other Hb derivatives such as carboxyhaemoglobin and methaemoglobin among other blood parameters (CO_2, HCO_3 (bicarbonate)).

The value of oxygen saturation is determined similarly to equation (1-1). The Beer-Lambert law is used to solve a system of linear equations and find the relative

concentrations of the absorbing substances in the haemoglobin solution. For example, if the solution is assumed to contain *O_2Hb*, *HHb, COHb* (carboxyhaemoglobin) and *MetHb* (methaemoglobin), the absorbance of the solution can be written as:

(1-7) $$A = a \cdot O_2Hb + b \cdot HHb + c \cdot COHb + d \cdot MetHb$$

where *a*, *b, c* and *d* are the respective concentrations of *O_2Hb*, *HHb, COHb* and *MetHb* present in the solution. The oxygen saturation is then given by:

(1-8) $$SO_2 = \frac{a}{a+b}.$$

1.3 Challenges of Retinal Oximetry

The challenges involved in measuring *in-vivo* retinal oximetry are many. The first attempts were made by Hickam *et al.* in 1963 [69] and at the time this chapter is being written, nearly 50 years later, there exists no commercial device that has received FDA (Federal Drug Administration) approval to accurately measure retinal oxygen saturation. The issues involved in retinal oximetry can be grouped into two categories; instrumentation and light-eye model. Both are described in the following sections.

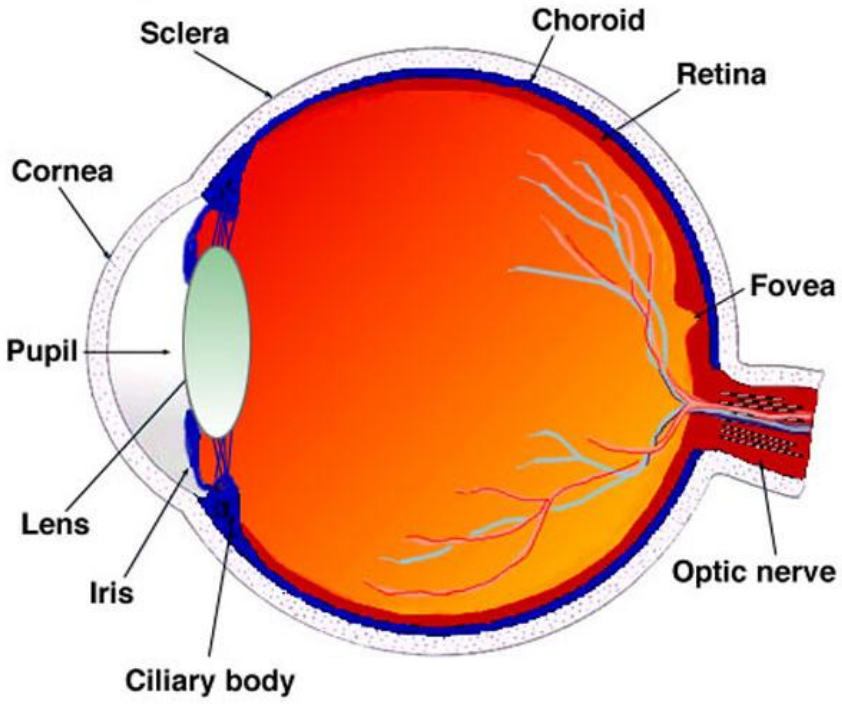

Figure 1.4: Diagram of the human eye showing main anatomical features (http://webvision.med.utah.edu) [70]

1.3.1 Instrumentation

Obtaining images from the ocular fundus is not an easy task. There are a number of design challenges that must be overcome to acquire high quality fundus images. The intensity of the incident light sent to the eye (figure 1.4) is limited by how much the retina can be exposed to without causing damage. In addition, only a small fraction of the light is reflected back out of the eye, resulting in low signal to noise ratios for image analysis. Eye alignment and corneal reflections are also issues that must be addressed when designing a retinal imaging system. Exposure times are limited by the amount of time that patients can keep their eyes still, which in most cases is less than 1 or 2 seconds. Despite these challenges, successful commercial fundus imaging devices have been

developed, and researchers have used these as a starting point to attempt retinal oximetry measurements.

The first attempts at retinal oximetry were performed by Hickam *et al.* in 1963 [69]. In the study, filters were used at 510 and 640 nm, and the ratio of reflectance was used to estimate the oxygen saturation. Since then, multiple studies [71-82] have used a small number of wavelengths to calculate oxygen saturation of retinal vessels. A significant improvement to retinal oximetry was achieved by Delori in 1988 [51], using 3 wavelengths and sampling only a small area of a vessel to calculate oximetry. Attempts were also made using multi-spectral imaging techniques to calculate oximetry using multiple bandpass filters coupled to a fundus camera [83-88]. Schweitzer *et al.* [89] used a fundus camera coupled with a spectrometer to simultaneously measure the fundus reflectance at 76 different wavelengths. Similar techniques were developed by Faubert *et al.* [90] and Diaconnu [91]. The advantage of this approach is that a higher number of wavelengths should result in a more accurate determination of oxygen saturation. A limitation of these techniques however, is that it only measures the reflectance spectrum at one specific location of the retina.

A scanning laser ophthalmoscope was used by Denninghoff *et al.* [92-94] equipped with 4 or 5 lasers in an interlaced mode to calculate oximetry. The choice of wavelengths was limited by the availability of lasers however and the calibration proved to be difficult. A promising method is the use of hyper-spectral imaging which uses an imaging spectrometer to record the spectrum of each pixel in an image to yield a spectral data cube [95-99]. The challenge in this method is that the calculation of spectral images from the diffraction patterns is laborious and perhaps dependant on the choice of initial

conditions of the iterative process [100]. In addition, the amount of light needed to obtain all the spectra with enough photons for the desired resolution is also a challenge.

Each different proposed technique to measure retinal oxygen saturation has advantages and limitations. Ultimately, the accuracy and possibly the reliability of the technique will depend on the calibration procedure and on the model used to describe the interaction that light has with blood vessels and the many layers of retinal tissue before exiting the eye.

1.3.2 Light-Eye Model

Oximetry is most reliable when the Beer-Lambert law is applied to spectroscopic measurements of a haemoglobin solution. In the eye, the haemoglobin molecules are contained inside RBCs, which are known to scatter light and cause deviations to the Beer-Lambert law. Many studies [101-115] have proposed methods of measuring oxygen saturation in whole blood with positive results. The situation is even further complicated in the eye however, since the light not only interacts with the RBCs, but has to interact with many layers of ocular tissue when entering and exiting the eye (figure 1.5). Consequently, studies have been conducted to measure the spectral properties of the eye [116-121] and the effect that scattering RBCs will have on retinal oximetry [78, 108, 122-126].

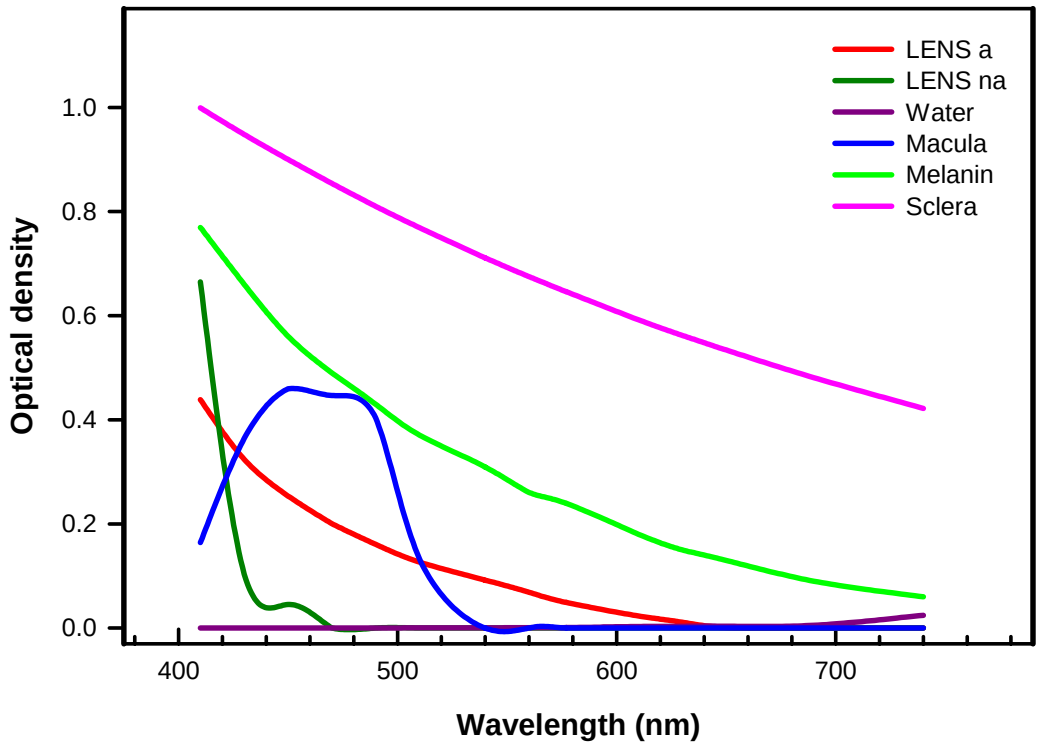

Figure 1.5: Spectral dependence of the transmittance of various ocular tissues and important compounds interacting with light in retinal oximetry optical pathways. Recreated from Handbook of Optics - Vol 3: Vision and Vision Optics [127].

When constructing an optical model of the light-eye interaction, there are 4 possible ways that light can interact with the blood before exiting the eye (figure 1.6). In one case, figure 1.6 c), light can enter a blood vessel and scatter from a RBC. Alternatively, light can pass through a vessel and be reflected by the back layer of the eye (sclera) or the retinal pigment epithelium (RPE). This is referred to as a single pass absorption model shown in figure 1.6 a). Also, light can pass through a vessel, be reflected by the sclera and then pass through a vessel a second time before exiting the

eye. This is referred to as a double pass absorption model shown in figure 1.6 b). Finally, light can reflect off a vessel wall without interacting with the blood at all as seen in figure

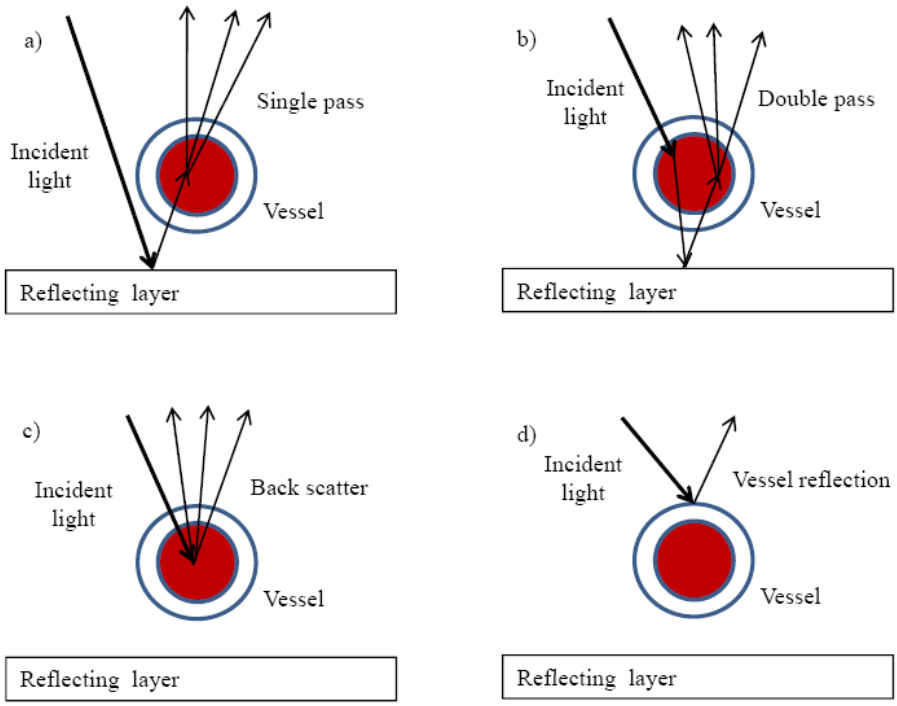

Figure 1.6: Possible relevant optical pathways of light from a retinal vessel in reflectance image for calculating oximetry. Figure 1.6 a) represents a single pass absorption while figure 1.6 b) is a double pass absorption. Figure 1.6 c) shows a RBC backscatter while figure 1.6 d) represents a vessel reflection. Recreated from Hammer et *al.* [128].

1.6 d). There is still debate in the literature on what type of light paths exist in retinal oximetry. Monte-Carlo simulations by Hammer *et al*. [128] suggest that most of the signal is from either light that has backscattered from a RBC or that went through a single pass through the blood vessel. However, double pass models have shown encouraging results to model the reflectance spectra [91].

A major problem with evaluating different retinal oximetry techniques is that it's impossible to know what the "actual" value of oxygen saturation really is when conducting a measurement. It isn't feasible to extract a blood sample from a retinal vessel just before or after the measurement to compare oximetry values. Dual wavelength oximeters, for example, require a calibration to calculate SO_2. Similar studies from Hardarson *et al.* [79] and Hammer *et al.* [100] found differences of 13% between the mean venous oxygenation due to different calibration procedures. The repeatability of consecutive SO_2 measurements has shown to be good using these techniques however. Mean standard deviation of repeated SO_2 measurement on arterioles was found to be 5% by Smith *et al.* [129], 3.7% for Hardarson *et al.* [79], 2.52% for Hammer *et al.* [100] and 2.1% for Delori *et al.* [51]. A repeatability of 4.6% was also found by Schweitzer *et al.* [89] using the fundus spectrometry technique. Research is continuing to improve the repeatability of the measurements and to develop a method that can prove to be accurate at measuring non-invasive *in vivo* retinal oxygen saturation.

1.4 Hypothesis and Approach

The approach in this thesis was to develop a retinal oximeter similar to the fundus spectrometry described by Schweitzer *et al.* [89], Faubert *et al.* [90] and Diaconnu [91]. The reflectance signal obtained by the instrument was normalized to a model eye as a reference to obtain the reflectance spectrum.

Before developing a model to calculate retinal oximetry from these measurements, whole blood spectroscopy experiments were conducted to gain a better understanding of the errors in the Beer-Lambert absorbance model. Oxygen saturation

was calculated using a multiple linear regression (MLR) analysis. The whole blood spectrum was assumed to contain only O_2Hb and HHb and the absorbance is given by:

(1-9) $$A_{blood}(\lambda) = a\varepsilon_{O_2Hb}(\lambda) + b\varepsilon_{HHb}(\lambda) + c$$

where the factors a, b and c are obtained from a MLR analysis and the oxygen saturation of the sample is calculated using equation (1-8). In equation (1-9), the value of c represents a constant (wavelength dependent) that offsets the value of A_{blood} and can represent other contributing factors to the absorbance such as scatter or device offset. The reason for using multiple wavelengths and a fundus spectrometer as opposed to 2 or 3 wavelengths using filters is that it reduces the requirement for the signal to noise ratio by the square root of the number of wavelengths used [71].

The thesis will attempt to prove or disprove 2 hypotheses: 1) The error in the Beer-Lambert model depends on the absorbance path length, 2) MLR can be used to calculate SO_2 and the coefficient of determination R^2 can be used to determine the accuracy of SO_2 calculation.

1.5 Scope of Thesis and Structure

The main goal of this thesis was twofold: 1) to better understand the influence of red blood cell scattering in optical pathways of retinal vessel oximetry, and 2) to design and develop an instrument capable of measuring *in-vivo* retinal oxygen saturation. The design principles and characterization of the retinal oximetry device are explained in Chapter 2, along with preliminary results of *in-vivo* retinal oximetry measurements

collected with the device. In Chapter 3, we investigate the possibility that the choice of the wavelength fitting range will have an impact on the calculated oxygen saturation value using a multiple linear regression. The linear independence of the O_2Hb and HHb extinction coefficient curves is examined and a method of determining a proper fitting range is proposed. The results of *in-vitro* whole blood experiments are presented in Chapters 4 and 5, which will be submitted as separate papers for publication. Finally, Chapter 6 summarizes the results found in the thesis and discusses possible future work.

1.6 Statement of Contribution

This research project was suggested to me by my supervisor Dr. Rejean Munger, but the directions that the thesis took were the results of many discussions between Dr. Munger and me. The concept of the retinal oximetry device described in this thesis was suggested to me by Dr. Munger, but the actual design, construction and characterization were performed by the author. Every experiment described in the thesis was designed and conducted by the author, with the help of Monica Atanya for some data collection. All chapters in this thesis, including the two papers, figure and tables were written by the author (except for figure 2.13 which was provided by David Priest) with extensive proof reading by Dr. Munger. The idea to investigate the covariance of the haemoglobin extinction coefficients in Chapter 3 was proposed by Dr. Munger and the analysis was performed by the author with numerous discussions with Dr. Munger. The concepts and experimental design described in Chapters 4 and 5 were the result of numerous discussions between the author and Dr. Munger.

CHAPTER 2 – DEVICE PRINCIPLES AND DESIGN

2.1 Introduction

Designing and developing an instrument to measure oxygen saturation at the surface of the retina is not an easy task. Many design challenges must be overcome, some due to the numerous limitations imposed by working with living tissue *in-vivo* i.e. the eye, others come from the optical demands of the eye itself. One of the main challenges faced when imaging the retina is the restriction on the amount of light that can be used to illuminate the retina without harming the patient's vision. At high intensity levels, retinal damage can occur, thus great care must be taken not to exceed what is called the damage threshold (usually associated with pain) when illuminating the retina (a more detailed explanation of the retinal pain threshold will be given in another section). In addition, only a small fraction (often < 1%) of the light illuminating the retina is reflected back into the imaging system due to losses from scattering, absorption and diffuse reflections in the eye, with the limited diameter of the pupil acting as a limiting aperture. This results in a low signal to noise ratio for the retinal image for most imaging technologies. Another difficulty encountered when attempting to image the retina is the large reflections from the cornea that get captured by the imaging optics. The cornea has an index of refraction of 1.376 [130] which potentially can result in a reflection of 2.5% of the incident light back into the optical system. This is more than twice the amount of light that is reflected from the retina, and therefore can completely saturate the image of the retina if not properly blocked. Furthermore, in the retinal image, this corneal reflection appears as a

bright spot where all the light from the cornea is further concentrated in a small area which is 10 times or more intense than the retinal image itself, thus overwhelming the image and degrading contrast of the retinal image. Finally, we are interested in obtaining the optical reflectance spectrum from the retina in selected areas of the retina, so we must include a methodology for collecting such spectra while imaging the retina so we know which part of the retina is under measurement.

In this chapter, an overview of the design of the system will be given along with details of each subsection of the device. The design of the device can be divided into 3 main systems: illumination system, which is responsible for illuminating the retina; imaging system, which captures the reflected light from the retina and images it by means of a CCD camera; and spectroscopic system, which captures the spectrum of a target area on the retina to measure oxygen saturation. All will be discussed in detail in this chapter. In addition, this chapter will also report results of the characterization of the instrument. The light source stability, spectroscopy validation, images of a model eye and an analysis of an ink mixture will be compared between this system and a commercial spectrometer. Finally, preliminary data taken with the retinal oximetry device are presented.

2.2 Conceptual Device Design

There are 2 main purposes that the device must fulfill; measure oxygen saturation on a selectable target area on the retina and capture an image of the retina with enough quality to determine the area where oxygen is being measured. The primary objective of the device is to measure oxygen, not to capture a high quality image of the retina capable of performing medical diagnostics. Therefore, the focus of the design was placed on the

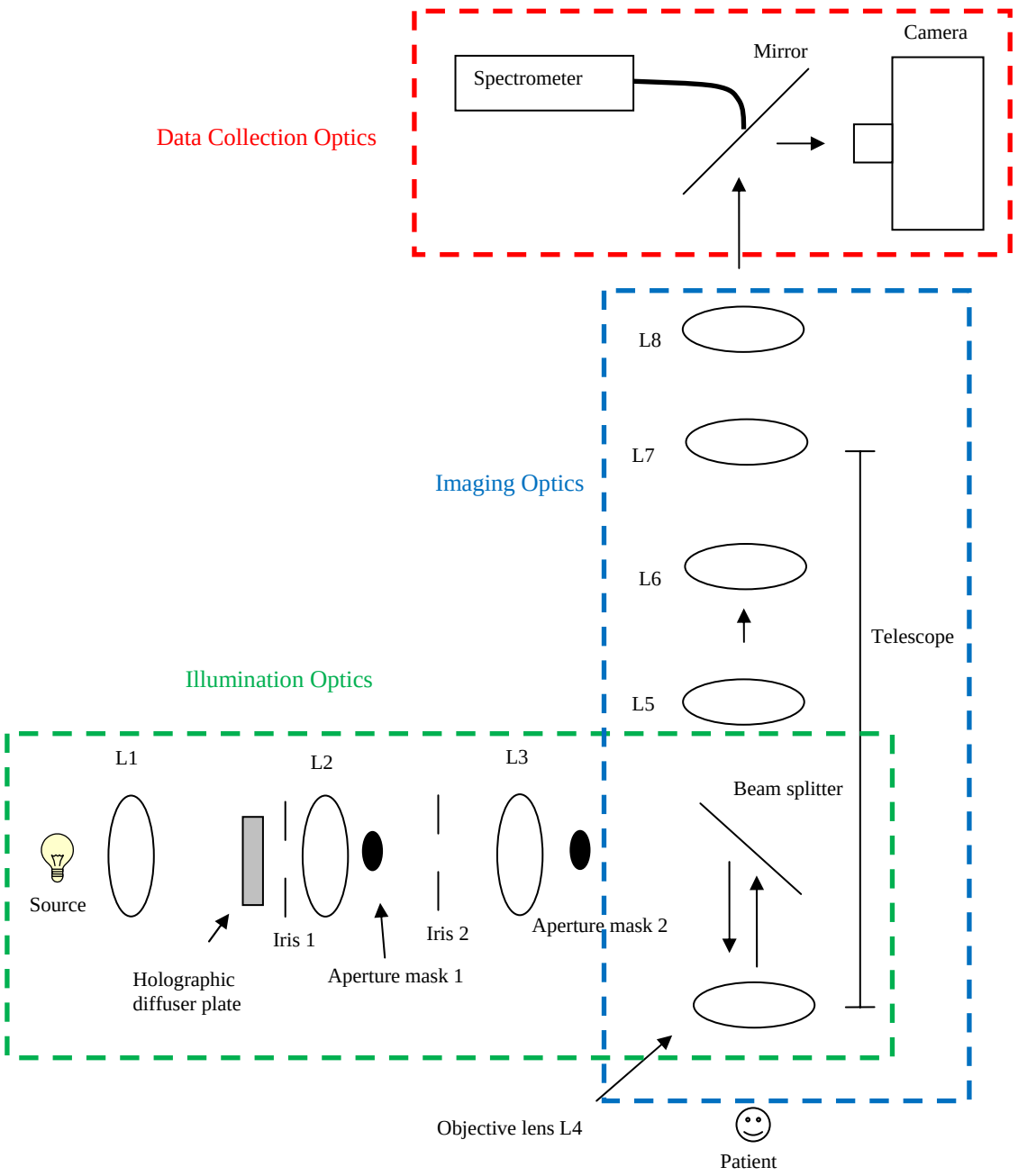

Figure 2.1: Block diagram of the retinal oximetry device showing the three different main sections of the device: illumination, imaging and data collection optics. The L's represent the different lenses with respective focal lengths f1 = 50 mm, f2 = 35.7 mm, f3 = 50 mm, f4 = 16.7 mm, f5 = 35.7 mm, f6 = 50 mm, f7 = 160 mm, f8 = 100 mm.

oxygen measurement capabilities, not on the image quality. A block diagram of the device is displayed below (figure 2.1).

In the device, light from a broad band light source is captured by the illumination optics and a uniform illumination is created on the retina. Light interacts with the retina and part of it is then reflected back into the imaging optics. The imaging optics creates an image of the retina on a mirror with a fiber mounted to the back. The mirror with fiber mount has a 100 μm hole in its center to let light through and be captured by the optical fiber. A camera focused on the mirror captures the retinal image including an image of the hole in the mirror, allowing the observer to know from which point on the retina the spectrum is obtained. Motors allow the mirror to be displaced so that the hole in the mirror can move anywhere along the surface of the retina in order to measure oxygen on a desired target area of the retina. This allows the user some flexibility to accommodate for different patients and eye movement. Finally, the camera can move with respect to the mirror position to compensate for any focusing errors resulting from the patients poorly focused natural optics. A more detailed explanation of each system is given in the next sections.

2.3 Illumination System

The illumination system of the device has 4 main requirements:

1. Illuminate a large area (> 35 degrees) of the retina uniformly with broad band light
2. Control illumination intensity while remaining below the retinal pain threshold
3. Block corneal reflections from entering imaging system

4. Block objective lens reflections from entering imaging system (discussed below)

To achieve these objectives, 4 lenses, 2 irises, 1 beam splitter, 2 blocking masks, 1 holographic diffuser and 1 tungsten halogen light source were employed (figure 2.2).

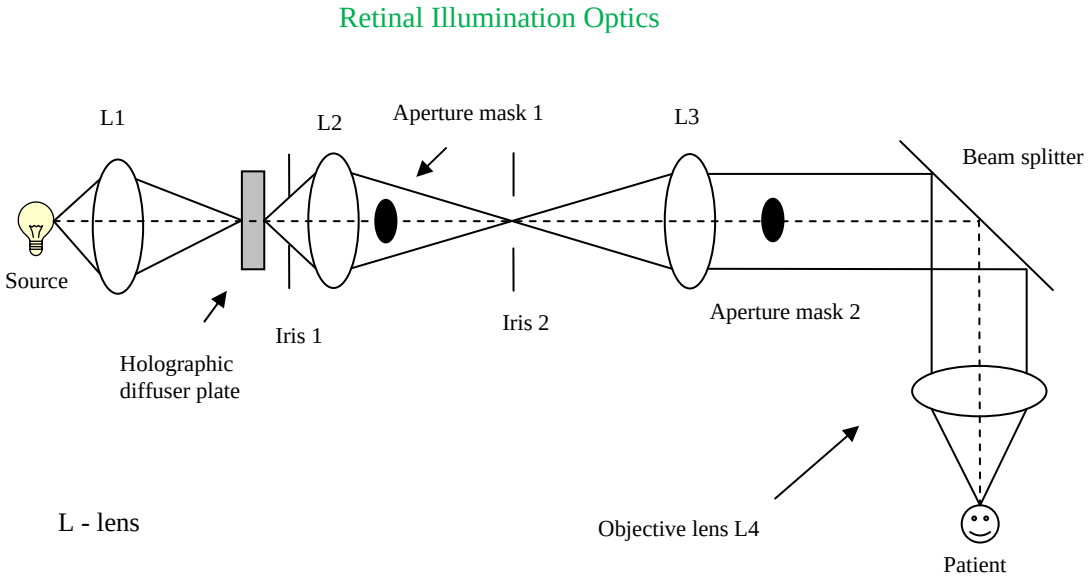

Figure 2.2: Schematic diagram of retinal oximetry device illumination system. System designed so the holographic diffuser is imaged in the patient's pupil, the mask 2 is conjugate with the cornea creating an annular illumination in the pupil of the patient and the mask 1 is conjugate with the surface of L4. Iris 1 is conjugate with the retina and iris 2 is conjugate with the holographic diffuser.

The rationale for the specific parts of the system is given in the following section but the need for the 4 requirements will be explained quickly here. As explained above, the cornea is an optical element that is shared by both the illumination path (brings light in to the retina) and imaging pathway (brings retinal light out to the imaging system). In

the proposed optical design we have to include one lens, the objective lens, which must also be shared by the illumination and imaging optics. The reflection from the first surface of this lens will thus be returned back through the imaging optics and interfere with the retinal image if not controlled. We can use anti-reflection coatings to reduce some of these reflections but wide band anti-reflection coatings do not eliminate all surface reflections for broad band imaging applications. The calculations for light exposure to the retina are shown, an explanation of how uniform retinal illumination was achieved is given, and finally the critical locations of the blocking masks are explained.

2.3.1 Maximum Permissible Exposure to Light

The light source utilized in the illumination system is a broadband Tungsten-Halogen source. Unlike lasers, these types of sources pose a low level danger since it is impossible for accidental exposure of a few milliseconds to cause damage to the eye. However, damage is still possible and depends on the exposure duration and the brightness at different wavelengths of light. Under normal circumstances, whenever a bright light is observed, the natural aversion responses of the eye (blinking, decreased pupil size) helps to protect against ocular injury for any illumination that is encountered in everyday living. In ocular instruments however, a patient is asked to keep their eyes open, sometimes with their pupils dilated, for extended periods of time. Because of this, we must be certain that the light levels used conform to the agreed upon safety standards.

According to the American National Standards Institute (ANSI) document RP-27.1-05: Recommended Practice for Photobiological Safety for Lamps and Lamp

Systems-General Requirements [131], different guidelines are employed depending on the wavelength of light and exposure time used in the system. For the broadband source used in the device, retinal photochemical injury (from mostly the shorter wavelength light exposure) poses the greatest danger based on the radiance of the source, the exposure time used (up to 4 minutes) and the retinal area exposed (35 degrees) (p. 6 [131]).

The radiance is an intrinsic property of an incandescent light source and depends only on its temperature. In a lossless optical system, the radiance of the source is conserved throughout the entire system. Therefore, when performing safety standards calculations, when the exposure limit depends on the radiance, we do not need to take into account the design of the optical system but only its total efficacy at delivering energy in the eye. This can be achieved by measuring the transmittance of the system for the design used.

The spectral radiance of an incandescent light source can be calculated using Planck's blackbody equation below:

(2-1) $$L_\lambda = \frac{2hc^2}{\lambda^5} \frac{1}{e^{hc/\lambda kT} - 1}$$ [132]

where L_λ is the spectral radiance, λ is the wavelength, h is Planck's constant, c is the speed of light in a vacuum, k is Boltzman's constant and T is the temperature. The blackbody curve is used in this case because the light source used in the system is a tungsten halogen bulb, which can be adequately represented by a blackbody. The light source used in our system has an effective colour temperature of 3000 K. A plot of the radiance of the light source is shown below (figure 2.3).

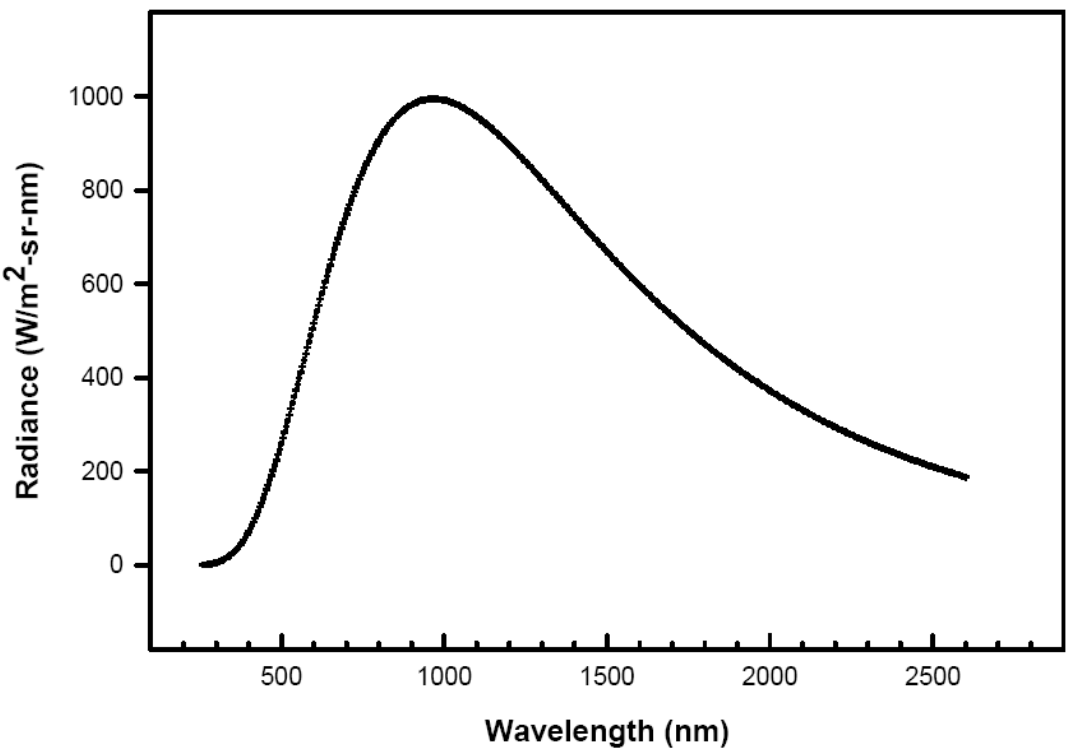

Figure 2.3: Calculated blackbody radiance at 3,000 degrees Kelvin representing the radiance of a tungsten halogen bulb used in the retinal oximetry device. Recreated from (ANSI) document RP-27.1-05 [131].

To protect against injury, the integrated spectral radiance of the light source weighted against the blue-light hazard function $B(\lambda)$ should not exceed the levels defined by:

$$(2\text{-}2)\quad L_B \cdot t = \sum_{400}^{700} L_\lambda \cdot B(\lambda) \cdot t \cdot \Delta\lambda \leq 100 \text{ W/cm}^2\text{·sr·s [131]}$$

where L_B is the blue light hazard weighted radiance between 400 nm and 700 nm in W/cm^2·sr, L_λ is the spectral radiance in W/cm^2·sr·nm, $B(\lambda)$ is the blue light hazard

weighting function, $\Delta\lambda$ is the calculation interval in nm and t is the exposure time in seconds. The wavelength range between 400 and 700 nm in equation (2-2) is chosen because it represents the range with the most potential danger. The optical components in the system are all optimized for visible light and block any light below 400 nm and above 700 nm. The blue light hazard function is plotted below (figure 2.4).

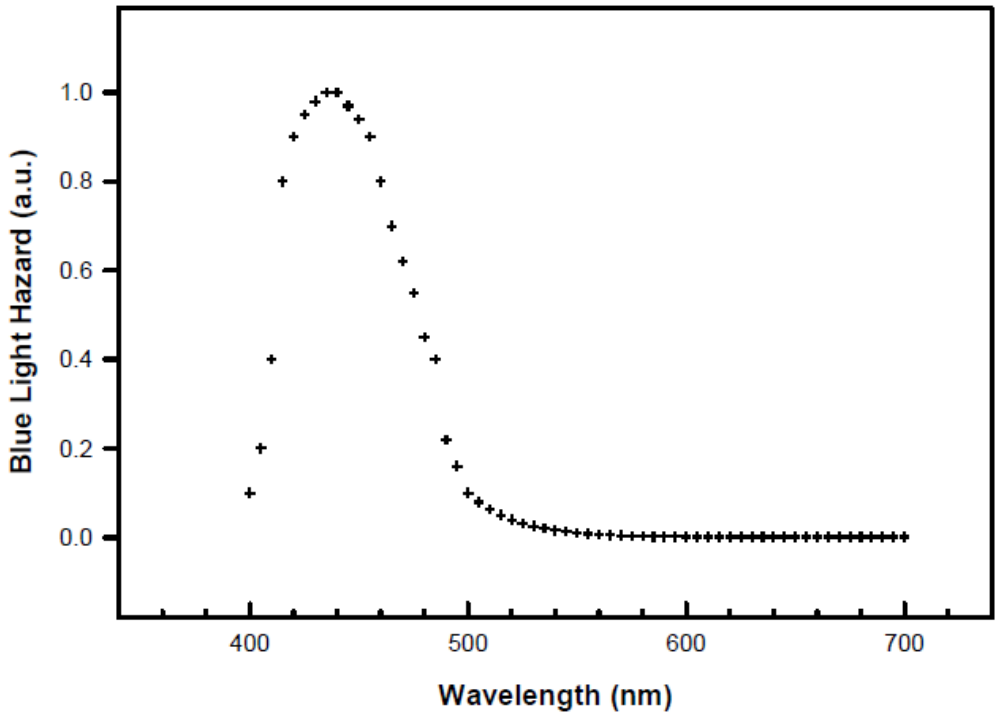

Figure 2.4: Blue light hazard function based on the ANSI standard showing the visible light wavelength regions more susceptible to produce retinal damage. Recreated from ANSI document RP-27.1-05 [131].

By rearranging equation (2-2), we can find a maximum exposure time based on the radiance of the source. This gives:

(2-3) $$t \le \frac{100}{\sum_{400}^{700} L_\lambda \cdot B(\lambda) \cdot \Delta\lambda}$$

The illumination optics as a whole has an average transmission of 21% over the 400-700 nm wavelength range from the light source to the patient's eye. This must be included in the calculations since it will reduce the radiance of the light source as seen by the patient. Also, equation (2-3) was derived based on an assumed pupil diameter of 3 mm. In most cases, the patient's pupils are under dilation will be approximately 9 to 10 mm in diameter, but our design will be limited to using a 6 mm area of the pupil. Thus, we have:

(2-4) $$t \le \frac{100}{\sum_{400}^{700} L_\lambda \cdot B(\lambda) \cdot \Delta\lambda \cdot \tau(\lambda)} \cdot \frac{A_3}{A_6}$$

where $\tau(\lambda)$ is the transmittance of the system, A_6 is the area of a 6 mm diameter pupil and A_3 is the area of a 3 mm pupil. Solving equation (2-4) gives

(2-5) $$t \le 125.66s$$

The result of the calculations shows that if the light source is at full power, it will take over 2 minutes before it becomes dangerous to the patient. In this study, the patients will be subject to an illumination of no more than 25% of full power and incident light will have a ring shape, reducing the intensity by an extra 50%, giving a threshold of more

than 16 minutes before it exceeds accepted illumination thresholds which are themselves approximately 10 times lower than damage thresholds. The maximum exposure time for patients will be limited to 4 minutes for our patients given the experimental conditions. This means that the light source used poses absolutely no threat to the patients even at full power. It is also important to note that the light beam entering the patient's eye has a diameter of 6 mm. In the event that a patient's pupil would dilate beyond 6 mm, there wouldn't be any additional light entering the eye. Therefore, a pupil diameter of 6 mm for the calculations accounts for the maximum amount of light that could possibly enter the eye if the source was at maximum and the mask not in place. It accounts for the worst case scenario that could ever cause any potential damage to the retina. Finally, before any experiments were performed, light levels were measured at the patient's eye position with a power meter to confirm that light source intensity was in the range of safe operation.

2.3.2 Uniform (Maxwellian) Retinal Illumination

Achieving a uniform retinal illumination is very important when performing any type of retinal imaging. In order to accomplish this task, a combination of 2 common types of illumination configurations was employed: Maxwellian and Kohler illumination.

Maxwellian illumination, commonly referred to as Maxwellian view, is the most common type of illumination configuration used when illuminating the retina [130]. In Maxwellian view, the illumination source is imaged at the entrance pupil of the eye which is conjugate with the pupil seen through the eye. This means that each point in the source image sends a cone of light (usually large angle but optics dependent) at the

retinal plane and each of these cones of light overlap for most of the illuminated retinal area. This mixing of light from each point source results in independence on the source uniformity and uniform retinal illumination (figure 2-5).

In the second illumination system (Kohler system), the lenses and irises are arranged in a way to have the sample be uniformly illuminated by matching the source's exit pupil with the retina while maintaining independent control on the light intensity and field size [130] (no change in source temperature or spectrum). This is the illumination system most commonly used in microscopes. A diagram of a Kohler illumination system is shown below (figure 2.6).

In this setup, the light source is imaged at the front focal plane of the condenser lens. The condenser lens then illuminates the sample object with parallel and uniform light because the sample is in the exit pupil plane of the illumination system. The auxiliary lens iris is placed at a position to be imaged at the sample object plane by the condenser lens. By opening and closing the auxiliary lens iris conjugate with the exit pupil of the system, the illumination field size can be controlled. The condenser lens iris is placed at the image plane of the light source image formed by the auxiliary lens. This iris gives control on the amount of light that illuminates the sample by limiting the area of the source used to project light on the sample. Using this type of illumination configuration, the object can be illuminated uniformly and the user can have independent control of the intensity of light and illuminated field size by opening and closing the respective irises. Our design described below incorporates elements from both systems so we can have control over illumination area and intensity with uniform illumination on the retina.

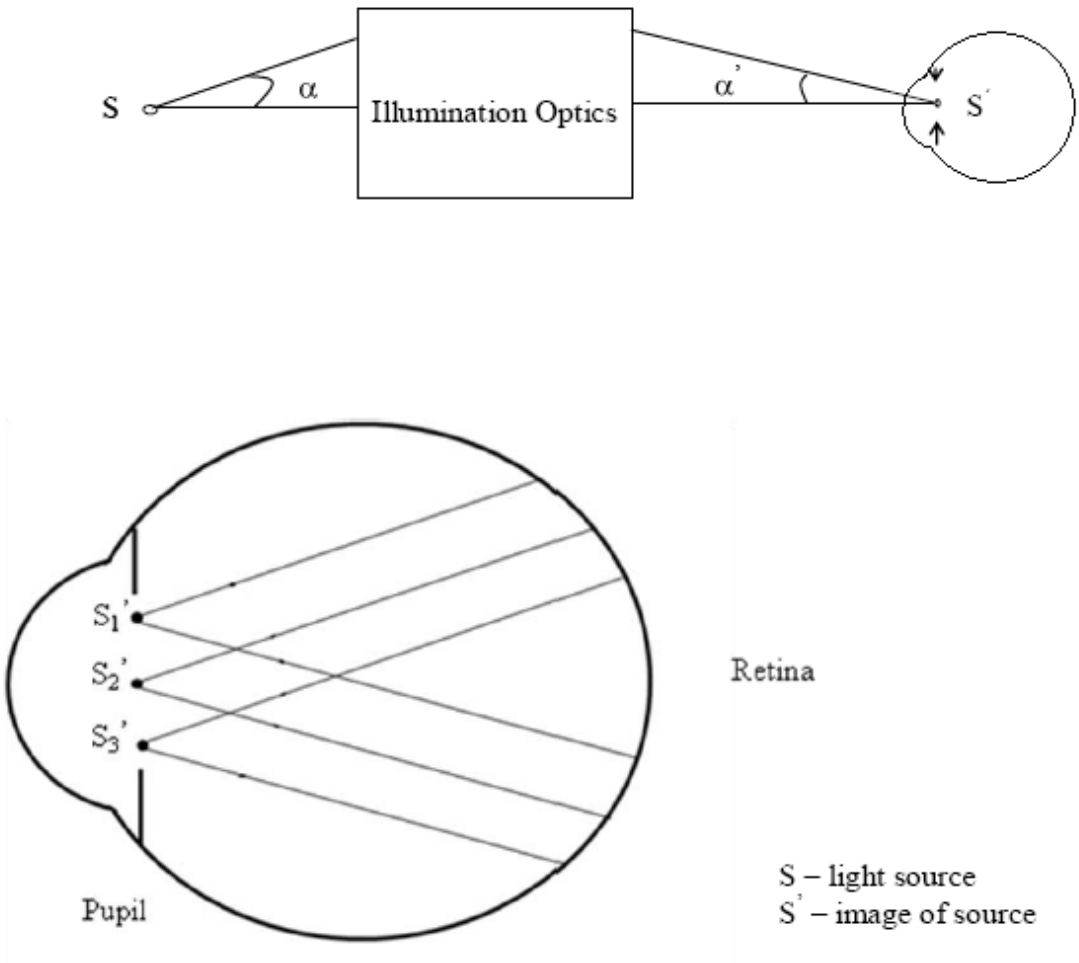

Figure 2.5: Diagram of Maxwellian illumination. Creating an image of the illumination source at the entrance pupil of the eye assures maximum coupling to the eye and a uniformly illuminated retina. Recreated from The Eye and Visual Optical Instruments [130]

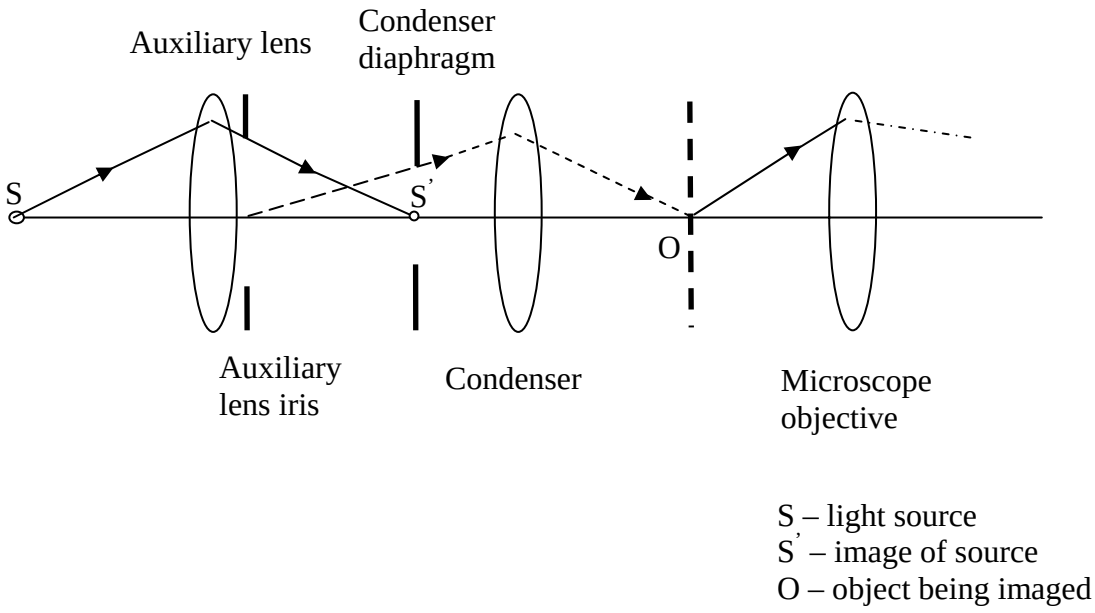

Figure 2.6: Diagram of a Kohler illumination system most commonly found in microscopes. Placements of an iris in a plane conjugate with the source (intensity control) and one conjugate with the object to illuminate (area control) provides for independent control of object brightness and field of view. Recreated from The Eye and Visual Optical Instruments [130].

The objective of the retinal oximetry device illumination system is to achieve uniform illumination of the retina while having independent control of light intensity and illuminated field size. Since the light source is a tungsten halogen (TH) broadband source, changing the voltage of the source would change its spectral radiance output. It is therefore preferred to have control of the intensity using irises instead of changing the light source voltage. A diagram of the device illumination system is shown below (figure 2.7).

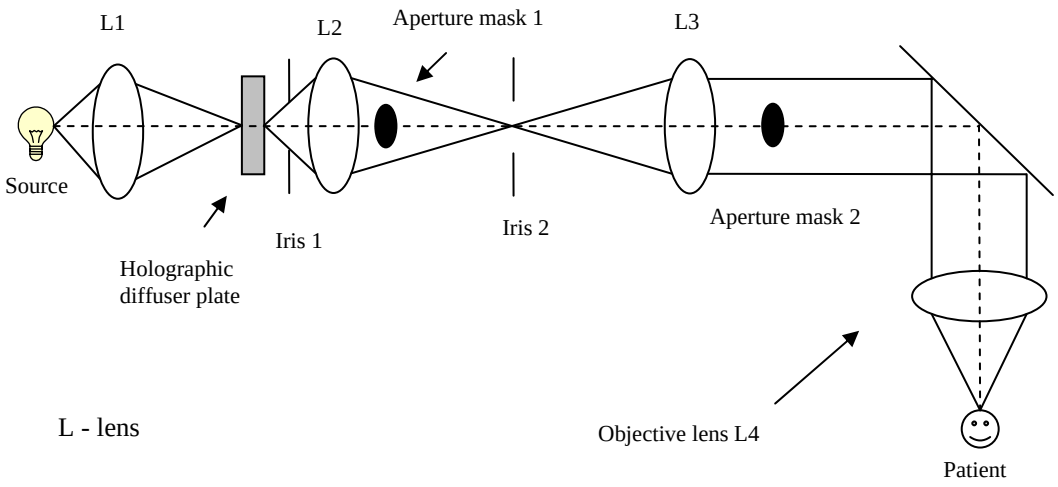

Figure 2.7: Diagram of retinal oximetry device illumination system showing light vergence used to create uniform retinal illumination

Figure 2.7 illustrates how a classic design for a Maxwellian illumination would look (a holographic diffuser is added to the classic design). One of the difficulties in this classic design is coupling an extended source to produce a small image of the source in the pupil, while controlling the area of uniform illumination. A novel approach, using the unique optical properties of holographic diffusers (beam shaping diffusers) was used in this design to overcome these difficulties. In this design, the light from the TH bulb is projected onto a holographic diffuser plate by a lens L1 and the diffuser is positioned to be conjugate with the eyes pupil. The diffuser effectively becomes the new light source for the eye. There are many designs of diffusers and a full discussion is beyond the scope of this thesis. For our particular use, we used diffusers which have the ability to control the angular diffusing of light exiting the diffuser. The purpose of the diffuser is twofold:

it helps create a uniform illumination by diffusing the image of the light source, and also helps to create a single image plane for the TH bulb, thus achieving a better overall control of the light vergence (reduces the requirement for exact coupling of the source to the illumination optics by creating a well defined plane for the source which is less sensitive to the source position and orientation). Because the TH bulb is in a light source housing that is equipped with a back mirror to increase the output intensity of the source, an imperfect positioning of the back mirror leads to an additional imaging plane for the TH bulb (i.e. one plane for the TH filament and one plane for the reflected image of the TH filament). In addition to the back mirror, the surfaces of the TH bulb create reflections as well, and all of these factors lead to multiple imaging planes for the TH bulb and poses some difficulty when controlling light vergence in the illumination system. By inserting a holographic diffuser at the source imaging plane, we eliminated these problems completely.

Iris 1 is placed in front of lens 2 so that lens 2 and lens 3 create an image of the iris at the front focal plane of the objective lens. The objective lens in turn creates an image of the iris at infinity and is thus focused on the surface of the retina by the eyes optics thus effectively acting as the illumination area aperture as per the Koehler design. By opening and closing the iris, the illuminated area of the retina can be controlled. As for iris number 2, it is conjugate with the holographic diffuser. Opening and closing the iris determines the area of the diffuser used and the amount of light that is sent to the retina. The combination of holographic diffuser plate and irises placed at the proper locations in the system allow for a uniform illumination of the retina and an independent control of intensity and illuminated field.

2.3.3 Corneal and Objective Lens Reflections

As mentioned previously in this chapter, corneal and objective lens reflections must be completely blocked from entering the retinal imaging system or they will saturate the retinal image. In order to achieve this objective, blocking masks were placed at strategic locations in the system. Blocking masks can be used in either the illumination or imaging pathway. We have used the former (discussed below) for two reasons, firstly because of the variance in the optical properties of human eyes, it is very difficult to control fully the light returning for both the objective lens and cornea simultaneously because the corneal image moves for each patient and the retinal image also moves slightly for each patient. Furthermore, as these two images move with eye alignment with the imaging system, the patient / imaging system alignment becomes very critical and difficult to maintain over an imaging session as patients move their eye. That is why most imaging systems for the eye use masking in the illumination pathway.

The 2 main objectives of the blocking masks in the illumination pathway are: to prevent light reflected from the cornea and the light reflected from the objective lens from entering the imaging system, all the while not interfering with the retinal illumination. The purpose of a mask is to ensure that no light is incident on the surface of the optical element in an area which would reflect the light back into the optical system (figure 2.8). To perform this task the mask has to be conjugate with the surface to block, therefore having 2 surfaces to block requires 2 individual masks.

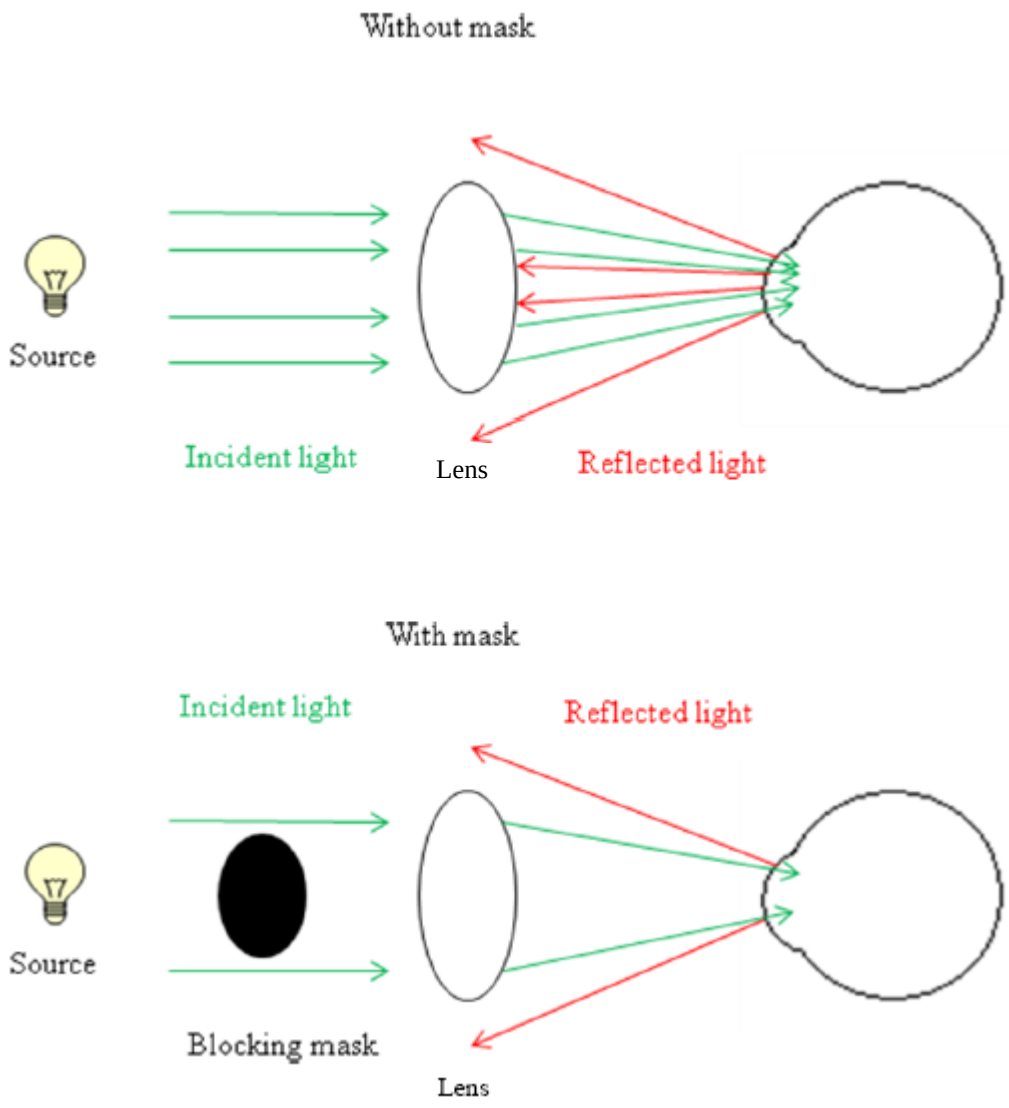

Figure 2.8: Function of corneal blocking mask. Without the blocking mask, the corneal reflection in the center of the cornea is captured by the lens and overwhelms the retinal image. The blocking mask prevents central corneal reflections from entering the imaging optical system.

The size of each mask is determined by the curvature of the reflecting surface. In the case of the objective lens, the curvature is very high, the lens having a power of 60 diopters. The blocking mask 1 in the illumination system is the one responsible for blocking the reflections from the objective lens; it has a size of 5 mm and is imaged by

lens 3 onto the front surface of the objective lens. As for the cornea, it has a curvature of approximately 7.7 mm [130] and requires a blocking mask of 4 mm imaged directly at the patient's corneal plane. The mask is placed after lens L3 in the illumination system and is imaged by the objective lens on the cornea. The position of this mask is critical, since it must block the corneal reflections but also can't be seen on the retinal illumination. The depth of field of the corneal blocking mask must therefore be very short so as not to cast any degree of shadow on the retina. The short focal length of the objective lens fulfills these criteria quite well.

2.4 Imaging System

The main purpose of the imaging system of the device is to capture the light exiting a patient's eye and image it on a CCD (Charge-Coupled Device) chip to be captured by computer. It must achieve this objective while providing sufficient image quality, magnification and allow for the spectroscopic system to be inserted somewhere in the system to be able to measure oxygen saturation on the retina. It is of paramount importance that the system be very efficient at capturing all the light exiting the eye and sending it to a digital camera with as little loss of light as possible, since the amount of light exiting the eye is very low compared to the light entering it. To achieve these objectives, great care must be taken when designing the imaging system to place the aperture stop in a location that will match the entrance and exit pupils of the system to the eye and camera pupils respectively. Failure to properly match the pupils results in a very poor quality and sometimes indistinguishable retinal image. Therefore, a discussion of these optical principles is necessary before an explanation of the design can be given.

2.4.1 Aperture and Field Stop

The aperture stop of an optical system can be defined as any optical element i.e. a diaphragm, iris or the rim of a lens, which determines the amount of light that reaches the image plane [133, 134]. The aperture stop of a system is dependent on the position of the object being imaged and determines the brightness of the image. That is, it determines the diameter of the cone of energy which the system will accept from an axial point on the object. A visual example is given below (figure 2.9).

In figure 2.9 ***(a)***, the object being imaged is from infinity. In this case, the aperture limiting the amount of light being captured by the optical system is the stop in front of lens 1. In figure 2.9 ***(b)***, the object is close enough to the objective lens that the aperture is not limiting the amount of light being captured by the optical system. In this case, the objective lens is the limiting aperture and is thus the aperture stop. In figure 2.9 ***(c)***, the object is further back from the objective than in figure 2.9 ***(b)***. Here, the second lens of the system is limiting the amount of light sent through the system and is therefore the aperture stop**.** It is very important to note that in these 3 cases, the optical system and stop positions and sizes remain the same. The aperture that determines the amount of light captured by the system depends on the position of the object being imaged by that system. This also means that the entrance and exit pupils will be different depending on the position of the object being imaged.

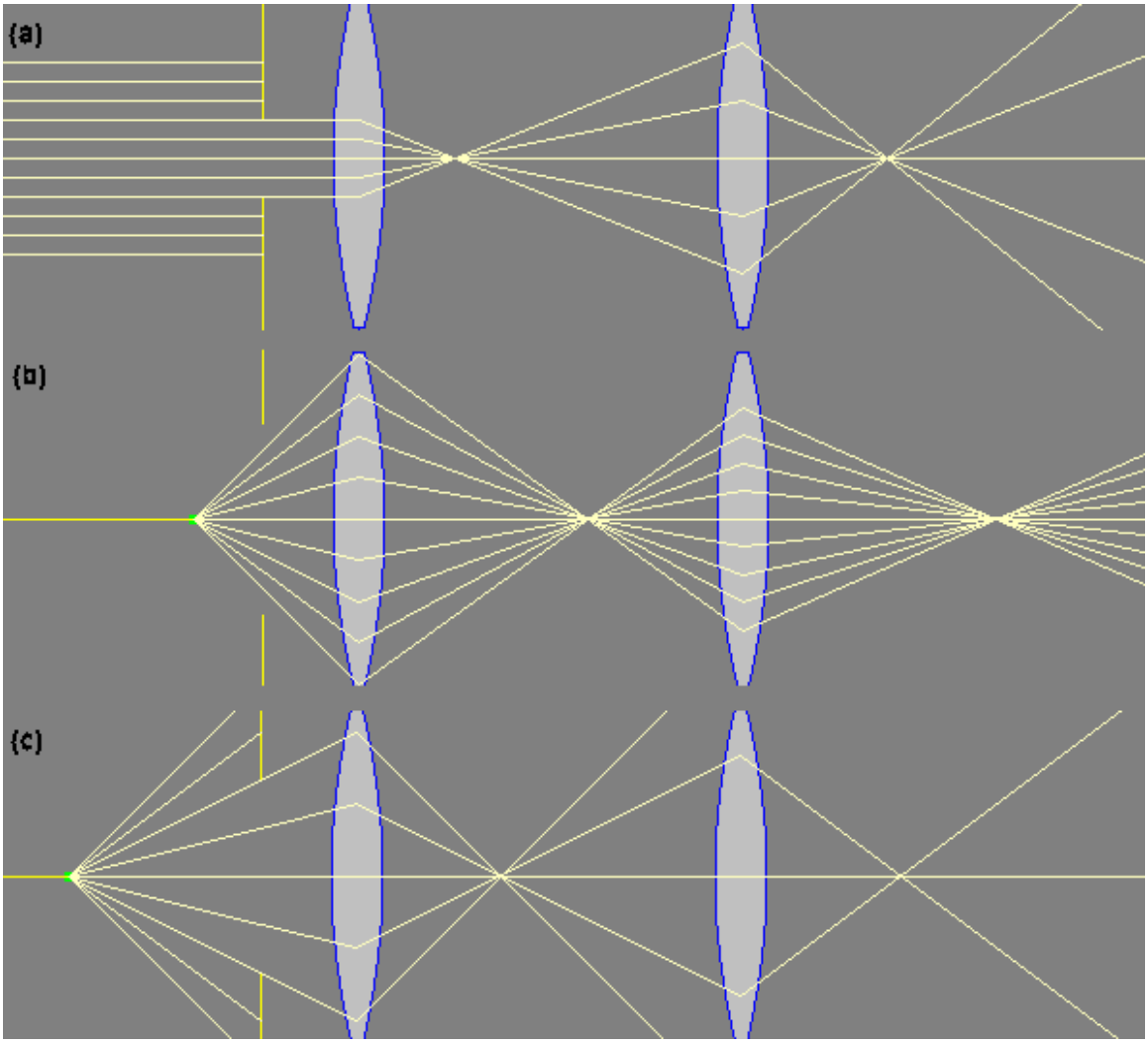

Figure 2.9: Example of light entering the same optical system from different object planes, resulting in different optical elements acting as the aperture stop in each system (http://electron9.phys.utk.edu/optics421/modules/m3/Stops.htm) [135]. In figure 2.9 *(a)*, the aperture stop is the stop in front of lens 1, while in figure 2.9 *(b)* the aperture stop is lens 1 itself. In figure 2.9 *(c)* the aperture stop of the system is lens 2.

The field stop of an optical system is defined by the element limiting the size or angular breadth of the object that can be imaged by the system. It determines the field of view of the system [133, 134]. The aperture stop controls the number of rays from an object point reaching the conjugate image point and the field stop determines which rays

reach the image plane. The aperture stop determines the brightness of the image while the field stop determines the size of the image.

2.4.2 Entrance and Exit Pupils

The entrance pupil of an optical system can be defined as “the image of the aperture stop as seen from an axial point on the object through the optical elements preceding the stop” [133]. In other words, it is the image of the aperture stop formed by the optical elements in front of the aperture stop when looking at the system from the object side. When there are no lenses between the object and the aperture stop, then the stop itself is the entrance pupil of the system and it can be real or virtual. Furthermore, the entrance pupil of a system depends on the position of the object being imaged (see above). The cone of light entering the optical system is determined by the entrance pupil. In the case where the aperture stop of an optical system is located in the back focal plane of that part of the system which precedes it, the entrance pupil will be at infinity and all the principal rays in the object space will be parallel to the axis [134]. The system is then telecentric on the object side.

The exit pupil of an optical system, on the other hand, is “the image of the aperture stop as seen from an axial point on the image plane through the optical elements succeeding the stop, if there are any” [133]. It will determine the cone of light leaving the optical system. The size and positions of the entrance and exit pupils are extremely important when coupling optical systems together. In order for two instruments to be coupled together effectively, the exit pupil of one instrument must be at the same plane as the entrance pupil of the other. This is known as pupil matching. In addition, in order for

all the light to be captured by the second optical system, the size of the exit pupil of the first system must be smaller than the size of the entrance pupil of the second. Failure to do so will result in a loss of light while coupling.

2.4.3 Imaging System Design

The imaging system is composed of 5 lenses, 1 mirror and a CCD camera with an additional camera lens. The objective lens of the imaging system is shared with the illumination system and acts as a double pass lens. The layout of the imaging system is shown below in figure 2.10 (ZEMAX model shown further).

The objective lens collects light exiting the eye, which normally will be projected to infinity for a well focused eye, and images it at its focal plane. Lens 4 and Lens 1 act together as a telescope to maintain focus at infinity so that lens 5 can focus the light onto the mirror with a known magnification. Lenses 2 and 3 are a set of relay lenses that act as an afocal condensing system between lens 1 and 4 to ensure no light loss. The camera is focused on the mirror image and projects the retinal image onto its' CCD chip. The imaging system was designed to have the iris of the patient as conjugate with its aperture stop so that it becomes the aperture stop for the combined eye / imaging system. This was done so that the instrument wouldn't limit the amount of light going through the imaging system as discussed above. By having the patient's iris as the aperture stop, all the light exiting the eye can pass through the optical system and not be limited by any element of the system. As for the exit pupil, it is located approximately 110 mm behind the imaging plane i.e. the mirror. The position was fixed at 110 mm to permit efficient coupling with the camera lens entrance pupil. Since the design specifications of the camera lens utilized

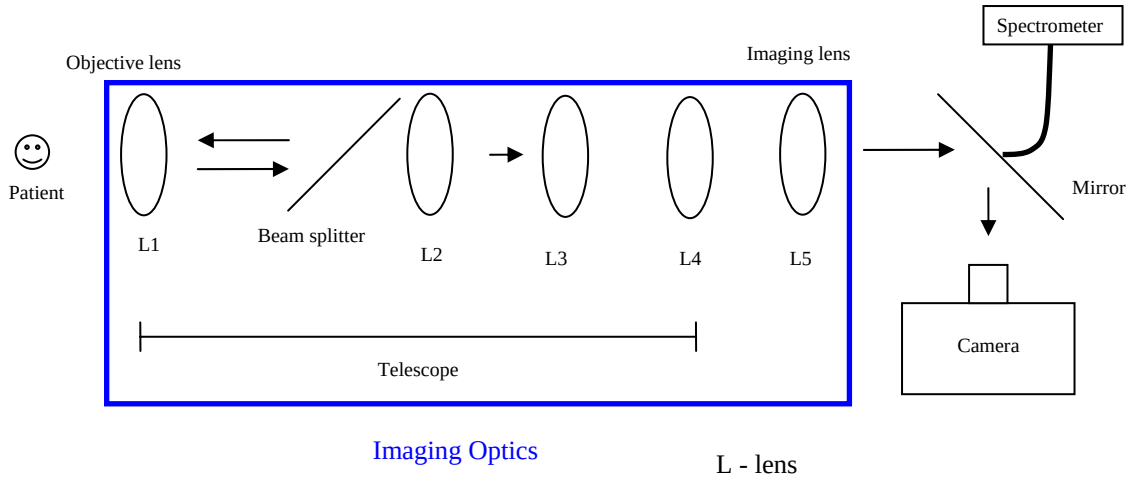

Figure 2.10: Layout of retinal oximetry device imaging system used to create an image of the retina at the mirror plane from the retinal reflectance signal

weren't available, a position close to the camera lens aperture was chosen as a suitable position for the exit pupil of the imaging system. The resulting image quality of the retina demonstrates that it was in fact a good choice. A model of the imaging system constructed in the optical modeling software ZEMAX is shown below (figure 2.11).

The total magnification of the system is approximately 1:1 so that the image size on the mirror is the same as the retina. This allows the camera to create an image of the retina that has decent resolution for a 35 degree field of view.

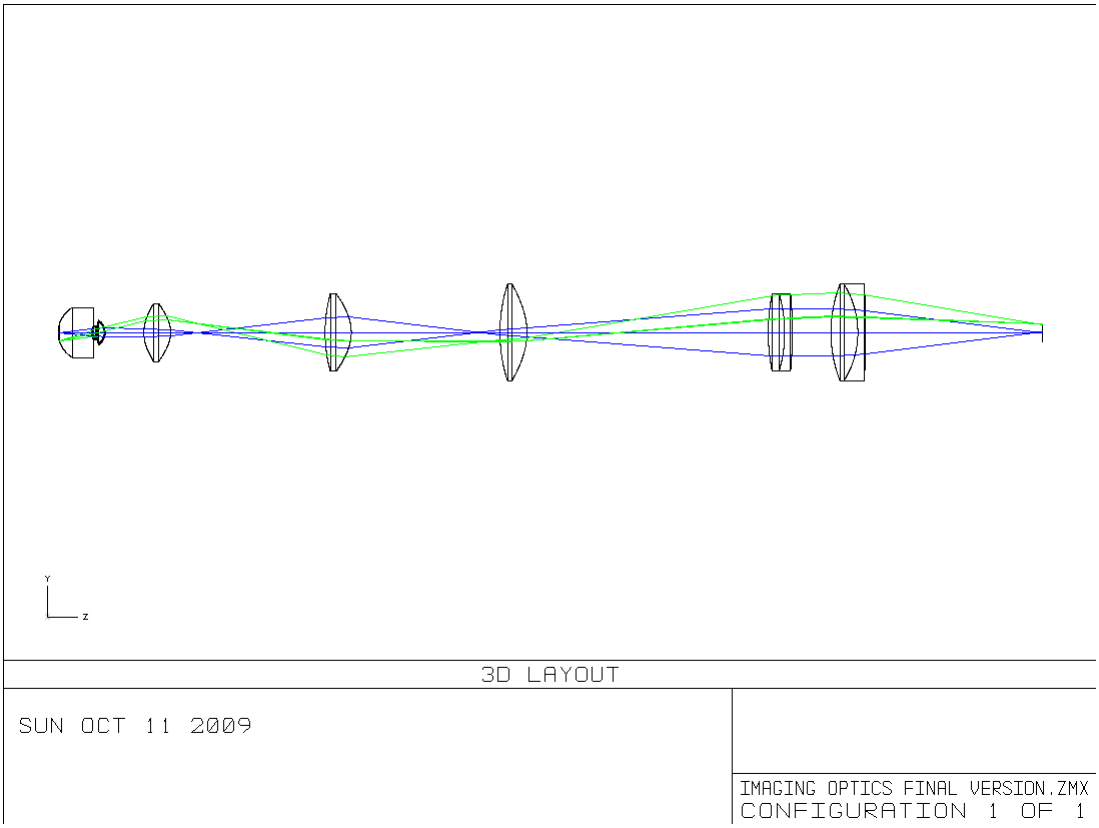

Figure 2.11: ZEMAX model of retinal oximetry device imaging system showing light vergence of retinal reflectance signal

2.5 Spectroscopic System

The main purpose of the spectroscopic system is to capture a spectrum of a target area on the retina in order to be able to calculate oxygen saturation. It must be able to select any desired area of the retina, and capture a signal from a target size that is comparable to a blood vessel (so that the spectrum is really from the vessel, not from the surrounding tissue). The system must also be very efficient at capturing the light from the retina, since low light levels could require long integration times, which would cause a problem with accuracy because of eye movement. For example, if an integration time of 5 seconds is required to capture a spectrum of a blood vessel, the patient would need to

maintain their eye in the exact same position for 5 seconds. This can pose quite a challenge for some patients. It is therefore preferred to keep the exposure times as low as possible, while maintaining an adequate signal to noise ratio for the spectrum.

2.5.1 Mirror Mount System

As previously discussed in the imaging system description, the optical fiber that captures the retinal spectrum is placed at an image plane of the retina. The mirror that directs the image from the imaging system to the CCD camera (and is also an image plane) has a small hole in it to allow light to be collected by an optical fiber. A diagram of the system is shown below (figure 2.12).

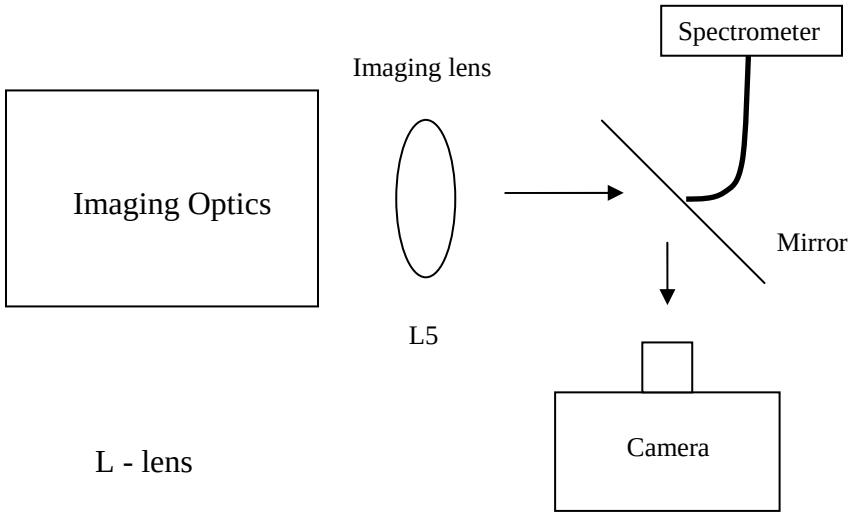

Figure 2.12: Diagram of spectrometer system used to measure the reflectance spectrum at a given target location of the retina

The mirror has a 100 micron angled hole drilled into it to allow the light to be coupled to an optical fiber at a normal angle to the fiber surface. A schematic diagram of the mirror mount is shown below (figure 2.13).

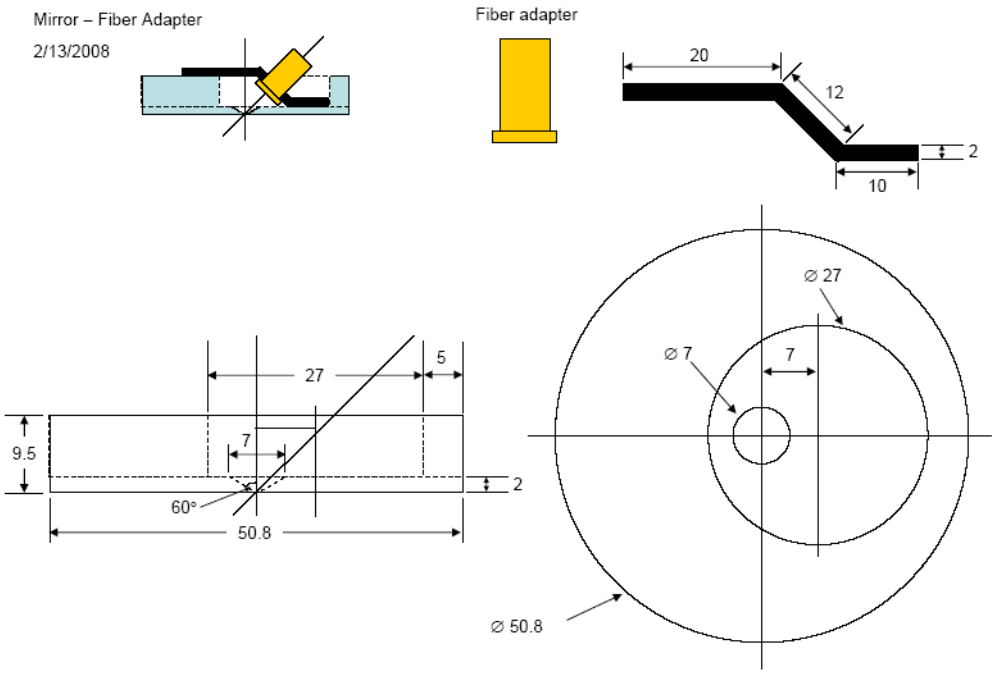

Figure 2.13: Diagram of the mirror mount system showing a 100 μm hole where light is coupled to a fiber and sent to a spectrometer for measurement

As can be seen from the diagram, the hole is drilled in a conic shape to allow light to pass through without any reflections. The hole is drilled at a 45 degree angle since this is the angle of the mirror to the CCD camera. A short focal length lens captures the light entering the hole and couples it to a broadband optical fiber. The fiber is connected to a USB (Universal Serial Bus) spectrometer with a linear array that has a range of 350 nm to

1000 nm. It is an Ocean Optics SD2000 spectrometer, with a 12 bit dynamic range (0 – 4096), a signal to noise ratio of 250 and integration times from 3 ms to minutes.

2.5.2 Motor System and Software

Since the fiber is attached directly to the mirror mount, the fiber moves with the hole when adjusting the mirror position. The mirror is mounted to an X-Y motor stage system that allows for the hole in the mirror, and thus the fiber, to be moved to any desired location on the retina. An image of the mirror and motor system is shown below (figure 2.14).

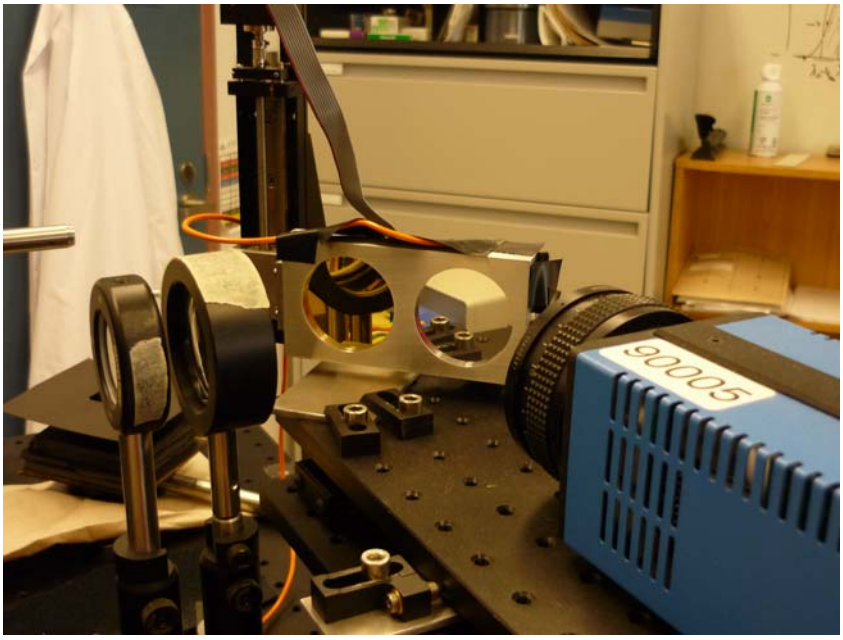

Figure 2.14: Picture of mirror mount and motor system of the retinal oximetry device

The motors used in the system are “Folded Motorized MicroMini Stages” from National Aperture Inc. They can be controlled by the help of a MicroMini Controller and

software that was adapted especially for this device. The user interface of the software is shown below (figure 2.15).

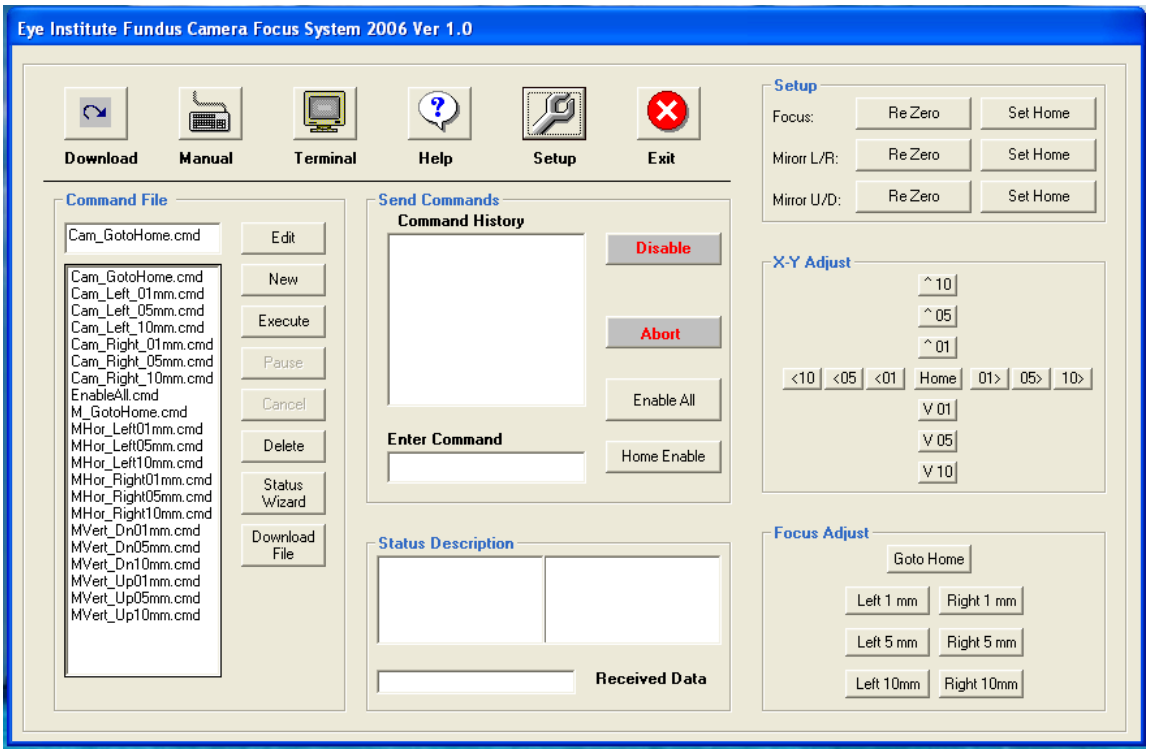

Figure 2.15: View of software GUI used to control motor stages

The software GUI (Graphic User Interface) allows for the control of the X and Y planes by moving the corresponding translation motors. The focus is controlled by a separate motor that translates the entire platform that the CCD camera and mirror mount system are mounted to. A patient with emmetropic (no refractive error) vision will have an image of the retina focused onto the mirror. However, if the patient doesn't have perfect vision, the image of the retina will be formed either in front or in back of the mirror plane. By translating the entire mirror stage back and forth while keeping the

distance between the CCD camera and the mirror constant, the patient's refractive error can be compensated.

2.6 Instrument Characterization

The device described above was designed to measure retinal oxygen saturation at user-targeted areas of the retinal vasculature in a non-invasive manner. Before the system can be used on human eyes however, it must first be characterized and validated. In the next section, the stability of the tungsten halogen light source will be measured, since this will affect the precision of the transmission spectra measurements. The spectrometer's wavelength calibration will be verified by measuring absorption peaks of known substances, and images will be taken on an artificial plastic eye to understand the image quality of the device along with its field of view. Finally, the multiple linear regression method described in Chapter 1 will be tested using measurements from a mixture of calligraphy inks performed on 2 different spectroscopy systems.

2.6.1 Light Source Stability

In any type of spectroscopy measurement, the stability of the light source is very important. In the device, the spectrum of a sample is taken by measuring the transmission spectrum through the sample and dividing by a reference spectrum. Since the reference and sample spectra are not taken simultaneously, any variation in the light source intensity will cause a variation in the calculation of the sample transmittance spectrum. In order to estimate the precision and repeatability of the spectroscopic measurements of the

device, the light source stability was measured at multiple intensities. Ten consecutive spectra were obtained for 4 different light source intensities. The repeatability of the light source for a particular intensity was calculated by equation (2-6):

$$\text{(2-6)}\quad \text{Repeatability}(\lambda) = \frac{Max(\lambda) - Min(\lambda)}{Mean(\lambda)}$$

where $Max(\lambda)$ and $Min(\lambda)$ are the highest and lowest intensity values respectively from the 10 measured spectra at wavelength λ and $Mean(\lambda)$ is the mean intensity value of the 10 measured spectra at wavelength λ. Results for light source intensities of 30%, 50%, 70% and 100% are shown in figure 2-16.

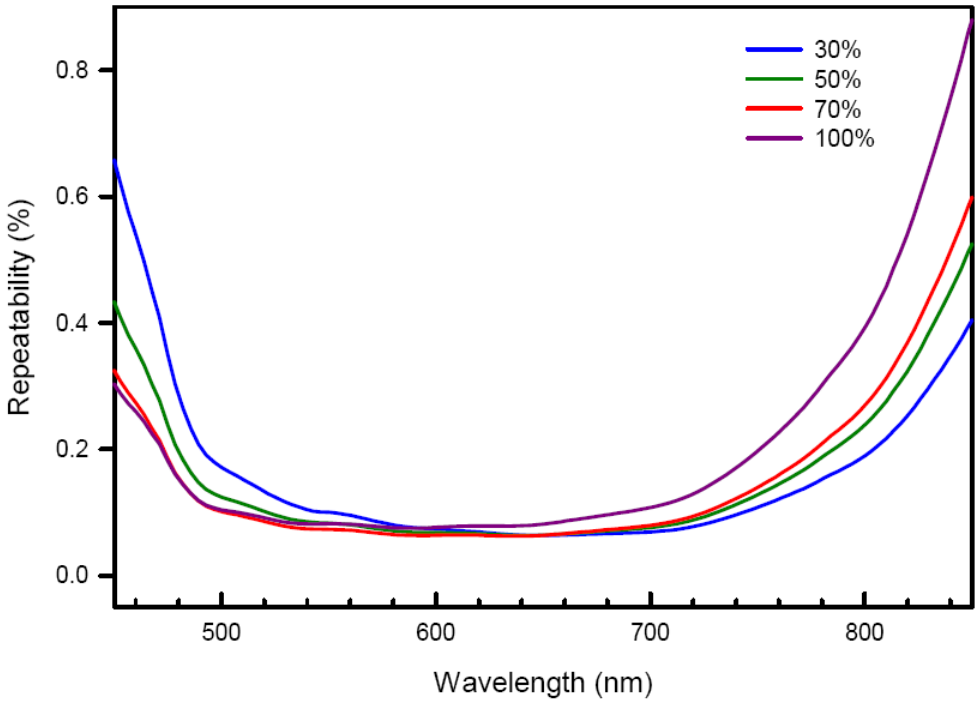

Figure 2.16: Variation of retinal oximetry device light source spectrum for different light source intensities. Calculations performed over 10 consecutive measurements.

In the wavelength range between 500 and 700 nm, the light source repeatability is better than 0.2% and never exceeds 0.6%. over the whole range of interest.

2.6.2 Spectroscopy Validation

The spectrometer used in the system was an Ocean Optics SD 2000 with a resolution of 8 nm, a maximum signal to noise ratio of 250 and a 12 bit dynamic range. Before any oximetry calculations can be performed, it is important to make sure that the spectrometer is property calibrated in its reported wavelength. This can be achieved by measuring the spectrum of a known substance or material and comparing to published results. An easy way to validate the spectrometer is by measuring the spectral lines of calibrated lasers. The spectral lines of a red (632.8 nm) and green (543.5 nm) HeNe (Helium-Neon) laser were measured and shown in figure 2-17.

The peaks of the red and green lasers were found to be 1.4 nm and 0.9 nm respectively from their expected value, which is well within the 8 nm resolution of the spectrometer. The full width at half maximum (FWHM) of the spectral peaks were calculated using the SigmaPlot (Systat Software Inc., San Jose, CA) function “fwhm” and were found to be 8.2 nm for the green laser and 7.6 nm for the red laser, which also corresponds well to the 8 nm resolution of the spectrometer (the bandwidth is actually wavelength dependent, but changes by only 3%, or 0.2 nm, between the wavelength range of interest in oximetry and will have no impact on the calculation of oxygen saturation). Even though the widths of the laser peaks are in the expected range for the spectrometer, the odd shape of the peaks and the difference between the measured and

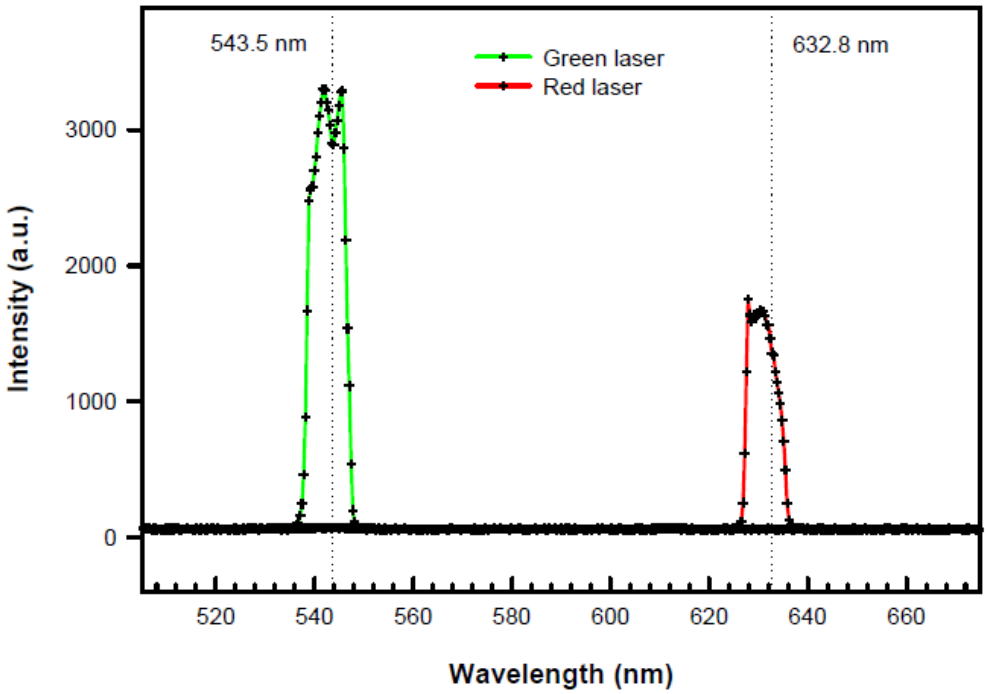

Figure 2.17: Spectra of 543.5 nm and 632.8 nm HeNe lasers taken with the Ocean Optics spectrometer

expected peak wavelength values suggest either a problem with the spectrometer or with the lasers themselves. Whole blood spectroscopy measurements discussed in Chapters 4 and 5 showed that the spectrometer measured oxyhaemoglobin absorption peaks at wavelength values that matched values found in the literature. This gave us confidence to use this spectrometer for all further oximetry measurements. Further experiments described in section 2.6.4 also reinforced our confidence in the spectrometer.

2.6.3 Model Eye Measurements

In order to verify the imaging capabilities of the device, a model eye was placed in the position where a patient's eye would normally rest. The image of the model eye

gives us a sense of the image quality we can expect from the retina and also verifies that the blocking masks described previously are performing as expected. Images of the model eye are shown in figure 2-18.

The images seen in figure 2-18 demonstrate that the blocking masks are performing as expected. There are no intense reflections saturating the images and interfering with the retinal image. The image quality is good enough to distinguish the optic disc, retinal vessels and some surface details as confirmed by an ophthalmologist. The whitish circle on the upper left corner represents the optic disc while the central black circle is a mechanical post supporting the eye to its mount. On the lower central part of the image, the hole in the mirror coupled to the optical fiber and spectrometer can be observed. As mentioned previously, the hole has the capability to move across the

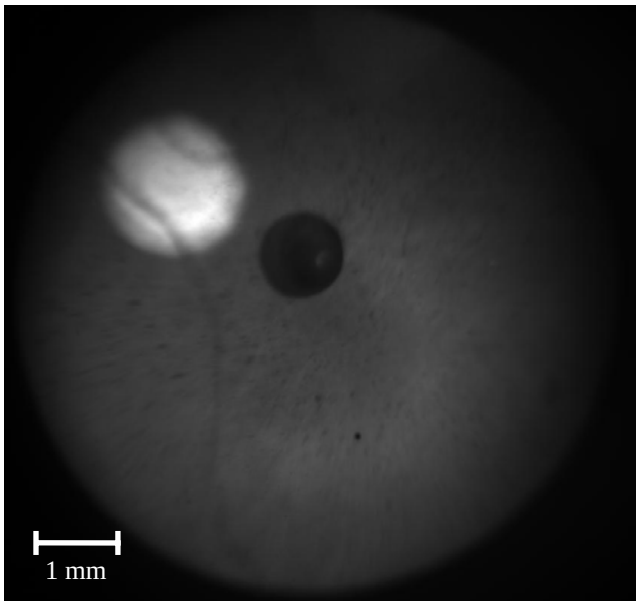

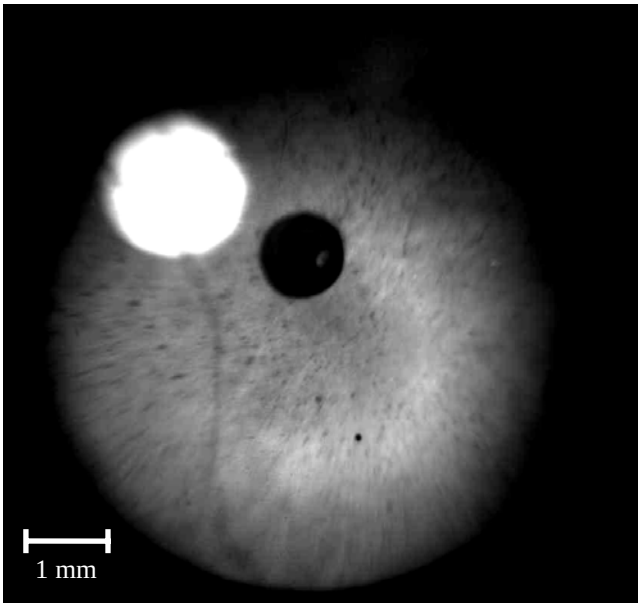

Figure 2.18: Fundus images of a model eye taken by retinal oximetry device. Lower image is same as upper with higher brightness level to highlight the retina features as opposed to the optic disc (upper image).

retina to capture the spectrum of any desired target area. The user can see the black dot move along the retinal surface and identify the location that the spectrum is being captured.

The image of the model eye was also taken by a commercial fundus camera for comparison. It is shown in figure 2-19.

2.6.4 Multiple Linear Regression Model Validation

The method described in Chapter 1 to calculate oxygen saturation of a blood sample relies on a multiple linear regression modeling of the absorbance of the blood sample. Before performing the analysis on blood, the approach was tested using a

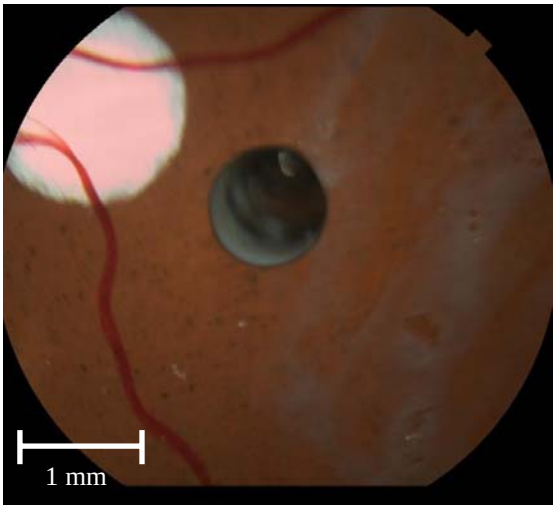

Figure 2-19: Fundus image of model eye taken by a Topcon fundus camera

mixture of calligraphy ink. In this experiment, the absorbance of red, green and a mixture of both red and green inks were measured. To reduce the absorbance of the ink to levels more easily measurable by the device, the inks were diluted with saline. Once the absorbance of each color inks were measured, the red and green ink were mixed in a 40% red 60% green ink mixture, and the absorbance of the mixture was also measured. Using a multiple linear regression analysis, the percentages of each ink in the mixture were extracted. The absorbance of the inks are shown in figure 2-20.

The results of the analysis predicted 41.1% - 58.9% mixture of red and green ink with a coefficient of determination R^2 value of 0.996 in the wavelength range between 550 and 750 nm. A similar analysis performed on an Olis Cary 14 spectrophotometer using the same mixtures found a predicted 39.6% - 60.4% mixture of red and green ink with an R^2 value of 0.997. The fact that results in both experiments were within 1.5% of each other suggest that the multiple linear regression analysis method may be promising to calculate the oxygen saturation of blood samples, and that the Ocean Optics

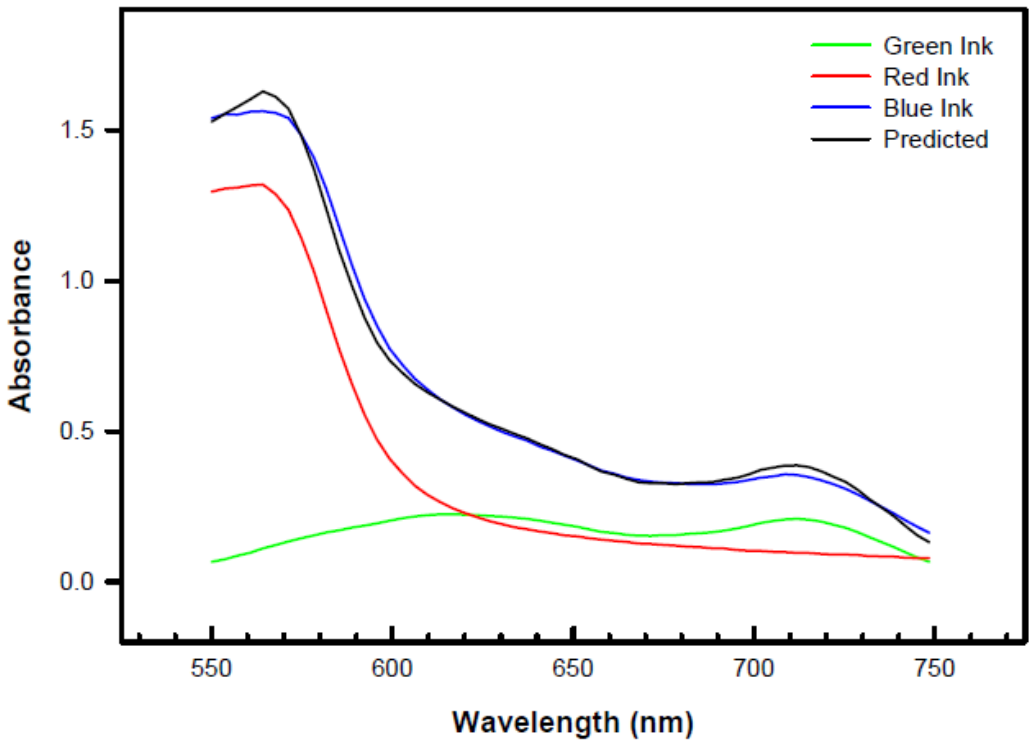

Figure 2.20: Absorbance of red, green and a red-green ink mixture measured with the retinal oximetry device. The blue curve is the absorbance of the red and green ink mixture while the black curve is the predicted curve found from the multiple linear regression analysis

spectrometer is appropriate for use in our experiments. In the following chapters, the method will be tested with whole blood samples using absorbance measurements performed with the retinal oximetry device.

2.7 Preliminary Retinal Oximetry Results

As mentioned in Chapter1, one of the objectives of this thesis was to design and construct an instrument capable of measuring *in-vivo* retinal oximetry. The purpose of the experiment described in this section was to attempt to validate the oximetry capabilities

of the retinal oximetry device described in the previous sections. Retinal images were acquired on five eyes from four healthy volunteers. In each measurement, a spectrum was acquired on the optic disc in order to calculate the oxygen saturation of the surface vessels. The inclusion criteria for this study were adults with normal ocular exams. Subjects were examined by an ophthalmologist prior to testing to ensure that the volunteers had good ocular health. The exclusion criteria were patients with retinal and optic nerve disease, any significant ocular media opacity including advanced cataract, any systemic vascular disease, including diabetes and hypertension.

Once the volunteers were cleared by the ophthalmologist to undergo the measurements, they were presented with a Patient Information Sheet and Consent Form (see Appendix E) which explained the purpose of the study, the study procedures and duration, along with the associated risks of participation. Upon accepted written consent, the volunteers were administered Mydriacyl eye drops which dilate the pupil to make retinal imaging easier. The dilating drops also relax the focusing muscles of the lens and thus prevent accommodation to allow for a constant focus of the imaging optics of the device.

Once the volunteers' eyes were fully dilated, they were asked to rest their heads on the device head mount and the instrument was aligned to acquire retinal images (figure 2.21). The dark spot on the optic disc represents the spectrum capture area of the device. Spectra from the optic disc were captured from five eyes and analyzed to calculate the oxygen saturation of the surface vessels. To calculate the absorbance of the reflected signal, the acquired spectrum was divided by a reference signal (both corrected for noise), which is a spectrum of a $BaSO_4$ reflective layer of a model eye that will be

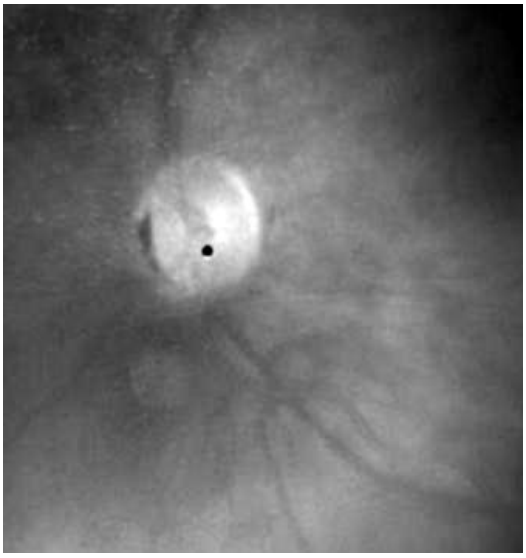

Figure 2.21: Retinal image of a healthy volunteer taken by retinal oximetry device. The dark circle is the area where the retinal reflectance signal is being measured. The white circle is the optic disc.

described in Chapter 4. The absorbance was then calculated by use of equation 1-4 (figure 2.22).

The reflectance spectra from different locations of the retina were also taken for comparison. An example for one subject is shown in figure 2.23. The relatively low signal to noise ratio of the Ocean Optics spectrometer made it difficult to resolve the retinal blood absorbance spectra and calculate oxygen saturation. Subsequent discussions with other authors using similar techniques to calculate *in-vivo* retinal oximetry on the optic disc confirmed that much higher signal to noise ratios are necessary to calculate oxygen saturation using this technique because of the high level of background scatter signal (white glow) on which it rides. Nerve head oximetry was thus not made possible with this version of the device. The results shown in figure 2.23 demonstrate the absorbance of different regions of the retina, but again due to the low signal to noise

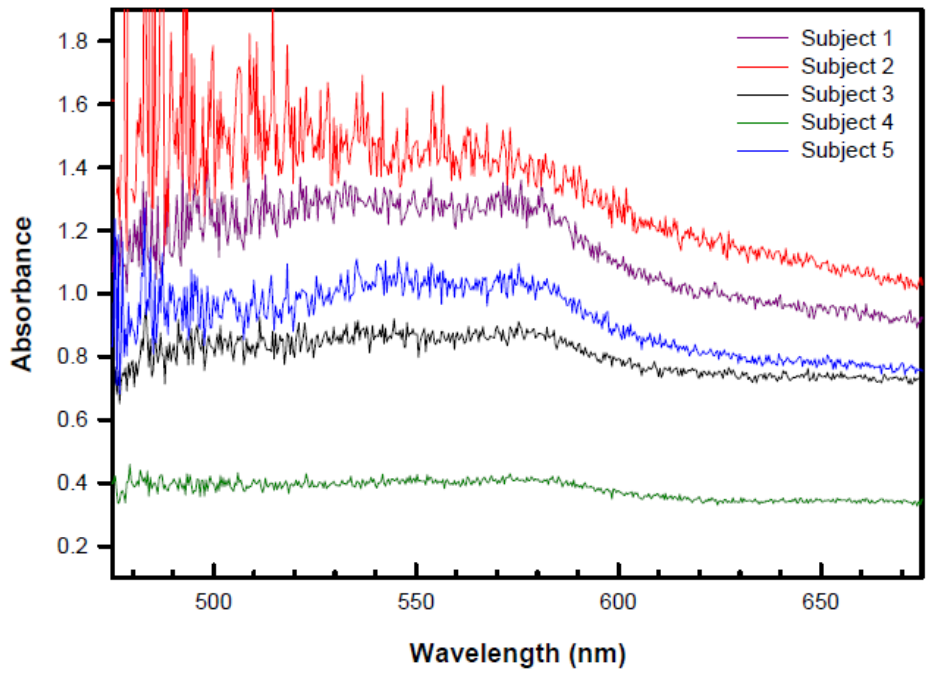

Figure 2.22: Absorbance spectra from the optic disc of 5 volunteer healthy eyes

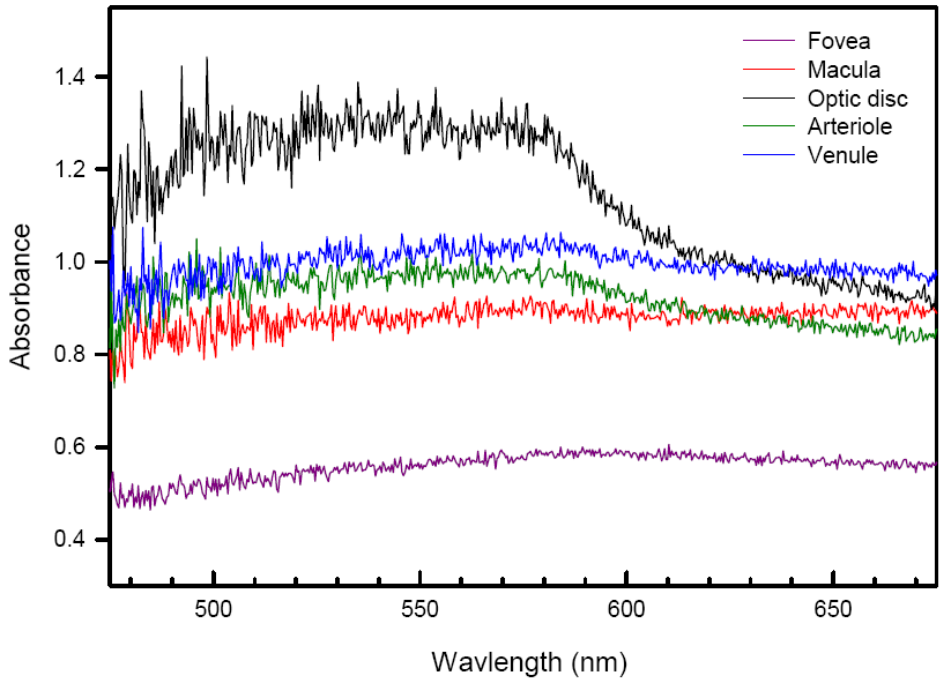

Figure 2.23: Absorbance spectra from 5 different locations of the retina for the same subject

ratio, calculating the oxygen saturation value was not possible. The other requirements of the device however, such as blocking corneal reflections and imaging the retina, were successfully accomplished. The device was able to acquire retinal images and select specific target areas of the retina to measure the reflectance spectrum. The knowledge gained from the first version of the device will be used to develop an upgraded version in the near future.

CHAPTER 3 - MULTIPLE LINEAR REGRESSION IN OXIMETRY

In Chapter 2, preliminary retinal reflectance spectra acquired using the retinal oximetry device were presented. From the absorbance spectrum, a value of oxygen saturation was calculated using an oxy - deoxyhaemoglobin mixture model to describe the measured blood spectrum (see section 1.4 for details) using a multiple linear regression methodology. The fit was obtained using a least squares fitting approach. The multiple linear regression methodology was chosen due to the linear nature of the widely used blood absorbance model described in equation (1-9), because it is easy to use, well studied, and commonly used in the literature for calculating oximetry. There are a number of assumptions built into this regression analysis however and the ones important for this project will be discussed below. More specifically, in this chapter, we explore the covariance of the two haemoglobin extinction coefficient curves across the 500 to 1,000 nm range to identify regions which would produce stable fit parameters in the Beer-Lambert model and assess the covariance of the regions to see if the correlation between the two curves could be a factor in the changes in oximetry seen in our data and discussed in future chapters.

3.1 Introduction to Multiple Linear Regression

Multiple regression analyses are some of the most widely used tools in statistics [136]. They are used to determine if the behavior of a dependent variable Y can be explained in terms of k independent variables (the predictors) $X_1, \ldots, X_k$. In the case

where a linear relationship can be found between Y and the predictor variables X_1, …, X_k, multiple regression analysis is referred to as multiple linear regression and takes the form:

(3-1) $\hat{Y} = \alpha + \beta_1 X_1 + ... + \beta_k X_k$ [136]

where $\hat{Y}$ is the expected value of Y, α is the intercept (a constant term) and the β_i are the regression coefficients [136]. In other words, Y is equal to a linear function of the X_i, plus an error term whose expectation is zero:

(3-2) $Y = \alpha + \beta_1 X_1 + ... + \beta_k X_k + \varepsilon$

with $\varepsilon = \hat{Y} - Y$ and the predicted error, $\hat{\varepsilon} = 0$ if the model is perfect [136]. The intercept α and coefficients β_i are usually found by a least squares fit. Given a set of $i = 1,\ldots, n$ data points, the least squares fit of the regression equation chooses a, $b_1,\ldots, b_k$ to minimize

(3-3) $\sum_{i=1}^{n}\left(Y_i - \hat{Y}_i\right)^2$ [136]

where $\hat{Y}_i = a + b_1 X_{i1} + ... + b_k X_{ik}$, $\hat{Y}_i$ being the predicted value of Y for the data point i. The b_i are the sample regression coefficients for data point i, a is the sample intercept for

data point i and the difference $Y_i - \hat{Y}_i$ is the residual for data point i [136]. The least squares fit determines the values of α and β_i that minimizes the sum of the squares of the residuals for all data points in the set ($i = 1,\ldots,n$).

There are a number of assumptions that are made in the multiple linear regression models. The assumptions that are important to the calculation of oxygen saturation of blood are described in this section. First, the multiple regression model assumes that a dependent variable Y for a single data point i can be written in terms of independent variables $X_{i1},\ldots, Xi_k$ as

(3-4) $$Y_i = \alpha + \beta_1 X_{i1} + ... + \beta_k Xi_k + \varepsilon_i$$

where the error terms ε_i for the n data points are statistically independent from each other and are normally distributed with mean of 0 and variance σ^2. This means that in order for the values of α and β_i to be interpreted correctly, there can be no systematic error in the regression model, all errors should be random. In the case of the blood absorbance modeled as

(3-5) $$A_{blood}(\lambda) = a\varepsilon_{O_2Hb}(\lambda) + b\varepsilon_{HHb}(\lambda) + c + \varepsilon(\lambda),$$

in order for the values of a and b to be reliable, the extinction coefficients of O_2Hb and HHb must be the only independent variables contributing to the absorbance A_{blood}. Any other contributing variables that are excluded in the model can result in systematic errors across all data points and yield values of a and b that incorrectly estimate the value of

oxygen saturation of blood. In other words, $\varepsilon(\lambda)$ should have a mean of zero and a normal distribution. The constant c in this equation represents an offset in the data and doesn't affect the values of a and b. This is important in light of the findings in the next two chapters which show systematic deviations from the pure absorbance model in whole blood samples.

Another important assumption built into any multiple linear regression model is that the independent variables are linearly independent from each other (any one independent variable cannot be reproduced as the sum of any other two or more independent variables). If two variables x and y are closely related (collinearity), it is difficult to estimate accurately their independent regression coefficients [136]. When the two variables x and y vary jointly, there is said to be covariance between them. There is positive covariance between two variables if when one variable increases so does the other. Oppositely, there is negative covariance between two variables if while one variable increases the other decreases. The sample covariance, s_{xy}, from a set of data points $i = 1,\ldots,n$ is defined as

$$(3\text{-}6)\quad s_{xy} = \sum_i \frac{(x_i - \bar{x})(y_i - \bar{y})}{(n-1)} \quad [136]$$

where $\bar{x}$ and $\bar{y}$ are the mean values of x and y respectively. The value of the covariance is difficult to interpret because it is composed of two parts; the variability of the individual variables as well as their linear association [136]. The measure of the degree of linear association between two variables is often measured by their correlation. There exists a correlation between two variables when the two variables vary together. The

degree of correlation, in other words the strength of the linear relationship between two variables, can be measured by a value *r* called the sample Pearson Product moment correlation coefficient:

$$(3\text{-}7)\quad r = \frac{\Sigma(x_i - \bar{x})(y_i - \bar{y})}{\sqrt{\Sigma(x_i - \bar{x})^2 \Sigma(y_i - \bar{y})^2}} \quad [136]$$

where x_i and y_i are measured data points for the variables *x* and *y* respectively, $\bar{x}$ and $\bar{y}$ are the mean values of *x* and *y* over the measured range and *r* is the called the coefficient of correlation. The value of *r* varies between -1 and 1, and measures the extent of linear association between the 2 variables [136]. From equations (3-6) and (3-7), we can see that the correlation coefficient is equal to the covariance of the two variables (s_{xy}) divided by the product of their standard deviations (s_x & s_y).

$$(3\text{-}8)\quad r = \frac{s_{xy}}{s_x s_y} \quad [136]$$

The correlation coefficient and the covariance are tools that we will use to determine possible impact of limiting ourselves to the proposed absorbance model when extracting oximetry from whole blood. Ideally, the wavelength range chosen to perform the MLR should have little to no covariance between the O_2Hb and *HHb* extinction coefficients i.e. the correlation coefficient between them should be small, so that any variance seen is a result of deviations from the absorbance model.

3.2 Correlation of the *O_2Hb* and *HHb* Extinction Coefficients

As previously discussed, for the multiple linear regression analysis to be useful in the Beer-Lambert absorbance model of determining the oxygen saturation of a blood sample, the *O_2Hb* and *HHb* extinction coefficients as a function of wavelength must not be highly correlated. We saw in the previous section that the correlation coefficient can be used to determine the extent of linear association between two variables. It should then be possible to calculate the coefficient of correlation between the *O_2Hb* and *HHb* extinction coefficients to measure the extent of their correlation. This poses a problem however because a closer look at equation (3-7) shows that the correlation coefficient depends on the range of data chosen for analysis. Equation (3-5) applied to the haemoglobin extinction coefficients can be written as

$$(3\text{-}9)\quad r = \frac{\sum\left(\varepsilon_{iO_2Hb} - \overline{\varepsilon_{O_2Hb}}\right)\left(\varepsilon_{iHHb} - \overline{\varepsilon_{HHb}}\right)}{\sqrt{\sum\left(\varepsilon_{iO_2Hb} - \overline{\varepsilon_{O_2Hb}}\right)^2 \sum\left(\varepsilon_{iHHb} - \overline{\varepsilon_{HHb}}\right)^2}}$$

where ε_{iO_2Hb} and ε_{iHHb} are the respective *O_2Hb* and *HHb* extinction coefficient values at data point *i* (i.e. at wavelength λ_i) and $\overline{\varepsilon_{O_2Hb}}$ and $\overline{\varepsilon_{HHb}}$ are the respective mean values of the *O_2Hb* and *HHb* extinction coefficients over the data range selected, $i = 1, \ldots, n$ (i.e. over the wavelength range $\lambda_1, \ldots, \lambda_n$).

There is an additional issue with applying the Pearson moment correlation coefficient calculation to the *O_2Hb* and *HHb* extinction coefficients. The Pearson moment correlation coefficient is only applicable to normally distributed data. When the data set

isn't normally distributed about the mean, the correlation between two variables is best described by the Spearman rank correlation coefficient given by

$$(3\text{-}10)\quad r_s = 1 - \frac{6\sum d_i^2}{n\left(n^2 - 1\right)} \quad [136]$$

where $d_i = x_i - y_i$ is the difference between ranks x_i and y_i of variables X_i and Y_i respectively for data point i. Since the O_2Hb and HHb extinction coefficients are not normally distributed (Shapiro-Wilk normality test), the Spearman rank correlation coefficient will be used to measure the extent of association between the haemoglobin extinction coefficients. Similarly to the Pearson moment correlation coefficient, the Spearman rank correlation coefficient will also depend on the wavelength range chosen for analysis.

Since the wavelength range chosen for the MLR analysis could possibly affect the accuracy of the oximetry calculation depending on the correlation between the two haemoglobin curves over that range, we need a way of finding potentially good fitting wavelength ranges which will have minimal correlation between the O_2Hb and HHb extinction coefficient curves, or else we could be searching an infinite number of combinations. The covariance is related to the correlation between 2 variables and can also be used to quantify how the variables vary with each other. One way to calculate the variation of a variable is by taking its derivative. We thus propose that we can relate the derivatives of the variables to their covariance. If we take the derivative of the O_2Hb and HHb extinction coefficient curves as a function of wavelength, the sign of the derivative will indicate how the curve is varying as a function of wavelength. We can then relate the

sign of the two derivatives to the correlation of the two curves. Wavelength ranges where the derivatives of the O_2Hb and HHb extinction coefficient curves have the same sign will indicate a strong positive correlation and ranges with opposite derivatives signs will indicate strong negative correlation. To find a wavelength region with low correlation, we need to look for a wavelength range where part of the range has same sign derivatives for the two curves and the other part of the range has opposite sign derivatives to create a zero sum. To verify if this hypothesis is applicable to the O_2Hb and HHb extinction coefficient curves, the derivative of the O_2Hb and HHb curves were analyzed to look for ranges that match the correlation criteria describe above (figure 3.1).

From figure 3.1, we can see that the wavelength range between 500-620 nm has the largest variation with wavelength than any other region of the spectrum, which could indicate that it is the best region to use the MLR analysis to calculate oxygen saturation. In order to test if the derivative analogy will correspond to correlation, three wavelength ranges were chosen from figure 3.1 to attempt to find ranges with the three types of correlation: strong positive, strong negative and very weak to zero correlation (figures 3.2, 3.3 and 3.4).

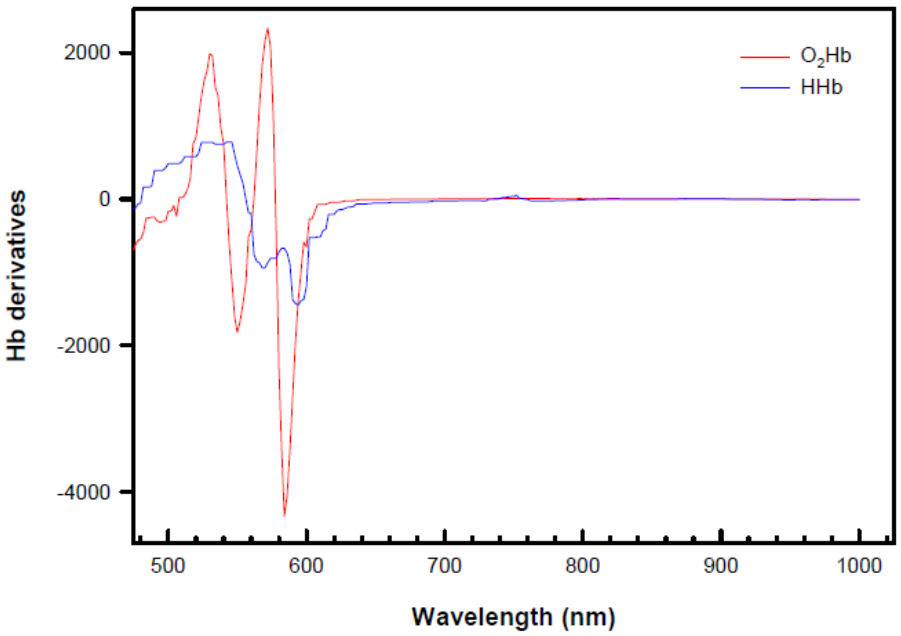

Figure 3.1: Wavelength dependence of the derivative of the *O_2Hb* and *HHb* extinction coefficient curves

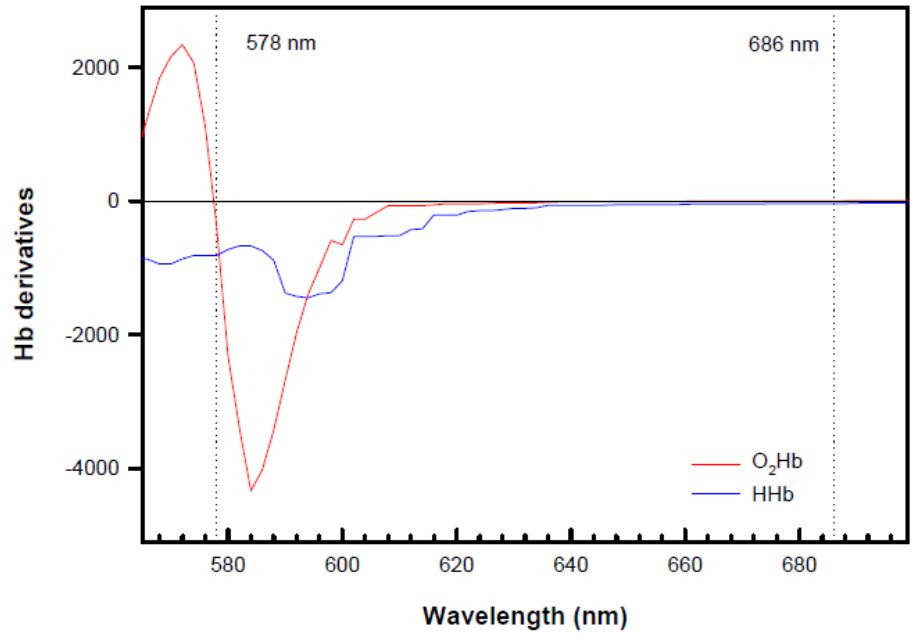

Figure 3.2: Wavelength range with same derivative signs between *O_2Hb* and *HHb* predicted to result in a strong positive correlation

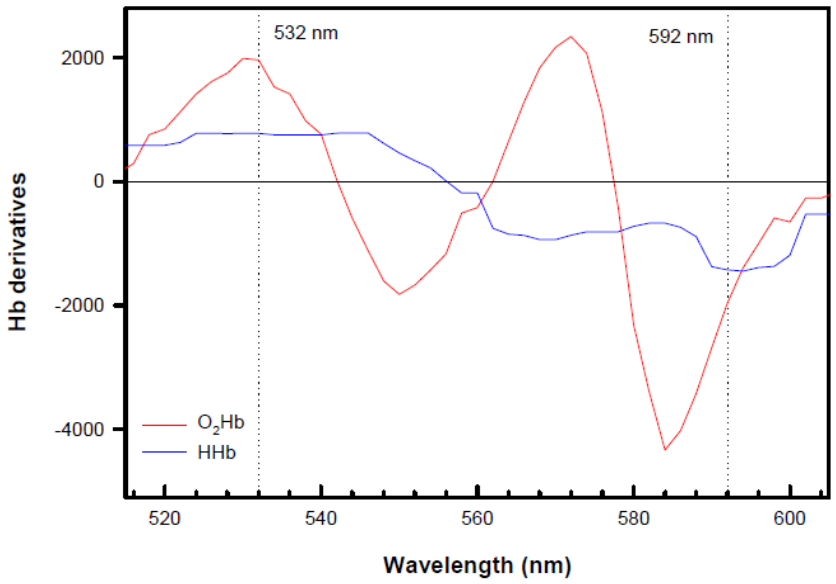

Figure 3.3: Wavelength range with mixed regions of same derivative signs and opposite derivative signs between *O_2Hb* and *HHb* predicted to result in a weak correlation

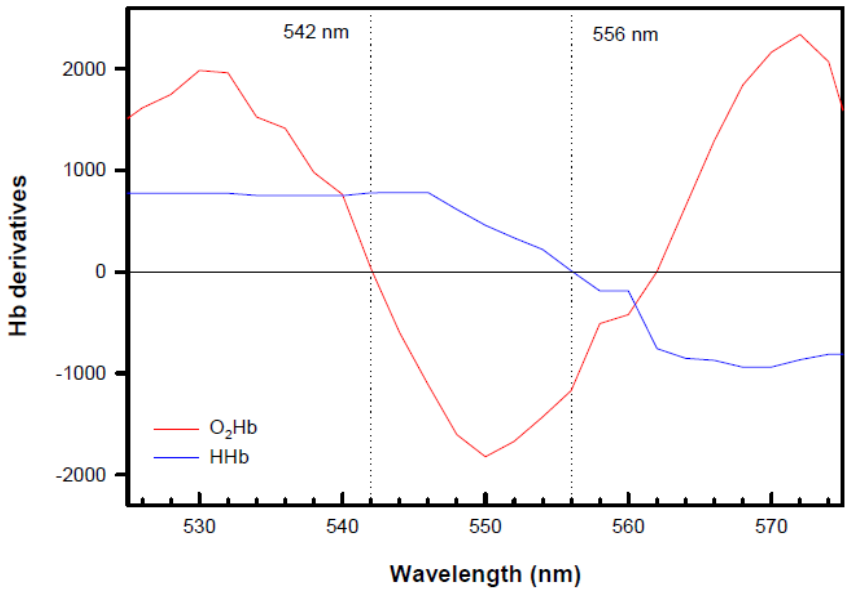

Figure 3.4: Wavelength range with opposite derivative signs between *O_2Hb* and *HHb* predicted to result in a strong negative correlation

Spearman rank correlation coefficients were calculated for the three wavelength ranges proposed in figures 3.2, 3.3 and 3.4 (table 3.1).

Wavelenth range (nm)	Spearman r_s	P value
542 - 556	-1.000	<0.05
532 - 592	-0.012	0.949
578 - 686	1.000	<0.05

Table 3.1: Comparison of Spearman rank correlation coefficients for different wavelength ranges

The results shown in table 3.1 confirm that the value of the correlation coefficient depends on the wavelength range chosen for analysis and that the covariance of the O_2Hb and *HHb* extinction coefficient curves can be related to their derivatives in this case. It is important to note however that this is not a proof for the general case between two variables, but that the result is applicable in this case. This brings up an interesting point to consider when applying a multiple linear regression approach to oximetry. Does the wavelength range chosen for analysis have an impact on the accuracy of the predicted oxygen saturation value? The impact of the wavelength range on oximetry will be investigated in the next section.

3.3 Experimental Results and Discussion

In the previous section, three wavelength ranges with different Spearman rank correlation coefficients were found from the theoretical curves for haemoglobin absorbance. Now we want to know what the impact of choosing wavelength regions with different correlation coefficients would be on oximetry using a MLR analysis on real data. The data from single pass measurements in 100 μm optical cells (described in Chapter 5) was refitted to obtain oxygen saturation using each of the three regions discussed above. The absorbance of the blood samples from the 10 subjects was calculated and a multiple linear regression analysis was used to calculate the oxygen saturation of each blood sample for each wavelength range previously proposed. The median R^2 values for each wavelength range were also calculated (table 3.2).

Wavelenth range (nm)	Median R^2	25%	75%
542 - 556	0.954	0.895	0.984
532 - 592	0.988	0.976	0.991
578 - 686	0.999	0.998	0.999

Table 3.2: Dependence of median R^2 value of oxygen saturation fits found by multiple linear regression on the fitted wavelength range

Median values of R^2 are shown instead of the mean because the data failed the normality test (Shapiro-Wilk) and a Kruskal-Wallis one way analysis of variance on ranks was performed for comparison of R^2 between groups. The 578-686 nm wavelength range had a median R^2 value statistically significantly greater ($p<0.05$, Tukey test) than

the other two wavelength ranges, while the difference between median R^2 values of the 542-556 nm and 532-592 nm wavelength ranges did not differ significantly.

To see if the wavelength range had an impact on oximetry, the SO_2 values were calculated for each sample and compared between ranges. Median SO_2 differences between ranges are presented in table 3.3

Wavelenth ranges	Median ΔSO_2	25%	75%
A-B	9.1%	4.7%	21.8%
A-C	8.7%	5.1%	20.8%
B-C	3.2%	1.3%	4.7%

Table 3.3: Median SO_2 differences between wavelength ranges. A = 542-556 nm, B = 532-592 nm and C = 578-686 nm.

Results show significant differences ($P<0.05$, Tukey test) in calculated SO_2 between wavelength ranges. It is interesting to note that the two wavelength ranges that had the least differences in calculated SO_2 values between them were the ones with the highest median R^2 values. This might suggest that high R^2 values can be a good predictor of calculated SO_2 values using this model. The relatively large variance in the data does not support this suggestion however. In one sample, R^2 values were above 0.99 in both the 542-556 nm and 578-686 nm wavelength ranges and the calculated SO_2 difference between the wavelength ranges was 25.4%.

In future Chapters 4 and 5, the wavelength range from 520-600 nm will be used for analysis to minimize the impact of the fitting model on the errors for oxygen

saturation calculations. To see how this wavelength range compares to the three ranges selected in this chapter, the difference between the calculated SO_2 value of the same blood sample for different wavelength ranges were calculated. Median values are presented in table 3.4.

Wavelenth ranges	Median ΔSO_2	25%	75%
A-D	7.9%	1.7%	22.3%
B-D	5.2%	3.9%	6.5%
C-D	8.6%	7.7%	9.2%

Table 3.4: Median SO_2 differences between wavelength ranges. A = 542-556 nm, B = 532-592 nm and C = 578-686 nm, D = 520-600 nm.

Significant differences in calculated SO_2 were found between the 520-600 nm range and the three ranges presented in this chapter. The Spearman rank correlation coefficient for the 520-600 nm range is 0.498 and therefore does not have significant correlation between *Hb* extinction coefficients (values greater than 0.7 are usually considered high correlation).

Without knowing the real values of oxygen saturation of the blood samples, it is difficult to conclude which wavelength range is more accurate at predicting SO_2 values using a multiple linear regression absorbance model. An attempt was made to compare calculated SO_2 values to CO-Oximetry results, but unavoidable (given our limited laboratory setup) exposure of our samples to air during the blood handling procedure prevented accurate comparison. However, there are a number of points that can be made. First, the results show conclusively that the predicted SO_2 value of a whole blood sample

using a multiple linear regression absorbance model depends on the wavelength range chosen for the fits. A systematic error in the model could be a possible explanation for the differences in calculated SO_2 values between ranges. The correlation between the O_2Hb and HHb extinction coefficients could also play a factor in the accuracy of calculated SO_2 values. The wavelength range of 532-592 nm was found to have no correlation between the O_2Hb and HHb extinction coefficients and this could be a potentially good wavelength region to use for oximetry, provided that there are no systematic errors in the absorbance model such as a scattering signal that is highly correlated to either of the O_2Hb and HHb extinction coefficients. Second, a high R^2 value does not guarantee an accurate oxygen saturation value if the wavelength range selected for analysis isn't appropriate. Some of the SO_2 fits had R^2 values above 0.99 in each of the wavelength ranges selected and still showed SO_2 differences of 25.4% between ranges. This is an important finding since numerous studies in the literature rely on the value of R^2 to determine the validity of their proposed model. This criterion can no longer be used in SO_2 calculations when using a multiple linear regression analysis. In a future study, calculated SO_2 values will be compared with SO_2 values determined by a CO-oximeter to attempt to isolate the impact of the wavelength range on the accuracy of calculated SO_2 values using a multiple linear regression approach.

CHAPTER 4 - QUANTITATIVE IMPACT OF SMALL ANGLE FORWARD SCATTER ON WHOLE BLOOD OXIMETRY USING A BEER-LAMBERT ABSORBANCE MODEL

Serge Emile LeBlanc

Monica Atanya

Kevin Burns

Rejean Munger

4.1 Abstract

It is well known that red blood cell scattering has an impact on whole blood oximetry as well as *in-vivo* retinal oxygen saturation measurements. The goal of this study was to quantify the impact of small angle forward scatter on whole blood oximetry for scattering angles found in retinal oximetry light paths. Transmittance spectra of whole blood were measured in two different experimental setups: one that included small angle scatter in the transmitted signal and one that measured the transmitted signal only, at absorbance path lengths of 25, 50, 100, 250 and 500 μm. Oxygen saturation was determined by multiple linear regression in the 520-600 nm wavelength range and compared between path lengths and experimental setups. Mean calculated oxygen saturation differences between setups were greater than 10% at every absorbance path length. The deviations to the Beer-Lambert absorbance model had different spectral dependences between experimental setups, with the highest deviations found in the 520-540 nm range when scatter was added to the transmitted signal. These results are consistent with other models of forward scatter that predict different spectral dependences of the red blood cell scattering cross section and haemoglobin extinction coefficients in this wavelength range.

Keywords: whole blood oximetry, blood spectroscopy, Beer-Lambert, blood absorbance, RBC scatter, forward scatter

4.2 Introduction

Non-invasive reliable *in-vivo* measurement of blood oxygen saturation has been a target of medical bioscience for years. An approach that has been discussed extensively because of its potential has been the measurement of retinal blood oxygen saturation. The retina is one of the most metabolically active tissues in the human body [48], consuming oxygen more rapidly than even the brain [49, 50] or kidney. Oxygen consumption has been linked to the pathogenesis and treatment of retinal diseases such as retinal vein occlusions [4, 5, 8, 9] as well as systemic diseases like diabetes (diabetic retinopathy) [20-23, 28, 29, 31, 32, 34, 35]. Consequently, an accurate, real-time, non-invasive *in-vivo* method of determining the oxygen saturation of retinal blood has high potential clinical value.

In clinical laboratories, optical techniques based on the optical properties of the haemoglobin molecule have been shown to be both reliable and accurate at measuring the oxygen saturation of blood samples [55]. These devices (CO-oximeters), now considered the clinical gold standard [55], rely on the differences in the absorption spectra (in the visible and near infrared, NIR) of haemoglobin's oxygen binding sites (heme sites) when they are empty or occupied. In these measurements, blood samples are lysed (break down of red blood cells) and an analysis of the absorption spectrum of the resulting haemoglobin solution is used to extract oxygen saturation using the Beer-Lambert law.

For *in-vivo* oximetry, where the oxygen saturation must be obtained from whole blood, the calculation of oxygen saturation becomes much more difficult. In whole blood, the haemoglobin molecules are contained inside red blood cells (RBC), whose substantial scattering cross section can be a significant contributor to the transmitted spectrum.

Because of its importance to the optical properties of whole blood and its possible impact on oxygen saturation measurements, RBC scattering has been well investigated [137-143]. The absorption cross section σ_a and the scattering cross section σ_s have been determined both theoretically and experimentally by a number of different groups [144-146]. Twersky (1970) [147] proposed equations for the absorption coefficient μ_a and scattering coefficient μ_s which were later verified experimentally by Steinke and Shepherd (1986) [123]. Phase functions for optically thin whole blood were also measured [146, 148, 149] and Hammer *et al.* (2001) [150] were able to determine the scattering phase function for blood with physiological haematocrit. An important result in these studies is that most of the RBC scatter occurs in the forward direction, with back scatter having a relative scattering power less than 2% of forward scatter. In addition, RBCs dominate over other blood components regarding absorption and scattering by two to three orders of magnitude [151].

In principle, the determination of retinal oximetry can be accomplished by measuring the reflectance spectrum from the ocular fundus. In addition to light that has been transmitted through retinal vessels once (single pass), the reflectance spectrum may contain light that has been scattered by RBCs, light reflected from the vessel wall and light that has undergone a double pass through a vessel before exiting the eye (figure 4.1).

Monte-Carlo simulations by Hammer *et al.* [128] predicted that for vessels smaller than 100 μm, most of the reflectance spectrum consists of light that has been back scattered from blood and light that has been transmitted through a vessel once and contributes forward-scatter. The reflectance spectrum thus contains light that has been

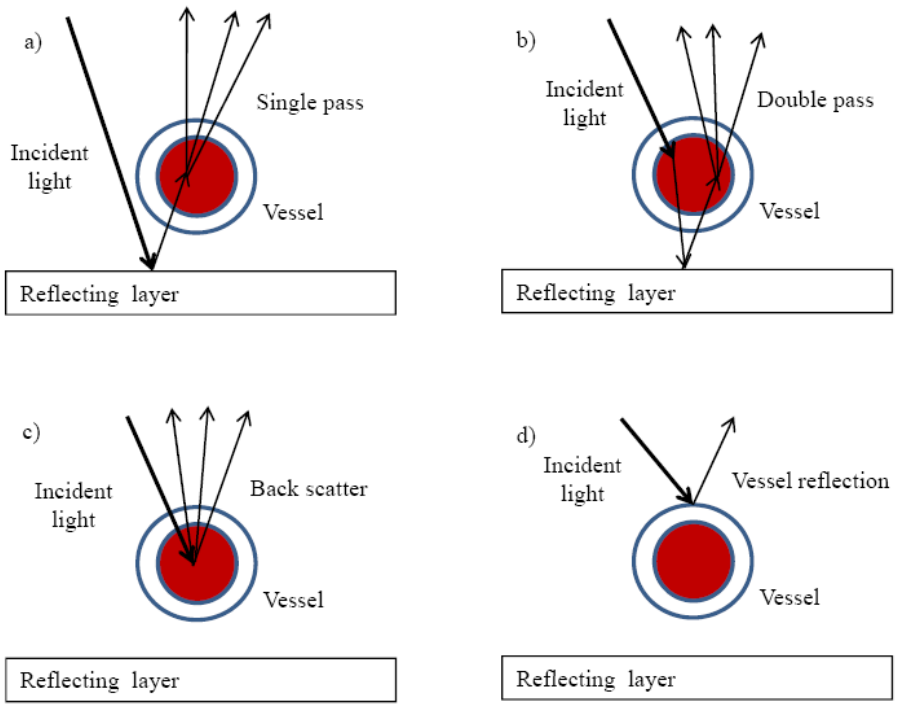

Figure 4.1: Possible pathways of light observed from a retinal vessel. Recreated from Hammer et *al.* [128]

transmitted through RBCs and forward scattered by RBCs. To be able to perform *in-vivo* oximetry of the retina, it is therefore critical to better understand the impact of forward scattered light on oximetry. The goal of the study presented in this paper was to experimentally quantify the impact of forward scattered light on whole blood oximetry in general and the retina specifically. Our approach was to investigate the transmitted spectrum of whole blood samples from healthy human volunteers for conditions where we control the amount of forward scattered light in the transmitted signals at absorbance path lengths of 25 to 500 μm, simulating different possible retinal vessel diameters. To better understand the impact of forward scatter on oxygen saturation calculations, deviations from the Beer-Lambert law are quantified and compared across absorbance

path lengths. Finally, calculated oxygen saturation values for the different optical configurations (controlling forward scatter contributions) are discussed.

4.3 Experimental

4.3.1 Subject Recruitment

Ten healthy volunteers (4 males, 6 females – median age 28, range 22 to 48 years) from a population of staff at the University of Ottawa Eye Institute were recruited for this study. The research protocol followed the tenets of the Declaration of Helsinki and all subjects provided informed written consent as per Ottawa Hospital Research Ethics Board (OHREB) requirements following an information session. The exclusion criteria for volunteers consisted of a recent or past history of systemic medical conditions which can affect blood composition (i.e. diabetes, anemia, leukemia, etc) , suspicion of active hepatitis B or C, or any other active infections as self reported by the subjects. The inclusion criteria consisted of individuals who self reported good health. Subjects were asked to fast at least 1 hour prior to blood draw, to abstain from alcoholic beverages at least 8 hours prior to the study and to perform no rigorous physical activities at least 1 hour prior to blood draw to ensure stable oxygen saturation at time of extraction so that the oxygen saturation measured in the sample was a good representation of the oxygen saturation in the blood at the location and time of extraction.

4.3.2 Blood Sample Acquisition and Preparation

For each subject, three venous blood samples of 1.5 ml each were drawn from the arm by a qualified phlebotomist in a blood gas syringe containing lithium heparin (7 units) as anti-coagulant. One of the blood samples was immediately placed on ice slurry and brought to the Visual Optics Laboratory of the University of Ottawa Eye Institute for blood spectroscopy analysis. Another sample was taken for clinical analysis to assure normal blood chemistry and the other was used for another study.

Whole blood from each subject was transferred to each of the 5 different size disposable optical cells made from UV transparent cyclo-olefin polymer (COP) films (SpecVette, Aline, Inc., Redondo Beach, CA) with absorbance path lengths of 25, 50, 100, 250 and 500 μm. Blood transfer was performed using a pipette (20 μL barrier tip) placed securely on the syringe containing the blood sample to match the entry port of the optical cells.

4.3.3 Measurement Apparatus and Procedure

The transmittance of the blood filled optical cells was measured under two different spectrometry setups: one that measures transmitted light by limiting the forward scatter collection angle to less than +/- 1 degree (this will be referred to as transmitted signal only), and one that intentionally measured transmitted plus scattered light over a 20 degree total angle. The transmitted light only system, an Olis-Cary 14 UV/Vis/NIR Spectrophotometer, is a scanning spectrophotometer that acquires the sample and reference spectra simultaneously resulting in a repeatability of 0.1% with a maximum signal to noise ratio of 10,000 and a 16 bit dynamic range. Spectra were obtained from

490 nm to 800 nm for each absorbance path length. A de-ionized (DI) water filled optical cell was placed in the reference path during data acquisition to account for reflections from the optical cell surfaces at sample cell interfaces, and the absorbance of water within the blood. The sample transmittance was calculated by dividing the sample path signal by the reference path signal. References were not adjusted for high absorbance path lengths to compensate for lower transmitted signal for reasons explained in the following section. All signals were corrected for background noise.

In order to measure the transmitted signal plus small angle scatter from the blood samples, an experimental setup was built with a collecting lens to capture small angle forward scatter (figure 4.2).

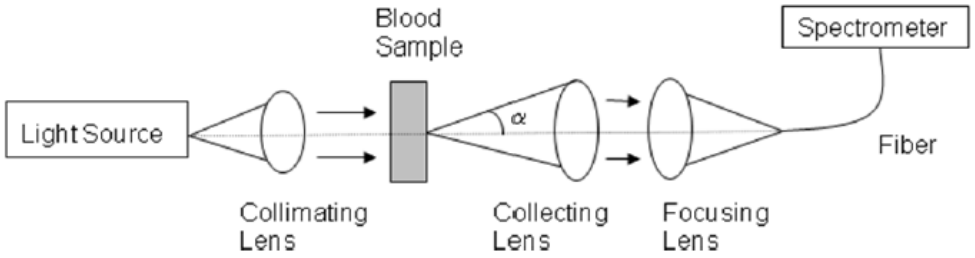

Figure 4.2: Schematic diagram of experimental setup collecting forward scatter

The experimental setup was designed to capture transmitted light through the blood samples plus light with forward scattering angles of +/- 10 degrees. An acceptance angle of 10 degrees was chosen firstly, because it has been shown experimentally that RBCs cause much of the scattering in the forward direction [138, 145] within that angular range. Therefore, an acceptance angle of 10 degrees will capture most of the scattered light by the blood samples. And secondly, for retinal oximetry, the exit pupil of the eye

will be the determinant factor in the angular size of the scattered signal exiting the eye and under average anatomical factors (an eye length of 24 mm and pupil size of 7 mm) the exit pupil acceptance angle is approximately 10 degrees.

The filled optical cells were placed in a sample holder in the experimental setup (figure 4.2) and illuminated with light from a current-stabilized 150 W tungsten-halogen lamp (Spectral Products, Inc., Putnam, CT). Spectra were obtained from 340 nm to 1022 nm using a SD2000 Ocean Optics (Dunedin, FL) spectrometer with a resolution of 8 nm, a maximum signal to noise ratio of 250 and a 12 bit dynamic range. Acquisition times ranged from 40 to 50 ms, depending on the RBC volume density in the blood, and were kept constant for all absorbance path lengths for the same sample to keep the maximum signal to noise ratio constant for each sample to better match the situation in the eye. Since retinal damage limits the amount of light that can be sent to the eye, once the light level is fixed and the spectrometer chosen, the maximum signal to noise ratio is a constant value for that instrument. Increasing the exposure time increases the noise level accordingly and the only way of increasing the signal to noise ratio is by upgrading the spectrometer.

Each blood sample was measured twice and the average spectrum was used for all subsequent analysis. The transmittance of whole blood was calculated by dividing the transmitted signal of the blood sample (all signals corrected for background noise) by the transmitted signal of an optical cell filled with DI water used as a reference as in the transmitted light only setup. All blood samples were measured at room temperature within 1 hour of extraction. Spectral data were acquired while the optical cell stood undisturbed for a period of 10 seconds.

4.3.4 Model for the Determination of Oxygen Saturation

Whole blood oximetry was determined using a Beer-Lambert absorbance model where absorbance is calculated from the transmitted light measurements. The absorbance of whole blood was modeled as a combination of the absorbance of oxyhaemoglobin (O_2Hb) and deoxyhaemoglobin (HHb):

(4.1) $$A_{blood}(\lambda) = a \cdot \varepsilon_{O_2Hb}(\lambda) + b \cdot \varepsilon_{HHb}(\lambda) + K$$

where A_{blood} is the absorbance of the blood sample, $\varepsilon_{O_2Hb}(\lambda)$ are the extinction coefficients of oxyhaemoglobin, $\varepsilon_{O_2Hb}(\lambda)$ are the extinction coefficients for deoxyhaemoglobin, a & b and K are fitting parameters. The fitting parameters are determined by a multiple linear regression over the wavelength range 520 to 600 nm with the blood absorbance as the dependent variable and the haemoglobin extinction coefficients as the independent variables. The wavelength range was chosen to A) match the optimal operating ranges of the light source, the Ocean Optics spectrometer and the Olis system and, B) to use a region rich in feature differences between the O_2Hb and HHb extinction coefficients spectra to ensure good separation between the contributions of the two signals. The choice of fitting range has also been validated in the literature to calculate retinal oxygen saturation [89, 91]. The oxygen saturation (SO_2) of the blood sample can then be determined by:

(4.2) $$SO_2 = \frac{a}{a+b}$$

The two haemoglobin extinction coefficient curves used were taken from the widely used Prahl data [68]. To match the Ocean Optics 8 nm resolution, a running average of 8 nm was applied to the haemoglobin extinction coefficient data from Prahl which is presented in 2 nm steps. This was not necessary for the fitting the OLIS data which had the same sampling rate as the Prahl data.

4.4 Results and Discussion

4.4.1 Blood Spectroscopy

Transmittance spectra of blood from 10 human volunteers were obtained with both experimental setups for absorbance path lengths of 25, 50, 100, 250 and 500 μm. The absorbance of each sample was then calculated from the transmittance (figure 4.3).

Figure 4.3, a representative set of data for one subject, illustrates clearly that the transmittance of the blood samples was measurably higher when a +/- 10 degree angle of scatter was accepted in the transmitted signal (Ocean Optics setup). All subjects followed the same trend as figure 4.3. Keeping exposure times constant with absorbance path length resulted in low signal to noise ratios for larger sample thicknesses, and neither experimental setups obtained reliable signals for the 500 μm absorbance path length and thus this data was not included in follow up analysis. Based on the Beer-Lambert model of absorbance only, it would be expected that the transmitted signal from the 250 μm absorbance path length be less than 1 % that of the 25 μm absorbance path length. This is below the signal detection capability of the Ocean Optics setup. However, reliable signals

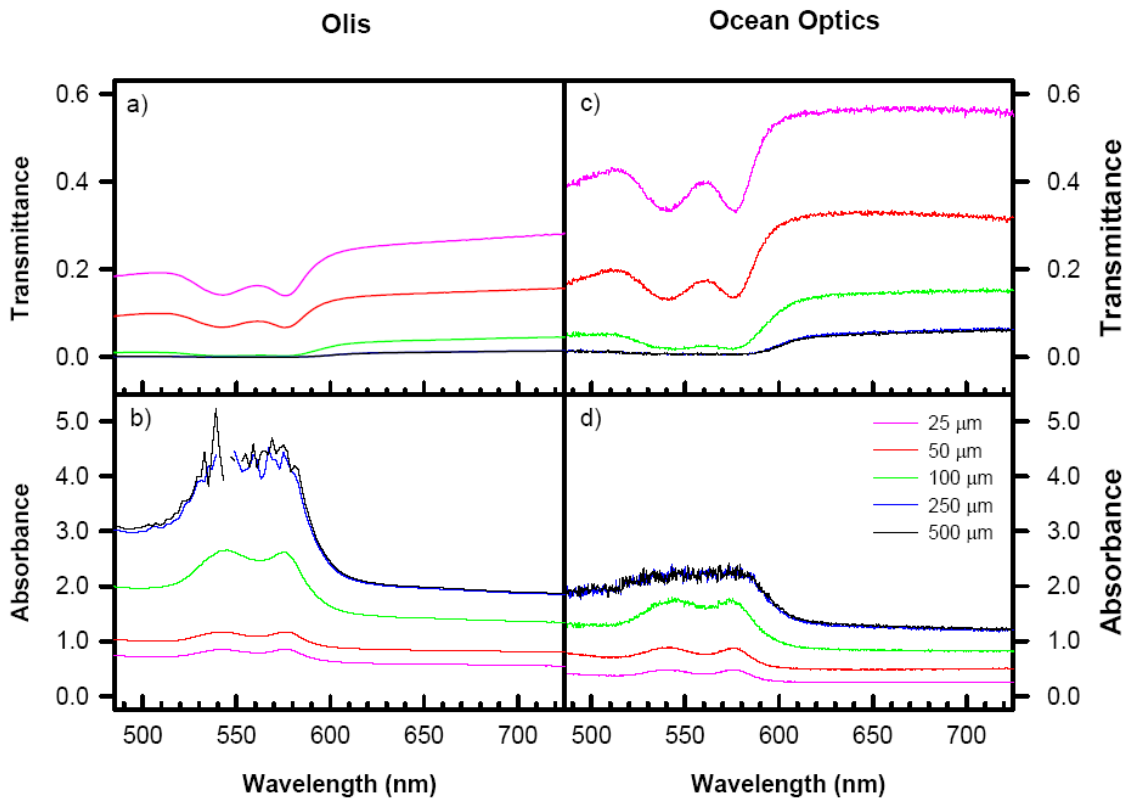

Figure 4.3: Dependence of transmittance and absorbance of blood on absorbance path length between experimental setups (illustrative example for one subject): a) & b) are for the transmitted signal (OLIS) and figures c) & d) are for the transmitted signal plus small angle scatter (Ocean Optics).

were obtained at the 250 µm absorbance path length due to the significant forward scatter added to the transmitted signal.

The difference in absorbance between the two experimental setups increased with absorbance path length (figure 4.3). To quantify the difference, the mean and standard deviation of the absorbance between 556 and 564 nm were calculated for each sample. The mean differences between experimental setups across the 10 subjects were statistically significant ($P<0.05$, Holm-Sidak method for 25 & 50 µm and Dunn's method for 100 & 250 µm) and are presented in figure 4.4.

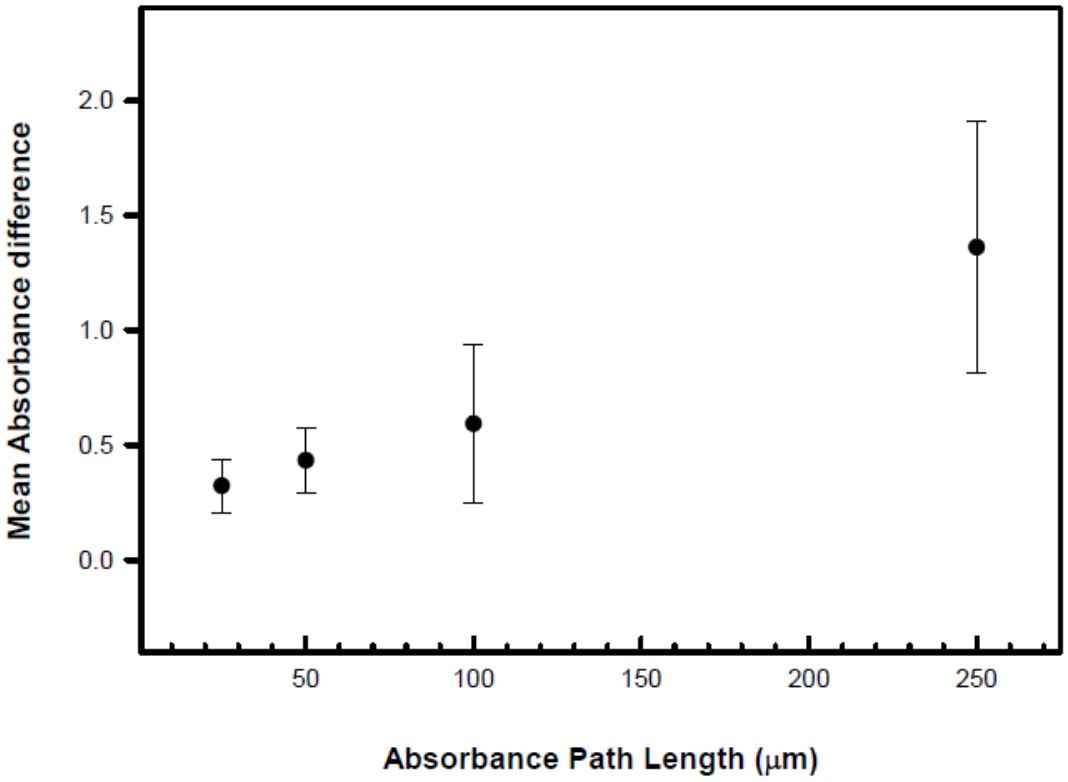

Figure 4.4: Dependence of mean absorbance (556-564 nm) difference and standard deviation between experimental setups with absorbance path length.

The mean absorbance difference between the Olis and Ocean Optics experimental setups increased with absorbance path length as expected for increased forward scatter.

4.4.2 Deviations from Beer-Lambert Model and Impact on Oximetry

The Beer-Lambert law, which is used to calculate oxygen saturation, holds only for non-scattering solutions, which is clearly not the case in whole blood. To assess the impact of scatter, the deviations from the Beer-Lambert law for each of the experimental setups were examined. The Beer-Lambert law predicts a linear dependence between

absorbance and absorbance path length. The mean absorbance of the blood samples in the 556-564 nm range (figure 4.5), for either setup, did not increase linearly with absorbance path length. The deviations from the Beer-Lambert law increased with increasing path length which is consistent with the scatter signal being increasingly important in the transmitted signal.

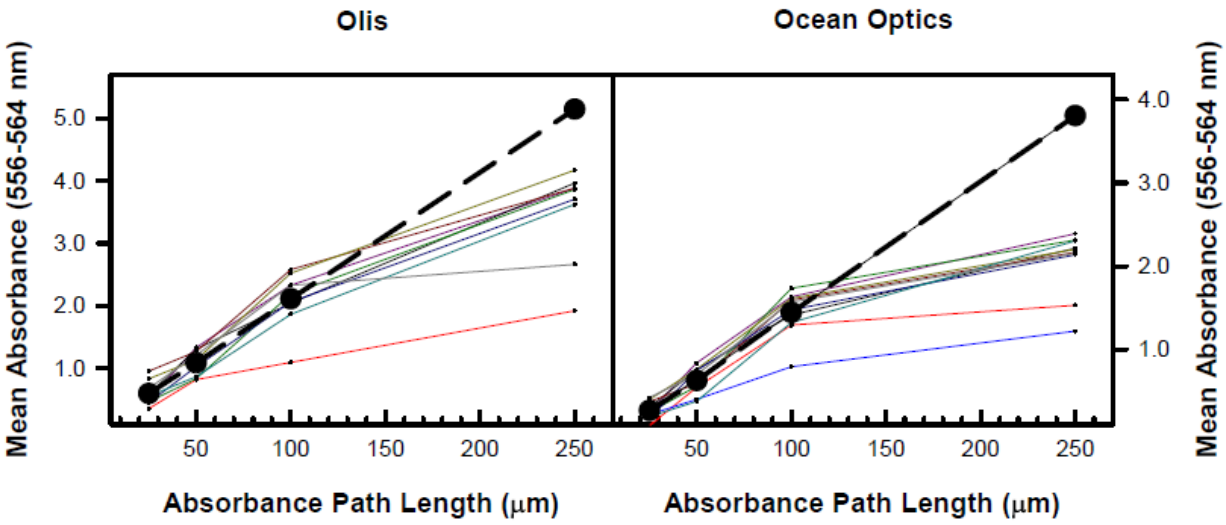

Figure 4.5: Comparison of Beer-Lambert law deviations between experimental setups. Cross points and solid lines represent measured data points for each subject. Large circles and dashed lines show mean of 25, 50 and 100 μm values. Extrapolated value calculated for 250 μm based on Beer-Lambert model.

In order to quantify the impact of small angle scattering on oximetry, the oxygen saturation values of each blood sample were calculated using the fitting parameters as per equation 4.2. Both oxygen saturation values and coefficients of determination (R^2) where obtained for each experimental setup and absorbance path length. Differences in calculated oxygen saturation between experimental setups for each blood sample were calculated (figure 4.6).

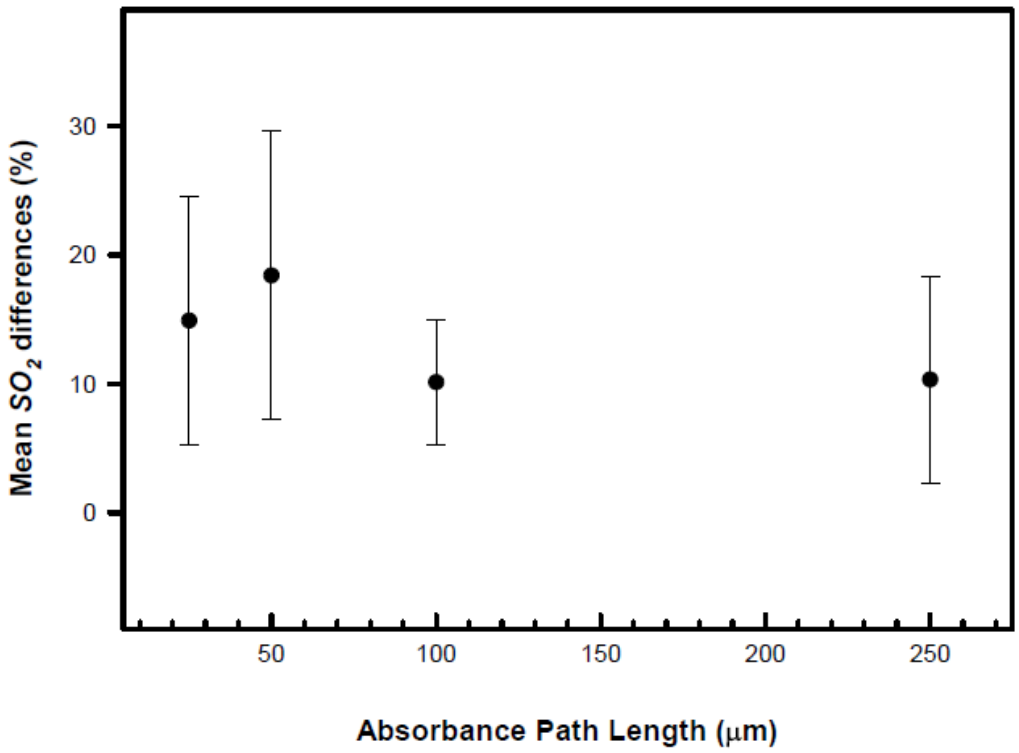

Figure 4.6: Mean calculated oxygen saturation difference between experimental setups and standard deviations for the 10 subjects.

Mean oxygen saturation differences between experimental setups for the 10 subjects are presented in figure 4.6 and the mean R^2 for the Beer-Lambert model fits are presented in figure 4.7. Mean differences were greater than 10% for every absorbance path length, with differences in predicted oxygen saturation exceeding 30% in 2 of the test samples in the 25 and 50 μm absorbance path lengths. The differences in mean oxygen saturation across absorbance path lengths are not statistically significant however (one way ANOVA, P=0.119).

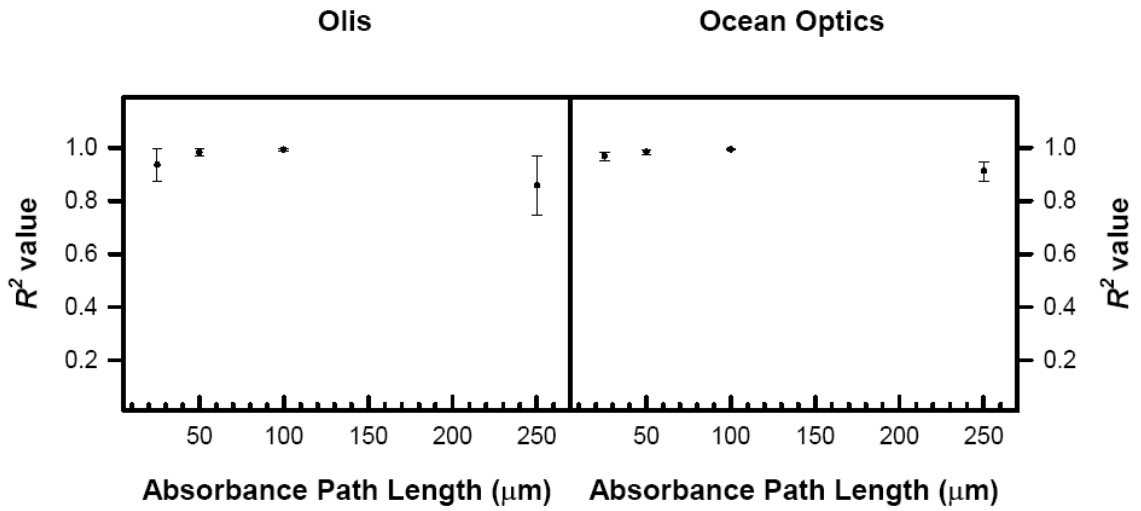

Figure 4.7: Dependence of R^2 value on absorbance path length

The difference in oxygen saturation values between optical setups shows that the added scatter in the signal influences the ability to extract accurate oxygen saturation values. This comes as no surprise since it is well known that RBC scattering has an impact on whole blood oximetry. An unexpected result however was that the mean R^2 values were the same between experimental setups. Since the Ocean Optics setup included scatter in the transmitted signal, the scatter was expected to increase the deviations from the Beer-Lambert model and result in lower R^2 values. This was not the case however. Even though the scattering resulted in a calculated oxygen saturation difference between experimental setups, it did not affect the R^2 value. The difference in the mean R^2 values of the oximetry fits between experimental setups were not statistically significant for any absorbance path length. In order to get a deeper understanding of the difference in the oximetry fits between experimental setups, error analysis was performed on the multiple linear regression model.

The R^2 value is a widely accepted means of measuring the quality of fit in oximetry but it can be misleading as an indicator of the confidence of the SO_2 values, as it cannot indicate if there are small but systematic errors in the fit which occurs when the model does not account for all effects in the data. In order to look more closely at deviations of the measured data from the oxy-deoxyhaemoglobin absorbance model, the difference between the measured spectra and the best fit absorbance model were calculated for each subject at each absorbance path length as a function of wavelength for both experimental setups (figure 4.8). The Beer-Lambert law deviations were calculated as the measured minus the predicted absorbance between the 520 nm to 600 nm range used in the oximetry calculation. The deviations are then normalized by dividing by the mean absorbance of each curve to allow for comparisons in patterns without affecting the fit quality and oximetry values.

The Beer-Lambert law deviations were consistent across subjects for every path length in both experimental setups. Low signals in the 250 μm absorbance path length resulted in larger deviations than the other path lengths in both the Olis and Ocean Optics setup. When comparing between experimental setups, the normalized Beer-Lambert law deviations were lower when less scatter was included in the transmitted signal. Furthermore, model deviations also had a different spectral dependence between experimental setups. The signals from the Ocean Optics setup had the highest deviations in the 520-540 nm region, while the Olis setup signals had Beer-Lambert model deviation

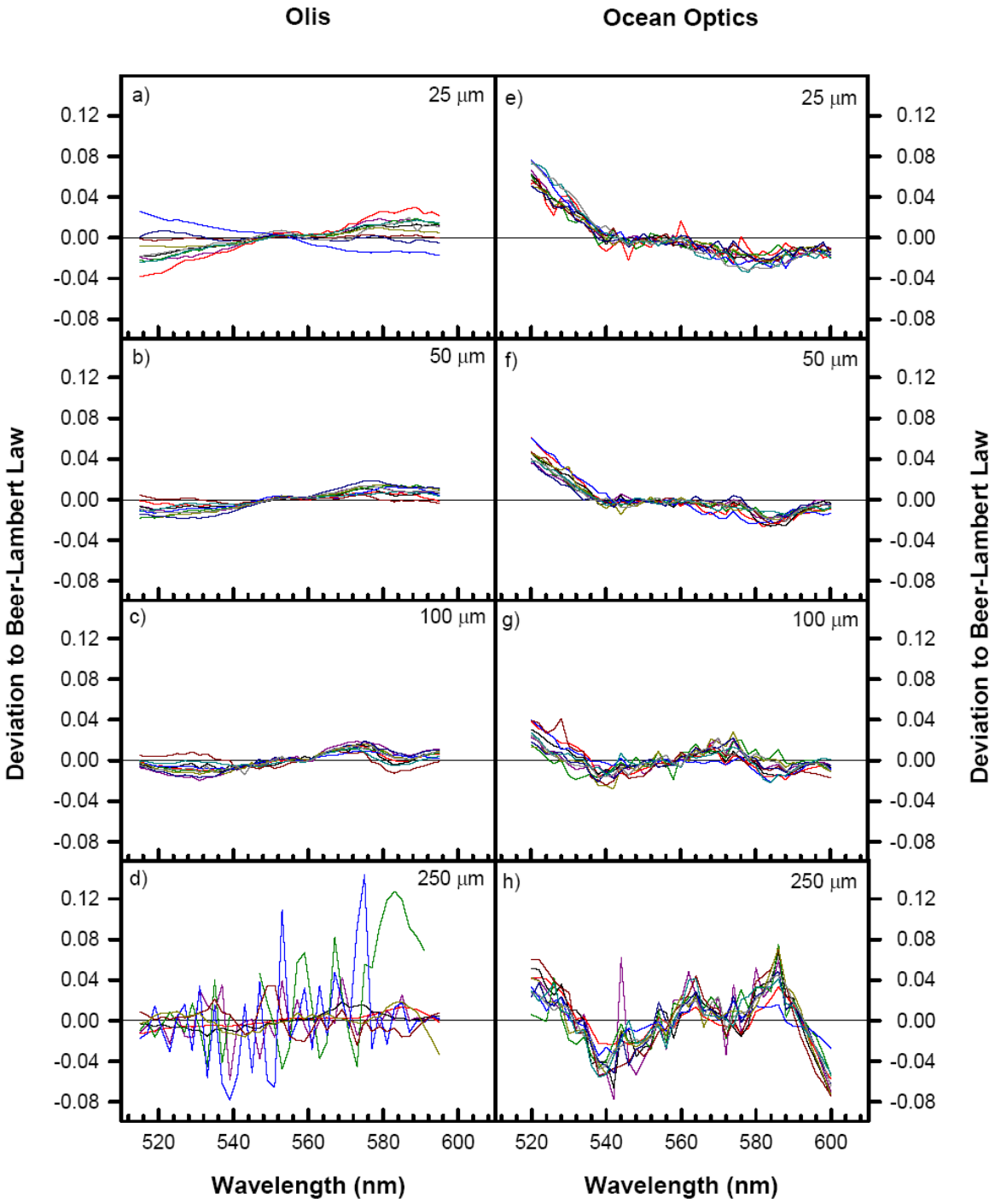

Figure 4.8: Comparison of Beer-Lambert law deviations of 10 subjects between experimental setups for different absorbance path lengths. The Beer-Lambert law deviations were calculated as a function of wavelength by taking the measured absorbance minus the predicted model absorbance and dividing by the mean of the

absorbance across the wavelength range of 520 nm to 600 nm. Figure 4.8 d) had 3 curves removed as outliers due to low signal to noise ratios.

profiles that were mostly flat in that range. This could be explained if the scattering cross section of RBCs was large in the same wavelength range. Whereas the extinction coefficients of both O_2Hb and HHb increase from 500 nm to 540 nm, Mie theory modeling performed by Faber *et al.* [152] found that the RBC scattering cross section has a maxima around 500 nm and decreases steadily with wavelength. This explains why the deviations are large in the 520-540 nm range when significant scatter is included in the transmitted signal and are smaller when less scattered signal is considered.

In conclusion we have shown that inclusion of forward scatter in whole blood transmittance measurement can result in a calculated mean SO_2 difference of 10% or more using a Beer-Lambert absorbance model for absorbance path lengths ranging from 25 to 250 μm. The mean SO_2 difference between experimental setups did not differ significantly between absorbance path lengths. We have shown that the deviations to the Beer-Lambert law are consistent with models of forward scatter which predict a different spectral dependence between RBC scattering and haemoglobin extinction coefficients. These deviations had little effect on the R^2 values however, with mean R^2 values of 0.94 and higher found for absorbance path lengths of 100 μm and below in both experimental setups.

4.5 Acknowledgements

The authors are thankful to all the people who helped in the realisation of these experiments. The authors would especially like to thank Gail Kayuk for performing the blood draws, and Dr. Mélanie Lalonde for her help with ethics approval.

CHAPTER 5 - WAVELENGTH DEPENDENCE OF DEVIATIONS TO THE BEER-LAMBERT MODEL FOR DIFFERENT LIGHT PATHS IN RETINAL OXIMETRY

Serge Emile LeBlanc

Rejean Munger

5.1 Abstract

The ability to measure *in vivo* retinal vessel oxygen saturation accurately and non-invasively has high potential clinical value. The Beer-Lambert law has proved useful for oximetry of haemoglobin solutions, but red blood cell scattering causes deviations to the law that result in errors to the oxygen saturation value. The goal of this study was to determine the spectral dependence of the deviations to Beer-Lambert absorbance model for different light paths involved in retinal oximetry. Transmittance spectra of whole blood were measured in single and double pass configurations that matched light paths in the eye with absorbance path lengths of 25, 50, and 100 μm. Oxygen saturation was determined by multiple linear regression in the 520-600 nm range and compared between path lengths and single and double pass configurations. Median oxygen saturation differences of 3.8% or more were found between single and double pass configurations at every absorbance path length. Deviations to the Beer-Lambert law varied with wavelength and spectra were different between configurations. Principal Component Analysis (PCA) performed on the deviations showed that 95% of the variations in the data can be accounted for by 3 principal components. Common mechanisms that cause deviations to the Beer-Lambert absorbance model were found between the single and double pass configurations.

Keywords: retinal oximetry, whole blood oximetry, blood spectroscopy, Beer-Lambert, light paths

5.2 Introduction

The ability to accurately measure retinal oxygen saturation *in-vivo* has high potential clinical value. The most promising non-invasive method of achieving this is an optical technique similar to that employed by the gold standard CO-oximeters used in laboratories around the world. These instruments measure the absorbance spectrum of a haemoglobin solution (extracted from the red blood cells, RBC) and use the dependence of the absorption spectra (in the visible and near infrared, NIR) of the solution on the number of occupied oxygen biding sites to quantify the oxygen content of blood by means of the Beer-Lambert law [55]. Complications arise however when attempting to use the Beer-Lambert law to calculate oximetry from whole blood, where the haemoglobin is located inside red blood cells which are known to be strong light scatter sites which are not accounted for by the Beer-Lambert law and therefore can affect the accuracy of oxygen saturation calculation using this simple absorbance model [64, 108, 123, 153].

In principle, it should be possible to calculate the oxygen saturation of retinal blood from the reflectance spectrum of the ocular fundus (the back of the eye). The retina contains superficial vessels and a vast network of surface capillaries which can be viewed through the eye's highly transparent optical elements (figure 5.1), the lens and cornea.

In addition to haemoglobin absorption and RBC scattering, the ocular reflectance spectrum is affected by the optical properties of the different tissues within the eye i.e. the ocular media, the retinal pigment epithelium (RPE), the sclera, melanin, photoreceptors, etc. Previous studies have been dedicated to measuring the optical properties of these ocular tissues [116, 117, 121]. Furthermore, studies have focussed on

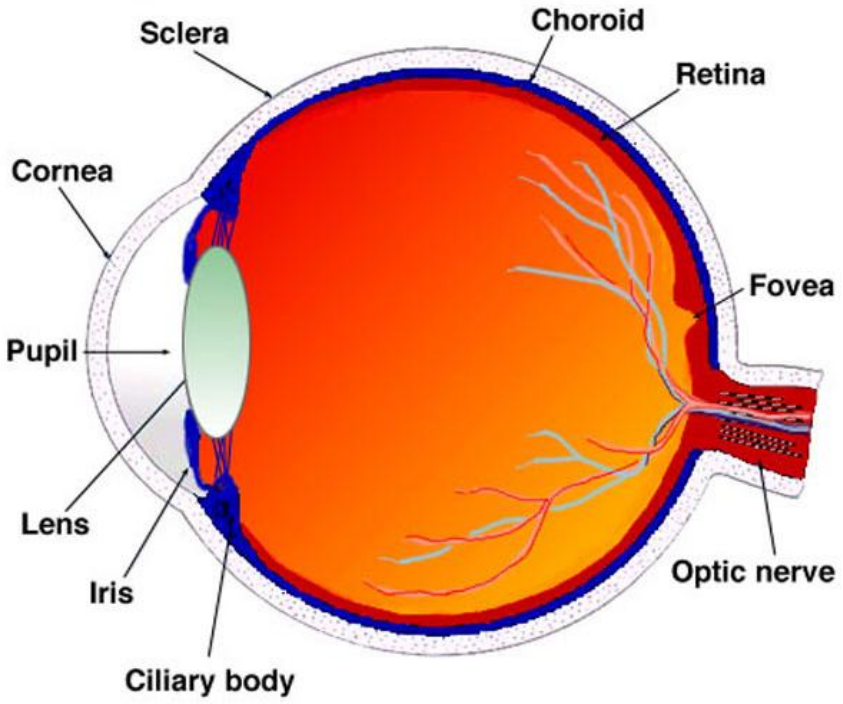

Figure 5.1: Diagram of the human eye (http://webvision.med.utah.edu) [70]

superficial vessels because their reflectance is dominated by the optical properties of the blood within and on the surface of the vessel. The optical properties of the capillary network are expected to be more difficult to extract because it is imbedded within the retinal tissues.

A complication of retinal vessel oximetry has been understanding the different light paths involved in retinal oximetry [122, 124-126]. Light observed from a retinal vessel can have come from any of 4 different light paths (figure 5.2) and there is still a debate in the literature as to the contribution of each path to the signal measured in fundus reflectance. Monte-Carlo simulations by Hammer *et al*. [128] suggest that most of the signal is from either light that has backscattered from a RBC or that went through a

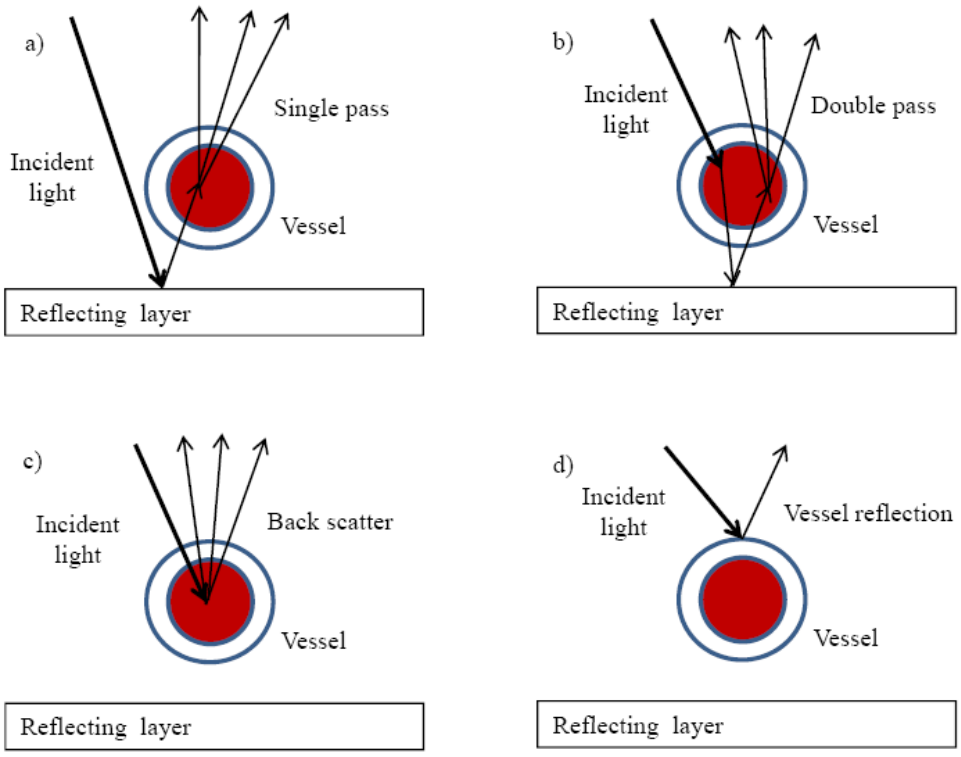

Figure 5.2: Possible pathways of light through a retinal vessel before exiting the eye. The vessels lie on the surface of the retina. Figure recreated from Hammer et *al.* [128].

single pass through the blood vessel. However, double pass models have shown encouraging results to model the reflectance spectra [91].

The first optical technique proposed to calculate retinal oximetry was by Hickham *et al.* [69] in 1963 who used a two-wavelength (510 nm and 640 nm) photographic technique to calculate the oxygen saturation of a vessel crossing the optic disk using the ratios of absorbance at these two wavelengths. A recent study by Hammer *et al.* [100] used a fundus camera equipped with a special dual wavelength transmission filter and color CCD camera, and were able to calculate mean arterial and venous oxygen saturations with reproducibility of 2.52% and 3.25%. The challenge is that the accuracy of a two-wavelength oximetry technique will depend on the calibration. In fact, Hammer

et al. found a difference in the mean venous oxygeneation of 13% compared to a study by Hardarson *et al.* [79] using a similar technique with different calibration. Other studies have expanded the work of Hickham *et al.* to improve the accuracy and repeatability of retinal oximetry measurements using the ratios of fundus reflectance at multiple wavelengths [51, 71, 74-76, 78, 79] but none have resulted in accuracies acceptable for clinical applications.

A different retinal oximetry technique was proposed by Schweitzer *et al.* [89] using the simultaneous measurements at 76 different wavelengths with a spectrometer. The drawback of this technique is that the measurement is limited to the cross-section of one or two retinal vessels. The advantages of this technique however are that a larger number of wavelengths could improve accuracy, lower the requirement for the signal to noise ratio [71] and allows for error analysis as a function of wavelength. It's known that RBC scattering must be taken into account in retinal oximetry and RBC scattering has been well studied [137-143], but no one has yet quantified the impact of scatter in retinal oxymetry in terms of the different light paths involved.

The goal of this study was to investigate the impact of red blood cells on the absorbance spectrum of blood for single and doubles pass optical paths and quantify its impact on the calculation of oxygen saturation based on the Beer-Lambert law model. To focus on the optical properties of whole blood, *in vitro* whole blood spectroscopy measurements were performed using an eye model and an instrument similar to Schweitzer *et al.* [89]. Beer-Lambert model deviations were calculated and compared for a single pass and double pass configuration (figure 5.2) for 3 different absorbance path lengths representing different vessel diameters. Finally, Principal Component Analysis

(PCA) was applied to the Beer-Lambert model deviations to see if deviation patterns could be linked to specific retinal oximetry optical pathways. To our knowledge, this is the first time PCA has been used to gain insight on different retinal oximetry optical pathways.

5.3 Experimental

5.3.1 Subject Recruitment

The same volunteers as described in section 4.3.1 were recruited for this study under the same inclusion and exclusion criteria (see section 4.3.1 for details).

5.3.2 Blood Sample Acquisition and Preparation

Blood samples were drawn using the same protocol as described in section 4.3.2 (see description in section 4.3.2 for details).

5.3.3 Measurement Apparatus and Procedure

The experimental setup (figure 5.3) was designed to allow the measurement of both single and double pass blood absorption spectroscopy. The retina is simulated as a spectrally flat diffuse reflectance surface ($BaSO_4$) and a bi-convex lens was used to represent the cornea. A specially designed light delivery system (not in diagram for

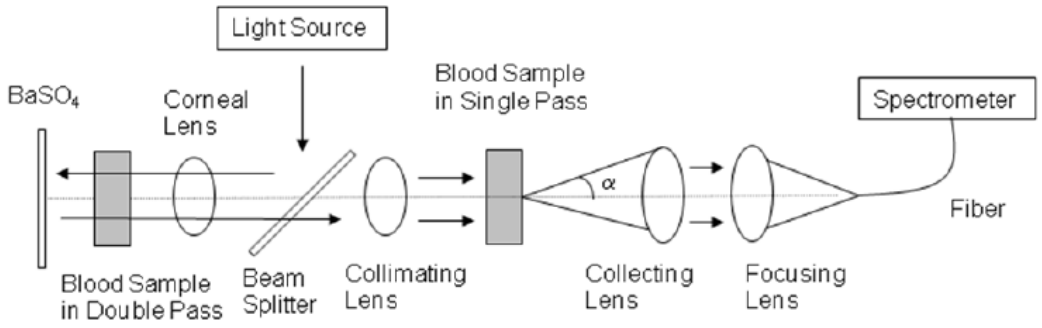

Figure 5.3: Schematic diagram of experimental setup allowing the measurement of the absorbance of blood in a single pass and double pass configuration

simplification, see section 2.3) was designed to use annular illumination with the eye and eliminate surface specular reflection from the corneal lens.

In the single pass configuration, the experimental setup was designed to capture transmitted light through the blood samples plus light with forward scattering angles of +/- 10 degrees (figure 5.3). An acceptance angle of 10 degrees was chosen for reasons explained in section 4.3.3.

In the double pass configuration, the blood sample is placed between a lens and a diffuse reflective surface ($BaSO_4$) to simulate a blood vessel on the retinal surface (figure 5.3), the lens representing the cornea and the reflective surface representing the retina. In this case, the transmitted signal is a combination of the double pass transmitted light and backward scattered light as well. The simulated corneal lens had an acceptance angle of 15 degrees for the light exiting the model eye.

The spectra of the blood filled optical cells were analyzed with the Ocean Optics spectrometer described in section 4.3.3. Acquisition times ranged from 40 to 150 ms, depending on the hematocrit level of the blood and on the configuration of the

measurement (single or double pass), and were kept constant for all absorbance path lengths for the same sample for reasons explained in section 4.3.3. The calibration procedure allowed corrections for the properties of the optical cell and optical cell holder in both single and double pass configurations.

5.3.4 Model for the Determination of Oxygen Saturation

The same model, fitting method and haemoglobin extinction coefficient source as in section 4.3.4 were used in the analysis of single and double pass blood spectra (see section 4.3.4 for details).

5.4 Results and Discussion

5.4.1 Blood Absorbance Spectra

Transmittance spectra of blood from 10 volunteers were obtained for optical absorbance path lengths of 25, 50 and 100 μm for each volunteer in both a single and a double pass configuration (example for one subject in figure 5.4).

The absorbance of blood for all subjects was dependent on the absorbance path length, with absorbance increasing with increased absorbance path length in both the single and the double pass configuration. The shape of the absorbance spectra differed between the single and double pass configuration. In single pass, the slope of the absorbance spectra in the region below 500 nm was steeper than in the double pass. In the wavelength region above 600 nm, the slope of the absorbance spectra in single pass was

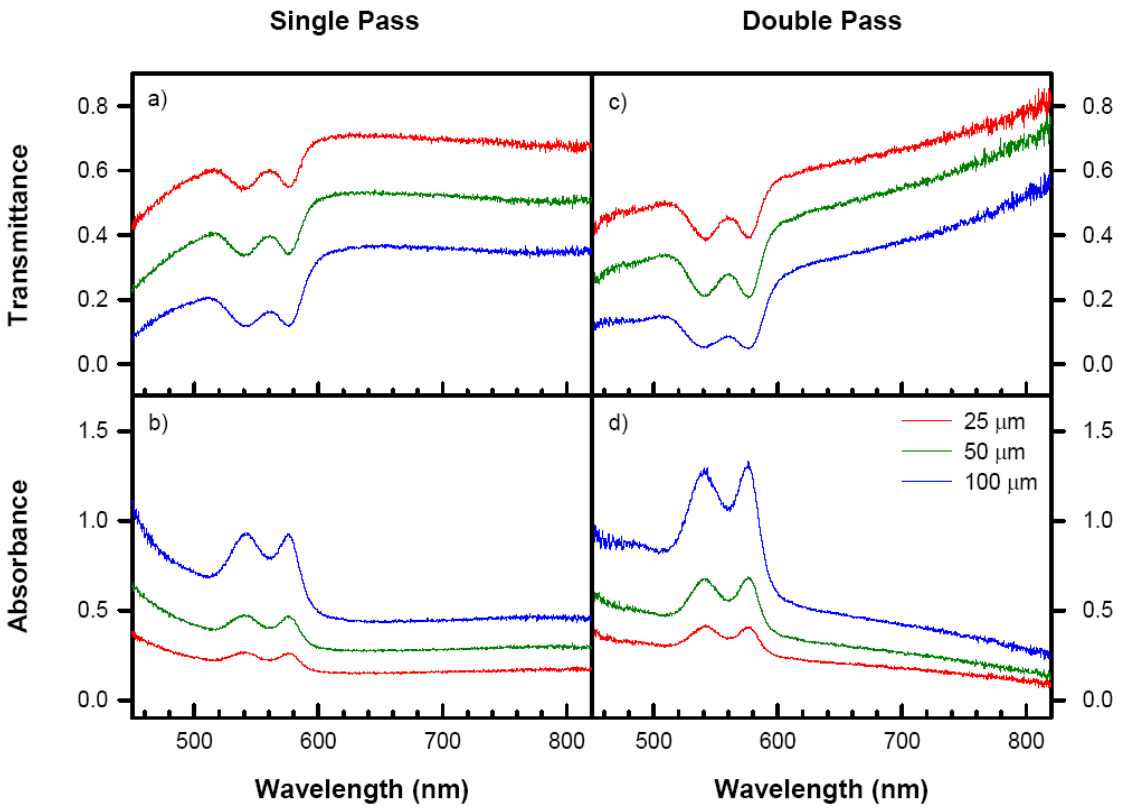

Figure 5.4: Dependence of the transmittance and the absorbance spectra of blood on absorbance path length in single and double pass configurations for one subject

almost flat while the slope of the absorbance spectra in double pass was negative and exhibited little change up to 800 nm. Also, the transmittance above 600 nm was higher in double pass than in single pass. This is due to the fact that haemoglobin absorption is low beyond 600 nm, and RBC scattering measured in the double pass configuration contributed significantly to the transmitted signal beyond 600 nm. Noise levels in the transmittance and absorbance curves are in the order of 1 – 2% between 500 and 700 nm, depending on transmittance and absorbance values, which correspond to the noise level of the spectrometer. Below 500 nm and above 700 nm, noise levels are significantly higher due to the low light intensity outside the optimal operating range of the system.

The constant background noise of the spectrometer across its operating wavelength range results in higher transmittance noise when light levels in the sample and reference signals are low, which is the case below 500 nm and above 700 nm.

5.4.2 Fitting to the Absorbance Model

The absorbance spectra were fitted to the Beer-Lambert model by multiple linear regression (equation 5.1) and the oxygen saturation of each blood sample was calculated using equation 4.2. For each sample, the difference between the predicted SO_2 value in single pass and the predicted SO_2 value in double pass (ΔSO_2) was calculated at each absorbance path length. The results were compared using a One Way Analysis of Variance (ANOVA). The data failed the Shapiro-Wilk normality test so a Kurskal-Wallis One Way ANOVA on Ranks was performed (table 5.1).

Path Length	Median ΔSO_2	25%	75%
25 μm	4.1%	1.0%	8.6%
50 μm	3.8%	0.9%	16.0%
100 μm	6.2%	2.2%	9.5%

Table 5.1: Dependence of median SO_2 difference between single and double pass SO_2 calculated from the same blood sample

There is no statistically significant difference (P = 0.938) between the median ΔSO_2 values when comparing between absorbance path lengths. This suggests that the scattering that cause deviations to the Beer-Lambert law, and possibly result in inaccurate oxygen saturation values, does not change with path length in these relatively short path

lengths, or if it does change with path length, the difference is too small between single and double pass configurations to cause a statistically significant difference in median SO_2 differences between the single and double pass configuration. It also suggests that backscatter, which is only present in double pass, does not contribute to the transmitted signal in the wavelength range used to calculate oxygen saturation enough to cause a significant change in the calculated SO_2 value. An attempt was made to compare calculated SO_2 values to CO-Oximetry results, but exposure to air during the blood handling procedure prevented accurate comparison as explained in section 3.3.

In the literature, the reliability of the predicted SO_2 is assessed from the quality of fit between the measured and fitted absorbance, using the coefficient of determination R^2. SO_2 reliability is considered high for high R^2 values and less reliable for lower values. The value of R^2 measures the proportion of the variability in the dependent variable that may be accounted for by the multiple linear regression equation [136]. The built in assumption in this interpretation is that the fit errors are randomly distributed, and that no systematic errors are present which would indicate the use of an inappropriate model for the absorbance. To see if there was any difference in the quality of fit between the single and double pass configurations as a function of path length, the R^2 values of all 10 subjects were compared between configurations and between path lengths using a Two Way ANOVA performed on R^2. The ANOVA revealed a statistically significant interaction between the absorbance path length and the configuration (single or double pass) indicating that quality of fit depends on both parameters but we cannot decouple their individual effects on R^2. For example, it is impossible to find a statistically significant difference between the R^2 values from the single pass 50 μm samples and the

R^2 values from the double pass 25 μm samples. A Pairwise Multiple Comparison Procedure (Holm-Sidak method) was performed to compare the R^2 values between single and double pass for the same absorbance path length (table 5.2).

	Single Pass		Double Pass		
Path Length	Mean R^2	SEM	Mean R^2	SEM	p value
25 μm	0.968	0.010	0.988	0.010	0.133
50 μm	0.985	0.010	0.987	0.010	0.862
100 μm	0.994	0.010	0.907	0.010	<0.001

Table 5.2: Comparison of mean R^2 values between single and double pass configurations as a function of absorbance path length

The standard error of the mean (SEM) is shown in table 5.2 instead of the standard deviation since the data failed the normality test (Shapiro-Wilk). The only absorbance path length that had a statistically significant difference ($P<0.001$) in quality of fit for single and double pass was the 100 μm path length, where the mean R^2 value found in single pass (0.994) was greater than the mean R^2 value found in double pass (0.907). This indicates that in terms of R^2, the fits were as reliable in single pass than in double pass for the path lengths of 25 and 50 μm, and were more reliable in single pass then in double pass for the 100 μm path length.

5.4.3 Wavelength Dependent Beer-Lambert Deviations

In order to look more closely at the wavelength dependence of the deviations of the measured data from the Beer-Lambert law model, the difference between the

measured spectra and predicted spectra was calculated for each subject at each absorbance path length as a function of wavelength for both the single and double pass configurations, and this will be referred to as the deviations from the model. The Beer-Lambert law deviations were calculated as the measured minus the predicted absorbance between the 520 nm to 600 nm range used in the oximetry calculation. The deviations are then normalized by dividing by the mean absorbance of each curve to allow for comparisons in patterns without affecting the fit quality and oximetry values. For each absorbance path length, there was a systematic deviation of the measured data from the oxy-deoxyhaemoglogin mixture model in both single and double pass configurations (figure 5.5).

In single pass, the spectral shapes of deviations from the model were consistent between subjects and were path length dependent. The wavelength region with the largest errors was the range of 520 to 540 nm, with the maximum error found at 520 nm for every path length. The rest of the wavelength range from 540 to 600 nm had less deviations and showed little spectral dependence. In double pass, there was more variance across the 10 subjects than for single pass, but general features were consistent across the 10 subjects and varied across path length. The largest deviations were found at the 100 μm path length. One reason the variance in the Beer-Lambert deviations are larger in double pass is due to the lower signals compared to single pass. Since light goes through blood twice in double pass, the transmittance will be lower and the same noise

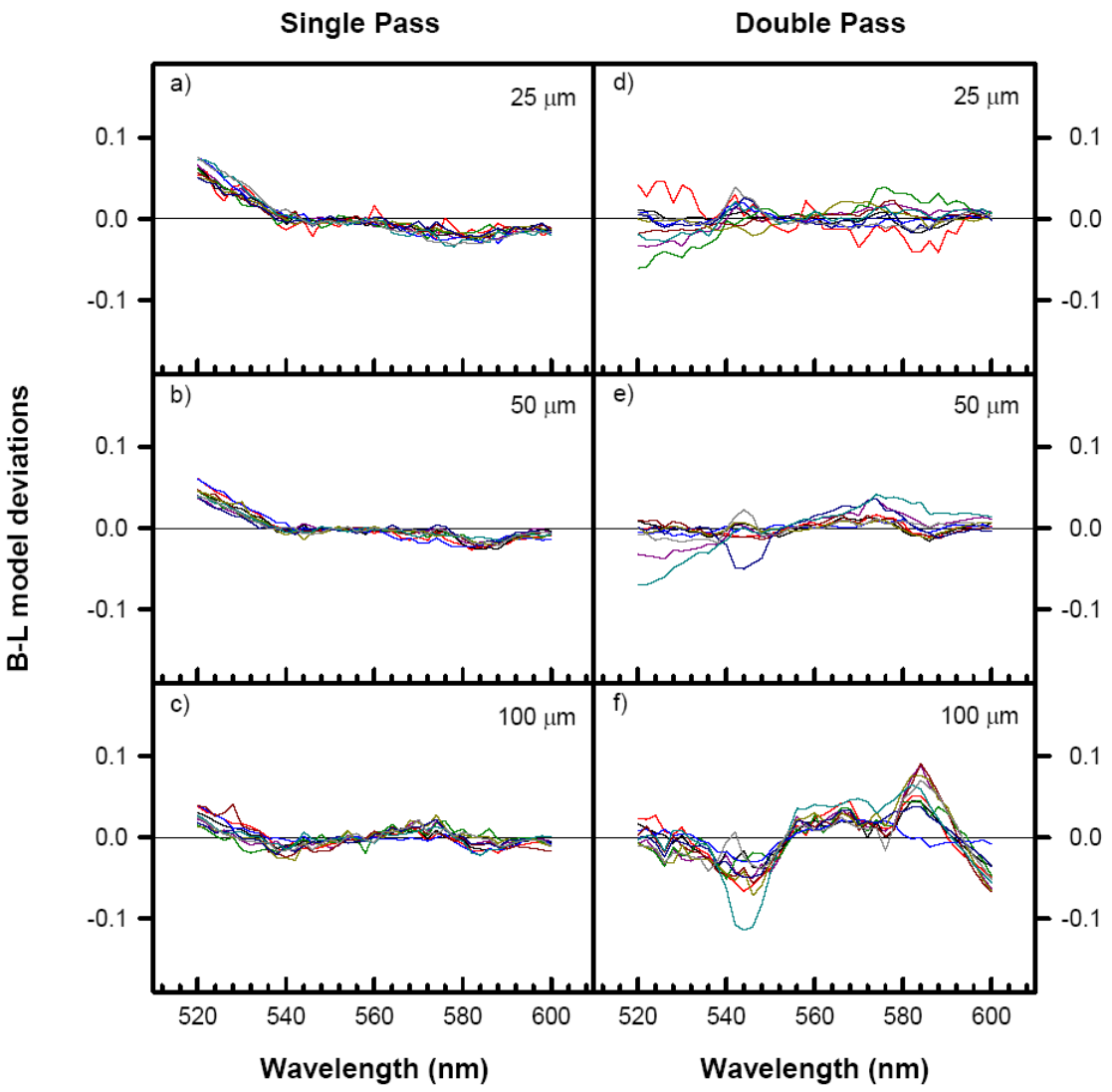

Figure 5.5: Beer-Lambert model deviations of 10 subjects (individual coloured lines) for different absorbance path lengths in single and double pass. The deviations were calculated as a function of wavelength by taking the measured absorbance minus the predicted model absorbance and dividing by the mean of the absorbance across the wavelength range of 520 to 600 nm.

level found in single pass will result in a larger percentage change in the double pass signal, thus making the transmittance and absorbance curves noisier in the double pass configuration. In addition, the backscatter present in double pass is dominated by surface

structure in blood samples (local density of RBC for example), which have much more variance between subjects compared to forward scatter where blood goes through the blood sample resulting in an averaging affect on the signal.

The shape of the model deviations is different between single and double pass configuration, suggesting that the different light paths cause different spectral deviations in the Beer-Lambert absorbance model. In order to determine if there were consistent patterns in the wavelength dependence of the Beer-Lambert model deviations across absorbance path lengths and experimental configuration (single and double pass), principal component analysis (PCA) was performed using the singular value decomposition (SVD) function in Mathcad (PTC, Needham, MA) (figure 5.6 and 5.7).

It was found that 95% of the variance across the data of Beer-Lambert deviations in the combined single and double pass configurations could be expressed in terms of three principal components (figure 5.6). The mean weighting factors across the 10 subjects for each principal component are plotted with their respective standard deviations (figure 5.7). The mean weighting factors of the first principal component had increased with the same slope as a function of path length for the single and double pass configurations (figure 5.7), but all double pass weighting factors were significantly ($P<0.05$) greater than the factors in single pass (Holm-Sidack method, table 5.3 and 5.4).

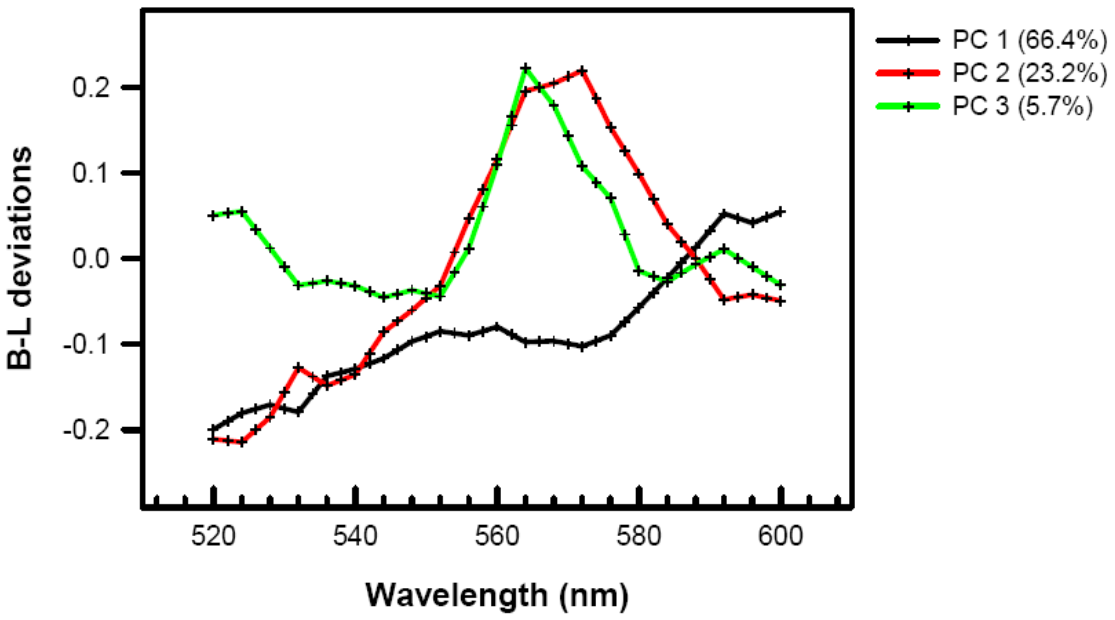

Figure 5.6: Dependence of the first three principal components resulting from the singular value decomposition of the Beer-Lambert model deviations on wavelength in both single and double pass data. Percentages in legend represent the amount of variation in the data accounted by the respective principal component.

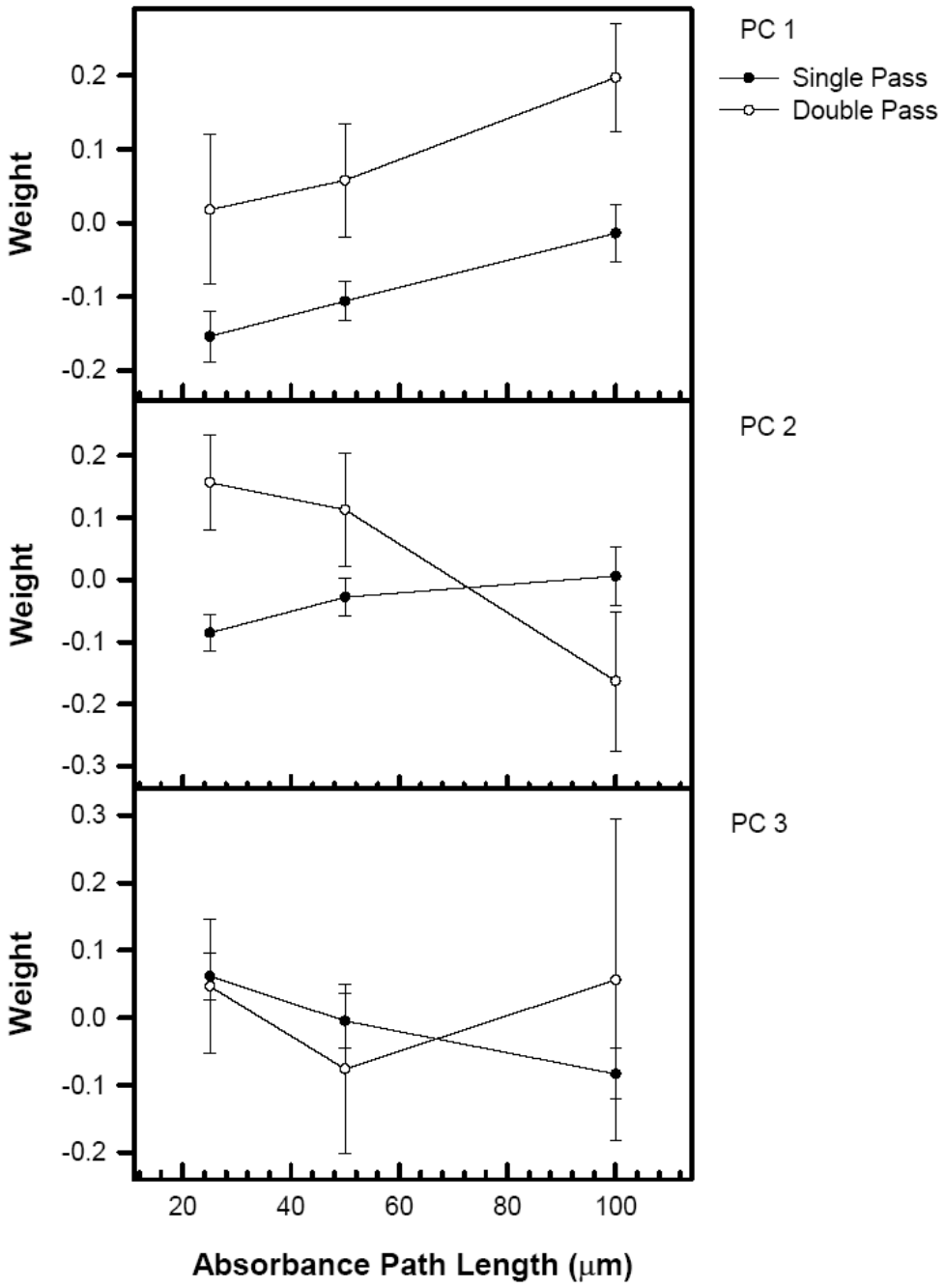

Figure 5.7: Dependence of the mean weighting factors of the singular value decomposition for the first three principal components on the absorbance path length for single and double pass data. Mean (data points) and standard deviations (whiskers) are calculated from the Beer-Lambert model deviations for 10 subjects.

Comparison	PC # 1		PC # 2		PC # 3	
	P (single)	P (double)	P (single)	P (double)	P (single)	P (double)
100 μm vs. 25 μm	<0.05	<0.05	<0.05	<0.05	<0.05	0.051
100 μm vs 50 μm	<0.05	<0.05	0.150	<0.05	0.277	0.052
50 μm vs 25 μm	0.104	0.173	0.297	0.177	0.222	0.862

Table 5.3: Results of ANOVA on principal component weighting factors comparing mean values of 10 subjects between absorbance path lengths in single and double pass configurations

Comparison	PC # 1		
	P (25 μm)	P (50 μm)	P (100 μm)
double vs. single	<0.05	<0.05	<0.05

Comparison	PC # 2		
	P (25 μm)	P (50 μm)	P (100 μm)
double vs. single	<0.05	<0.05	<0.05

Comparison	PC # 3		
	P (25 μm)	P (50 μm)	P (100 μm)
double vs. single	0.782	0.191	<0.05

Table 5.4: Results of ANOVA on principal component weighting factors comparing mean values of 10 subjects between single and double pass configurations at every absorbance path length

For the second principal component, in single pass, the weighting factors increased with path length, although only the difference between the 25 μm and 100 μm path length was statistically significant ($P<0.05$). For the double pass configuration, the weighting factors decreased with path length with the 25 μm and 100 μm path length

being the only path lengths with statistically significant differences between the mean weighting factors. The difference between the mean weighting factors of the single and double pass configurations was statistically significant at every absorbance path length. The mean weighting factors of the third principal component showed a similar trend between the single and double pass configurations and only the 100 μm path length had mean weighting factors that were statistically significantly different.

It is not possible from the analysis to assign specific principal components to different path ways of light in the experiments. However, the first principal component, which accounted for 66.4% of the variance in the data, had the same trend between the single and double pass configurations suggesting a common mechanism for deviations to the Beer-Lambert absorbance between single and double pass. Forward scatter is present in both the single and double pass configurations and could be the source of this signal. In theory, forward scatter should increase with absorbance path length and be greater in double pass than in single pass. The weighting factors of the first principal component follow this trend and could possibly be associated with forward scatter. The different trends between the mean weighting factors of the second principal component might be a result of the different pathways between the single and double pass configurations, and since backscatter is only being found in double pass, it could be associated with the second principle component. The mean weighting factors in double pass decreased with path length and were significantly different from values in single pass at every absorbance path length. In a future set of experiments, we will attempt to determine if it is possible to associate principal components of the Beer-Lambert model fit errors to different pathways of light in retinal oximetry.

5.5 Acknowledgements

The authors are thankful to all the people who helped in the realisation of these experiments. The authors would especially like to thank Monica Atanya for her help with the measurements, Gail Kayuk for performing the blood draws, and Dr. Mélanie Lalonde for her help with ethics approval.

CHAPTER 6 – CONCLUSIONS AND FUTURE WORK

6.1 Summary of Results

The influence of red blood cell scattering in different possible optical pathways of retinal oximetry was investigated experimentally by *in-vitro* whole blood spectroscopy measurements. Custom-designed experimental setups were developed to measure the absorbance of whole blood samples in configurations that matched the light paths in retinal vessel oximetry for absorbance path lengths ranging from 25 to 500 μm, representing different retinal vessel thicknesses. Deviations from the Beer-Lambert absorbance model were calculated which gave some insight into the spectral dependence of scattering for the different pathways in retinal oximetry.

In chapter 3 the correlation between the O_2Hb and HHb extinction coefficient spectra was examined to identify wavelength regions suitable for oximetry and to determine if the correlation between these variables has an impact on oximetry calculation independently of the identified deviations from the Beer-Lambert law. It was found that the Spearman rank correlation coefficient between the O_2Hb and HHb extinction coefficients is dependent on the wavelength range chosen for analysis. Median oxygen saturation differences on our data showed that SO_2 can vary by up to 9.1% across the 10 subjects between wavelength ranges. The quality of fit measures, R^2, were found not to be good predictors of accurate oxygen saturation values, with oxygen saturation differences of up to 25.4% found when calculating SO_2 of the same blood sample of one subject at two different wavelength ranges when the R^2 value was above 0.99 in both

ranges. A wavelength range, 532-592 nm, was found to have no significant correlation (r = -0.012 and P = 0.949) between O_2Hb and HHb extinction coefficients, and it will be verified in another experiment if it is a reliable range for oximetry using a MLR. Our selected range of 520-600 nm (r = 0.498 and P = 0.001) had some correlation (but small), and is not likely to be the major source of the SO_2 differences reported in the previous two chapters. These findings are important since it shows that some wavelength ranges might be more reliable for oximetry than others when using a multiple linear regression model to calculate oxygen saturation, and that the R^2 value might not be a reliable indicator of oxygen saturation accuracy if using an inappropriate wavelength range for analysis, or an inappropriate absorbance model.

In Chapter 4, the impact of small angle forward scatter on whole blood oximetry was quantified for different absorbance path lengths by using two different optical systems allowing either minimal or a significant amount of forward scatter in the transmittance path. Firstly, we found that forward scatter increases the transmitted signal significantly – allowing signal detection in thicker blood samples where absorbance was well beyond the signal detection limit of our instrument. There were significant calculated oxygen saturation differences between the high and low forward scatter experimental setups of 10% or more for every absorbance path length calculated. The oxygen saturation difference between experimental setups did not affect the quality of fit as assessed by the coefficient of determination for the regression fits. The mean R^2 value was not statistically significantly different between experimental setups at either of the absorbance path lengths. Both setups showed significant systematic deviations from the Beer-Lambert law, but patterns were different for the two setups and were absorbance

path length dependent. Deviations from the Beer-Lambert model were largest with the larger scatter setup, and were maximum in the 520-540 nm range, which is consistent with the other studies [152] which also found that out of the 520-600 nm range used for analysis, the biggest difference in the spectral dependence between the spectra of the RBC scattering cross section and haemoglobin extinction coefficients are in the 520-540 nm range. The presence of systematic fit errors across subjects suggests that the absorbance model proposed does not account for all contributing factors to the absorbance signal and that this unaccounted signal affects SO_2 calculations significantly.

In Chapter 5, the wavelength dependence of Beer-Lambert model deviations was examined for 2 different potential light paths in retinal oximetry at absorbance path lengths of 25, 50 and 100 μm. As in chapter 4, both single and double pass spectra deviated systematically from the Beer-Lambert law. The pattern for single and double pass for a given absorbance path length showed some similarities but were different. Both pathway deviations from the Beer-Lambert law were dependent on absorbance path length. Median calculated oxygen saturation differences between single and double pass (up to 6.2%) pathways were significant but were not dependent on absorbance path length. Principal component analysis performed on the deviations from the Beer-Lambert law for both single and double pass configurations found that 95% of the variance in deviations across subjects, setup and path length, could be expressed in terms of three principal components. The mean weighting factor of the first principal component had the same dependence on absorbance path length for the single and double pass configuration, suggesting a common mechanism responsible for the Beer-Lambert model deviations between the two configurations. The mean weighting factor of the second

principal component showed a different dependence on path length, suggesting a second mechanism acting differently in the single and double pass configurations. This is consistent with the first component having a correlation with forward scatter which would contribute to the measured signal in both setups, and the second having a correlation with back scatter which would be significant only in the double pass setup.

6.2 Future Work

There are a number of steps that can be taken in order to continue the work done in this thesis. Since the ultimate goal of this research is to perform *in-vivo* non-invasive retinal oximetry on clinical patients, the first step would be to develop an upgraded version of the retinal oximetry device. The Ocean Optics spectrometer needs to be replaced with a spectrometer that has a much higher signal to noise ratio in order to be able to calculate oxygen saturation from the absorbance spectrum. Cooling the spectrometer detector array would significantly reduce the noise level and improve the signal to noise ratio. Having a narrower bandwidth is not necessary in this case, because the features that we are attempting to measure are in the order of 20 – 30 nm, and the 8 nm bandwidth of the existing spectrometer is adequate for this purpose. Reducing the bandwidth would not improve the measurement capabilities of retinal oximetry. The design of the instrument will allow for an easy replacement of the spectrometer without having to do any dismantling of the device. Another feature in the device that should be changed is the motor controls to adjust the position of the captured fundus reflectance spectrum along with the focus of the image. While software and motor control of these parameters seems attractive at first, the implementation proved to be difficult. The lack of

fine adjustment and slow response time of the motors made it difficult to reach and stay on the desired target area for oximetry as subjects moved their eyes during examinations. A manual adjusting knob system would be much easier to use in this case. Finally, adapting the system with a hyperspectral camera could improve our ability to calculate retinal oximetry. Provided that the camera can capture enough light, a hyperspectral imaging system gives multispectral imaging information in a single image capture. This would allow us to obtain oxygen saturation values across the entire retina form a single image.

The analysis in Chapter 3 showed that the wavelength range chosen for analysis can have an impact on the calculated oxygen saturation value of blood when using a multiple linear regression. Two possible explanations are that systematic errors were present in the absorbance model that resulted in inaccurate predicted oxygen saturation values, and that strong correlation between O_2Hb and HHb extinction coefficient spectra make multiple linear regression impractical for oximetry in certain wavelength ranges. To verify which factor is dominating the difference in oxygen saturation values found between different wavelength ranges, an experiment should be conducted to measure the absorbance spectrum of a haemoglobin solution (to eliminate the effects of scatter) with known oxygen saturation and calculate the predicted oxygen saturation of the sample by multiple linear regression for different wavelength ranges. Wavelength ranges should be chosen to have different correlation coefficients ranging from strong positive, strong negative and zero correlation. If the calculated oxygen saturation values are the same at each wavelength, it shows that the correlation between O_2Hb and HHb extinction coefficient spectra does not affect the accuracy of oxygen saturation calculations using a

multiple linear regression approach. In addition, the hypothesis that the covariance (or correlation) between the O_2Hb and HHb extinction coefficients can be associated to their derivatives, and that the sign of the derivatives can be used to predict wavelength regions of different correlations was confirmed by the findings in Chapter 3. This was not a mathematical proof for a general case of two variables however. In a future study, we will attempt to demonstrate how the covariance is linked to the derivatives and provide a mathematical proof of the method used to find the different wavelength ranges.

As a follow up to the experiments described in Chapters 4 and 5, it would be interesting to repeat the experiments and compare the oxygen saturation values to CO-oximetry measurements. To do so would require a different procedure to transfer the blood from the blood gas syringes into the optical cells so that the blood never comes in contact with air during the transfer in order to keep its oxygen saturation value constant. One interesting variation to the experiment in Chapter 4 would be to vary the acceptance angle of the scattered light in the experimental setup to add to the transmitted signal. It would be interesting to see how the oxygen saturation difference between experimental setups varies with acceptance angle. The Beer-Lambert model deviations would also be expected to vary with acceptance angle. The deviations should increase in the 520-540 nm wavelength range with increasing acceptance angle, while the 540-600 nm wavelength range would not be expected to vary much with acceptance angle.

Finally, principal component analysis performed on the Beer-Lambert deviations in Chapter 5 found that 95% of the variations in the data can be accounted for by 3 principal components. Further analysis would be useful to attempt to associate principal components to specific light paths in retinal oximetry. Trends in principal component

weighting factors suggest both common and separate mechanisms that cause deviations to the Beer-Lambert model. Linking the principal components to specific light paths could prove useful in retinal oximetry.

REFERENCES

1. Osborne NN, Casson RJ, Wood JPM, Chidlow G, Graham M, Melena J, *Retinal ischemia: mechanisms of damage and potential therapeutic strategies.* Progress in Retinal and Eye Research, 2004. **23**(1): p. 91-147.
2. Beatty S, Koh H-H, Phil M, Henson D, Boulton M, *The role of oxidative stress in the pathogenesis of age-related macular degeneration.* Survey of ophthalmology, 2000. **45**(2): p. 115-134.
3. Wangsa-Wirawan ND, Linsenmeier RA, *Retinal oxygen.* Archives of Ophthalmology, 2003. **121**.
4. Pournaras C J, Tsacopoulos M, Strommer K, Gilodi N, Leuenberger PM, *Experimental retinal branch vein occlusion in miniature pigs induces local tissue hypoxia and vasoproliferative microangiopathy.* Ophthalmology, 1990. **97**: p. 1321-1328.
5. Stefansson E, Novack RL, Hatchell DL, *Vitrectomy prevents retinal hypoxia in branch retinal vein occulsion.* Investigative Ophtalmology & Visual Science, 1990. **31**: p. 284-289.
6. Pournaras CJ, Tsacopoulos M, Strommer K, Gilodi N, Leuenberger PM, *Scatter photocoagulation restores tissue hypoxia in experimental vasoproliferative microangiophathy in minuature pigs.* Ophthalmology, 1990. **97**: p. 1329-1333.
7. Pournaras CJ, *Retinal oxygen distribution. Its role in the physiopathology of vasoproliferative microangiopathies.* Retina, 1995. **15**: p. 332-347.
8. Yoneya S, Saito T, Nishiyama Y, Deguchi T, Takasum M, Gil T, Horn E, *Retinal oxygen saturation levels in patients with central retinal vein occlusion.* Ophthalmology, 2002. **109**: p. 1521-1526.
9. Pournaras JA, Petropoulos IK, Munoz JL, Pournaras CJ, *Experimental retinal vein occlusion: effect of acetazolamide and carbogen (95% O_2/5% CO_2) on preretinal PO_2.* Investigative Ophtalmology & Visual Science, 2004. **45**: p. 3669-3677.

10. Alder VA, Ben-Nun J, Cringle SJ, *PO_2 profiles and oxygen consumption in cat retina with an occluded retinal circulation.* Investigative Ophtalmology & Visual Science, 1990. **1990**: p. 1029-1034.
11. Braun RD, Linsenmeier RA, *Retinal oxygen tension and the electroretinogram during arterial occlusion in the cat.* Investigative Ophtalmology & Visual Science, 1995. **36**: p. 523-541.
12. Lewis G, Mervin K, Valter K, Maslim J, Kappel, PJ, Stone J, Fisher S, *Limiting the proliferation and reactivity of retinal Muller cells during experimental retinal detachment: the value of oxygen supplementation.* American Journal of Ophthalmology, 1999. **128**: p. 165-172.
13. Stefansson E, *Ocular oxygenation and neovascularization.* 1981.
14. Mervin K, Valter K, Maslim J, Lewis G, Fisher S, Stone J, *Limiting photoreceptor death and deconstruction during experimental retinal detachment: the value of oxygen supplementation.* American Journal of Ophthalmology, 1999. **128**: p. 155-164.
15. Linsenmeier RA, Padnick-Silver L, *Metabolic dependence of photoreceptors on the choroid in the normal and detached retina.* Investigative Ophtalmology & Visual Science, 2000. **41**: p. 3117-3123.
16. Lewis GP, Talaga KC, Linberg KA, Avery RL, Fisher SK, *The efficacy of delayed oxygen therapy in the treatment of experimental retinal detachment.* American Journal of Ophthalmology, 2004. **137**: p. 1085-1095.
17. Sakai T, Lewis GP, Linberg KA, Fisher SK, *The ability of hyperoxia to limit the effects of experimetnal detachment in cone-dominated retina.* Investigative Ophtalmology & Visual Science, 2001. **42**: p. 3264-3273.
18. Yu D-Y, Cringle SJ, *Retinal degeneration and local oxygen metabolism.* Experimental Eye Research, 2005. **80**(6): p. 745-751.
19. Zarbin MA, *Current concepts in the pathogenesis of age-related macular degeneration.* Arch Ophthalmol, 2004. **122**(4): p. 598-614.
20. Dean FM, Arden GB, Dornhorst A, *Partial reversal of protan and tritan colour defects with inhaled oxygen in insulin dependent diabetic subjects.* British Journal of Ophthalmology, 1997. **81**: p. 27-30.

21. Drasdo N, Chiti Z, Owens DR, North RV, *Effect of darkness on inner retinal hypoxia in diabetes.* Lancet, 2002. **359**: p. 2251-2253.
22. Wangsa-Wirawan ND, Linsenmeier RA, *Retinal oxygen: fundamental and clinical aspects.* Archives of Ophthalmology, 2003. **121**: p. 547-557.
23. Tiedeman JS, Kirk SE, Srinivas S, Beach JM, *Retinal oxygen consumption during hyperglycemia in patients with diabetes without retinopathy.* Ophthalmology, 1998. **105**: p. 31-36.
24. Ernest JT, Goldstick TK, Engerman RL, *Hyperglycemia impairs retinal oxygen autoregulation in normal and diabetic dogs.* Investigative Ophtalmology & Visual Science, 1983. **24**: p. 985-989.
25. Isenberg SJ, McRee WE, Jedrzynski MS, *Conjunctival hypoxia in diabetes mellitus.* Investigative Ophtalmology & Visual Science, 1986. **27**: p. 1512-1515.
26. Sutherland FS, Stefansson E, Hatchell DL, Reiser H, *Retinal oxygen consumption in vitro; the effect of diabetes mellitus, oxygen and glucose.* Acta Ophthalmology (Copenh), 1990. **68**: p. 715-720.
27. Alder VA, Y DY, Cringle SJ, Su EN, *Changes in vitreal oxygen tension distribution in the streptozotocin diabetic rat.* Diabetologia, 1991. **34**: p. 469-476.
28. Augsten R, Konigsdorffer E, Schweitzer D, Strobel J, *Multisubstance analysis of reflection spectra before and after laser photocoagulation for proliferative diabetic retinopathy.* European Journal of Ophthalmology, 1997. **7**: p. 317-321.
29. QD Nguyen, S.S., E Van Anden, J. U. Sung, S. Vitale, P. A. Campochiaro, *Supplemental oxygen improves diabetic macular edema: a pilot study.* Investigative Ophtalmology & Visual Science, 2004. **45**: p. 617-624.
30. Berkowitz BA, Ito Y, Kern TA, McDonald C, Hawkins R, *Correction of early subnormal superior hemiretinal DeltaPO(2) predits therapeutic efficacy in experimental diabetic retinopathy.* Investigative Ophtalmology & Visual Science, 2001. **42**: p. 2964-2969.
31. Berkowitz BA, Kowluru RA, Frank RN, Kern TS, Hohman TC, Prakash M, *Subnormal retinal oxygenation response precedes diabetic-like retinopathy.* Investigative Ophtalmology & Visual Science, 1999. **40**: p. 2100-2105.

32. Berkowitz BA, Luan H, Gupta RR, Pacheco D, Seidner A, Roberts R, Liggett J, Knoerzer DL, Connor JR, Du Y, Kern TS, Ito Y, *Regulation of the early subnormal retinal oxygenation response in experimental diabetes by inducible nitric oxide synthase.* Diabetes, 2004. **53**: p. 173-178.
33. Luan H, Leitges M, Gupta RR, Pacheco D, Seidner A, Liggett J, Ito Y, Kowluru R, Berkowitz BA, *Effect of PKCbeta on retinal oxygenation response in experimental diabetes.* Investigative Ophtalmology & Visual Science, 2004. **45**: p. 937-942.
34. Trick GL, Berkowitz BA, *Retinal oxygenation response and retinopathy.* Progress in Retinal and Eye Research, 2005. **24**: p. 259-274.
35. Berkowitz BA, Roberts R, Luan H, Peysakhov J, Knoerzer DL, Connor JR, Hohman TC, *Drug intervention can correct subnormal retinal oxygenation response in experimental diabetic retinopathy.* Investigative Ophtalmology & Visual Science, 2005. **46**: p. 2954-2960.
36. J Flammer, Orgul S, Costa VP, Orzalesi N, Krieglstein GK, Serra LM, Renard JP, Stefansson E, *The impact of ocular blood flow in glaucoma.* Progress in Retinal and Eye Research, 2002. **21**: p. 359-393.
37. Flammer J, Haefliger IO, Orgul S, Resink T, *Vascular dysregulation: a principal risk factor for glaucomatous damage?* Journal of Glaucoma, 1999. **8**: p. 212-219.
38. Stefansson E, Landers MB 3rd, Wolbarsht ML, *Increased retinal oxygen supply following pan-retinal photocoagulation and vitrectomy and lensectomy.* Transactions of the American Ophthalmological Society, 1981. **79**: p. 307-334.
39. Stefansson E, *Oxygen and diabetic eye disease.* Graefes Archives of Clinical and Experimental Ophthalmology, 1990. **228**: p. 120-123.
40. Stefansson E, *The therapeutic effects of retinal laser treatment and victrectomy; a theory based on oxygen and vascular physiology.* Acta Ophthalmol Scand, 2001. **79**: p. 435-440.
41. Landers MB 3rd, Stefansson E, Wolbarsht ML, *Panretinal photocoagulation and retinal oxygenation.* Retina, 1982. **2**: p. 167-175.

42. Molnar I, Poitry S, Tsacopoulos M, Gilodi N, Leuenberger PM, *Effect of laser photocoagulation on oxygenation of the retina in miniature pigs.* Investigative Ophtalmology & Visual Science, 1985. **26**: p. 1410-1414.
43. Stefansson E, Hatchell DL, Fisher BL, Sutherland FS, Machemer R, *Panretinal photocoagulation and retinal oxygenation in normal and diabetic cats.* American Journal of Ophthalmology, 1986. **101**: p. 657-664.
44. Novack RL, Stefansson E, Hatchell DL, *The effect of photocoagulation on the oxygenation and ultrastructure of avascular retina.* Experimental Eye Research, 1990. **50**: p. 289-296.
45. Stefansson E, Machemer R, de Juan E Jr , McCuen BW 2nd, Peterson J, *Retinal oxygenation and laser treatment in patients with diabetic retinopathy.* American Journal of Ophthalmology, 1992. **113**: p. 36-38.
46. Funatsu H, Wilson CA, Berkowitz BA, Sonkin PL, *A comparitive study of the effects of argon and diode laser photocoagulation on retinal oxygenation.* Graefes Archives of Clinical and Experimental Ophthalmology, 1997. **235**: p. 168-175.
47. Yu DY, Crincle SJ, Su E, Yu PK, Humayun MS, Dorin G, *Laser-induced changes in intraretinal oxygen distribution in pigmented rabbits.* Investigative Ophtalmology & Visual Science, 2005. **46**: p. 988-999.
48. Cohen LH, Noell WK, *Relationships between visual function and metabolism.* Biochemistry of the Retina, 1965: p. 36-50.
49. Anderson B, Saltzman HA, *Retinal oxygen utilization measured by hyperbaric blackout.* Archives of Ophthalmology, 1964. **72**: p. 792-795.
50. Ames A 3rd, *Energy requirements of CNS cells as related to their function and to their vulnerability to ischemia: a commentary based on studies on retina.* Canadian Journal of Physiology and Pharmacology, 1992. **70**: p. S158-S164.
51. Delori F, *Noninvasive technique for oximetry of blood in retinal vessels.* Applied Optics, 1988. **27**(6): p. 13.
52. Cringle SJ, Yu D-Y, Yu PK, Su E-N, *Intraretinal oxygen consumption in the rat in vivo.* Investigative Ophthalmology & Visual Science, 2002. **43**(6): p. 1922-1927.

53. Johnson PC, *The microcirculation and local ad humoral control of the circulation.* International Review of Physiology, 1974. **1**: p. 163-195.
54. Robinson F, Riva CE, Grunwald JE, Petrig BL, Sinclair SH, *Retinal blood flow autoregulation in response to an acute increase in blood pressure.* Investigative Ophtalmology & Visual Science, 1986. **27**(5): p. 722-726.
55. Moyle JTB, *Pulse Oximetry*. 1998. 140.
56. http://www.ganfyd.org/index.php?title=Haemoglobin_dissociation_curve.
57. Leow MK, *Configuration of the hemoglobin oxygen dissociation curve demystified: a basic mathematical proof for medical and biological sciences undergraduates.* Advances in Physiology Education, 2007. **31**: p. 198-201.
58. Heck H, Hollmann W, *Berechnung der werte des saure-basen-status mit hilfe eines tischcomputers.* Sportarzt Sportmed, 1975. **25**: p. 154.
59. Marsoner HJ, Harnoncourt K, *Berechnung der sauerstoffsattigung als funktion von pO_2, pH, temperatur und basenabweichung.* Anaesthesist, 1976. **25**: p. 345.
60. Keys A, *The oxygen saturation of the venous blood in normal human subjects.* 1938.
61. Drabkin DL, *The crystallographic and optical properties of the hemoglobin of man in comparison with those of other species.* Journal of Biological Chemistry, 1946. **164**: p. 703-723.
62. Benesch RE, Benesch R, Yung S, *Equations for the spectrophotometric analysis of hemoglobin mixtures.* Analytical Biochemistry, 1973. **55**: p. 245-248.
63. Van Assendelft OW, Zijlstra WG, *Extinction coefficients for use in equations for the spectrophotometric analysis of haemoglobin mixtures.* Analytical Biochemistry, 1975. **69**: p. 43-48.
64. Pittman RN, *In vivo photometric analysis of hemoglobin.* Annals of Biomedical Engineering, 1986. **14**: p. 119-137.
65. Zijlstra WG, Buursma A, Meeuwsen-van der Roest WP, *Absorption spectra of human fetal and adult oxyhemoglobin, de-oxyhemoglobin, carboxyhemoglobin, and methemoglobin.* Clinical Chemistry, 1991. **37**(9): p. 1633-1638.
66. Kuenstner JT, Norris KH, McCarthy WF, *Measurement of hemoglobin in unlysed blood by near-infrared spectroscopy.* Applied Spectroscopy, 1994. **48**(4).

67. Kuenster JT, Norris KH, Kalasinsky VF, *Spectrophotometry of human hemoglobin in the midinfrared region.* Biospectroscopy, 1997. **3**(3): p. 225-232.
68. Prahl, S., *http://omlc.ogi.edu/spectra/hemoglobin/index.html.*
69. Hickam JB, Frayser R, Ross JC, *A study of retinal venous blood oxygen saturation in human subjects by photographic means.* Circulation, 1963. **27**: p. 375-385.
70. *http://webvision.med.utah.edu/anatomy.html.*
71. Schweitzer D, Leistriz L, Hammer M, Scibor M, Bartsch U, Strobel J, *Calibration-free measurement of the oxygen saturation in retinal vessels of men.* Proc. SPIE, 1995. **2393**: p. 210-218.
72. Scott VA, Tarassenko L, Glynn CJ, Hill AR, *Retinal pulse oximetry: Towards a method for measuring cerebral oxygen saturation.* IEEE-EMBC and CMBEC, 1995. **Theme 7**.
73. Smith MH, *Optimum wavelength combinations for retinal vessel oximetry.* Applied Optics, 1999. **38**(1).
74. Drewes J, Smith M, Derminghoff K, Hiliman L, *An Instrument for the measurement of retinal vessel oxygen saturation.* Ophthalmic Technologies, 1999. **9**.
75. Smith MH, Denninghoff KR, Lompado A, Hillman LW, *Retinal vessel oximetry: Toward absolute calibration.* Proc. SPIE, 2000. **3908**.
76. Beach JM, Schwenzer KJ, Srinivas S, Kim D, Tiedeman JS, *Oximetry of retinal vessels by dual-wavelength imaging: calibration and influence of pigmentation.* Journal of Applied Physiology, 1999. **86**: p. 748-758.
77. Beach J, *Spectral reflectance technique for retinal blood oxygen evaluation in humans.* Proc. AIPR, 2002. **31**.
78. Hammer M, Thamm E, Schweitzer D, *A simple algorithm for in vivo ocular fundus oximetry compensating for non-haemoglobin absorption and scattering.* Physics in Medicine and Biology, 2002. **47**: p. 233-238.
79. Hardarson SH, Harris A, Karlsson RA, Halldorsson GH, Kagemann L, Rechtman E, Zoega GM, Eysteinsson T, Benediktsson JA, Thorsteinsson A, Jensen PK,

Beach J, Stefánsson E, *Automatic retinal oximetry.* Investigative Ophthalmology & Visual Science, 2006. **47**(11).

80. Narasimha-Iyer H, Beach JM, Khoobehi B, Ning J, Kawano H, Roysam B, *Algorithms for automated oximetry along the retinal vascular tree from dual-wavelength fundus images.* Journal of Biomedical Optics, 2005. **10**(5).
81. Ramella-Roman JC, Mathews SA, *Spectroscopic measurements of oxygen saturation in the retina.* IEEE Journal of Selected Topics in Quantum Electronics, 2007. **13**(6).
82. Hammer M, Vilser W, Riemer T, Schweitzer D, *Retinal vessel oximetry-calibration, compensation for vessel diameter and fundus pigmentation, and reproducibility.* Journal of Biomedical Optics, 2008. **13**(5).
83. Üzümcü M, Vos FM, Vossepoel AM, van der Heijde GL, *theoretical analysis of a spectrophotometric technique for measuring oxygen saturation in retinal vessels.* Proc. ASCI, 2000. **6th Annual Conf. Adv. School Comp. Imag.**: p. 117-121.
84. Lompado A, Smith MH, Hillman LW, Denninghoff KR, *Multi-spectral confocal scanning laser ophthalmoscope for retinal vessel oximetry.* Proc. SPIE, 2000. **3920**.
85. Arimoto H, Furukawa H, Hangai M, *PLS Regression approach for oxygen saturation in spectroscopic fundus imaging.* Ophthalmic technologies, 2006. **6138**: p. 8.
86. Styles IB, Calcagni A, Claridge E, Orihuela-Espina F, Gibson JM, *Quantitative analysis of multi-spectral fundus images.* Medical Image Analysis, 2006. **10**: p. 578–597.
87. Khoobehi B, Ning J, Puissegur E, Bordeaux K, Balasubramanian M, Beach J, *Retinal oxygen saturation evaluation by multi-spectal fundus imaging.* Medical Imaging (proc of SPIE), 2007. **6511**: p. 6.
88. Arimoto H, Furukawa H, *Retinal blood oxygen saturation mapping by multispectral imaging and morphological angiography.* IEEE Engineering in Medecine and Biology Society 2007. **29th Annual International Conference**: p. 1627-1630.

89. Schweitzer D, Hammer M, Thamm JK, Konigsdorffer E, Strobel J, *In vivo measurement of the oxygen saturation of retinal vessels in healthy volunteers.* IEEE Transactions on Biomedical Engineering, 1999. **46**(12): p. 1454-1465.
90. Faubert J, Diaconnu V, *On-line and real-time spectroreflectrometry measurement of oxygenation in a patient's eye.* U.S. Patent 5,919,132, 1999.
91. Diaconnu V, *Multichannel spectroreflectometry: a noninvasive method for assessment of on-line hemoglobin derivaties.* Applied Optics, 2009. **48**(10): p. 52-61.
92. Heaton LC, Smith MH, Denninghoff KR, Hillman LW, *Handheld four-wavelength retinal vessel oximeter.* Ophthalmic Technologies X, 2000: p. 227-233.
93. Denninghoff KR, Smith MH, *Optical model of the blood in large retinal vessels.* Journal of Biomedical Optics, 2000. **5**(4): p. 371–374.
94. Denninghoff KR, Smith MH, Lompado A, Hillman LW, *Retinal venous oxygen saturation and cardiac output during controlled hemorrhage and resuscitation.* Journal of Applied Physiology, 2003. **94**: p. 891-896.
95. Harvey AR, Lawlor J, McNaught AI, Williams JW, Fletcher-Holmes DW, *Hyperspectral imaging for the detection of retinal diseases.* Proc. SPIE, 2002. **4816**.
96. Khoobehi B, Beach J, Kawano H, Lanoue M, Chander D, *Non-invasive measurement of oxygen saturation in optic nerve head tissue.* Proc. SPIE, 2004. **5325**.
97. Khoobehi B, Beach J, Kawano H, *Hyperspectral imaging for measurement of oxygen saturation in the optic nerve head.* Investigative Ophthalmology & Visual Science, 2004. **45**(5): p. 9.
98. Alabboud I, Muyo G, Gorman A, Mordant D, McNaught A, Petres C, Petillot YR, Harvey AR, *New spectral imaging techniques for blood oximetry in the retina.* Proc. SPIE-OSA Biomedical Optics, 2007. **6631**.
99. Johnson WR, Wilson DW, Fink W, Humayun M, Bearman G, *Snapshot hyperspectral imaging in ophthalmology.* Journal of Biomedical Optics, 2007. **12**(1).

100. Hammer M, Riemer T, Vilser W, Gehlert S, Schweitzer D, *A new imaging technique for retinal vessel oximetry – principles and first clinical results in patients with retinal arterial occlusion and diabetic retinopathy.* Ophthalmic Technologies, 2009. **19**.

101. Tsao MU, Sethna SS, Sloan CH, Wyngarden LJ, *Spectrophotometric determination of the oxygen saturation of whole blood.* Journal of Biological Chemistry, 1955. **217**: p. 479-488.

102. Brown LJ, *A new instrument for the simultaneous measurement of total hemoglobin o/o oxyhemoglobin, o/o carboxyhemoglobin, o/r, methemoglobin and oxygen content in whole blood.* IEEE Transactions on Biomedical Engineering, 1980. **27**(3): p. 132-138.

103. Schmitt JM, Mihm FG, Meindl JD, *New methods for whole blood oximetry.* Annals of Biomedical Engineering, 1986. **14**: p. 35-52.

104. Schmitt JM, Meindl JD, Mihm FG, *An integrated circuit-based optical sensor for in vivo measurement of blood oxygenation.* IEEE Transactions on Biomedical Engineering, 1986. **33**(2).

105. Takatani S, Noda H, Takano H, Akutsu T, *A miniature hybrid reflection type optical sensor for measurement of hemoglobin content and oxygen saturation of whole blood.* IEEE Transactions on Biomedical Engineering, 1988. **35**(3): p. 187-198.

106. de Kock JP, Tarassenko L, *In vitro investigation of the factors affecting pulse oximetry.* Journal of Biomedical Engineering, 1991. **13**.

107. McCormick PW, Lewis GD, Dujovny M, Ausman JI, Stewart M, Widman RA, *Correlation of results obtained by in-vivo optical spectroscopy (INVOS®) with measured blood oxygen saturation using a positive linear regression fit.* Proc. SPIE, 1992. **1641**.

108. Fine I, Weinred A, *Multiple-scattering effects in transmission oximetry.* Medical & Biological Engineering & Computing, 1993. **31**: p. 516-522.

109. Takatani S, Ling J, *Optical oximetry sensors for whole blood and tissue.* IEEE Engineering in Medecine and Biology 1994. **13**.

110. Cysewska-Sobusiak A, *A modern approach to the determination of expanded uncertainty in noninvasive blood oximetry.* Measurement, 1999. **25**: p. 123-134.
111. Wu C, Kenny MA, Huang M-C, Afromowitz MA, Yager P, *Feasibility study of the spectroscopic measurement of oxyhemoglobin using whole blood without pre-treatment.* Analyst, 1998. **123**: p. 477-481.
112. Ushizima MR, Muhlen SS, Cestari IA, *A low-cost transmittance transducer for measurement of blood oxygen saturation in extracorporeal circuits.* IEEE Transactions on Biomedical Engineering, 2001. **48**(4): p. 495-499.
113. Cysewska-Sobusiak A, *Optoelectronic blood oximetry as a tool of health safety monitoring.* Proc. SPIE, 2001. **4535**.
114. Franceschini MA, Boas DA, Zourabian A, Diamond SG, Nadgir S, Lin DW, Moore JB, Fantini S, *Near-infrared spiroximetry: noninvasive measurements of venous saturation in piglets and human subjects.* Journal of Applied Physiology, 2002. **92**: p. 372–384.
115. Yang S, Batchelder PB, Raley DM, *Effects of tissue outside of arterial blood vessels in pulse oximetry: a model of two-dimensional pulsation.* Journal of Clinical Monitoring and Computing, 2007. **21**: p. 373–379.
116. Van Norren D, Tiemeijer LF, *Spectral reflectance of the human eye.* Vision Research, 1986. **26** (2): p. 313-320.
117. Delori FC, Pfilbsen KP, *Spectral reflectance of the human ocular fundus.* Applied Optics, 1989. **28**(6).
118. Delori FC, *Spectrophotometer for noninvasive measurement of intrinsic fluorescence and reflectance of the ocular fundus.* Applied Optics, 1994. **33**(31).
119. Thamm E, Schweitzer D, Hammer M, *A data reduction scheme for improving the accuracy of oxygen saturation calculations from spectrometric in vivo measurements.* Physics in Medicine and Biology 1998. **43**: p. 1401-1411.
120. Hammer M, Schweitzer D, *Quantitative reflection spectroscopy at the human ocular fundus.* Physics in Medicine and Biology, 2002. **47**: p. 179-191.
121. Berendschot TT, DeLint PJ, van Norren D, *Fundus reflectance—historical and present ideas.* Progress in Retinal and Eye Research, 2003. **22**: p. 171–200.

122. Cohen AJ, Laing RA, *Multiple scattering analysis of retinal blood oximetry.* IEEE Transactions on Biomedical Engineering, 1976. **23**(5).
123. Steinke JM, Shepherd AP, *Role of light scattering in whole blood oximetry.* IEEE Transactions on Biomedical Engineering, 1986. **33**(3): p. 294-301.
124. van de Kraats J, Berendschot TT, van Norren D, *The pathways of light measured in fundus reflectometry.* Vision Research, 1996. **36**(15): p. 2229-2247.
125. Smith MH, Denninghoff KR, Lompado A, Hillman LW, *Effect of multiple light paths on retinal vessel oximetry.* Applied Optics, 2000. **39**(7).
126. Hammer M, Leistritz S, Leistritz L, Schweitzer D, *Light paths in retinal vessel oxymetry.* IEEE Transactions on Biomedical Engineering, 2001. **48**(5).
127. Bass M, *Handbook of Optics-Vol 3: Vision and Vision Optics.* McGraw Hill. **3**.
128. Hammer M, Leistritz S, Leistritz L, Schweitzer D, Thamm E, Donnerhacke K-H, *Monte-Carlo simulation of retinal vessel profiles for the interpretation of in-vivo oxymetric measurements by imaging fundus reflectometry* Proc. SPIE, 1997. **3192**.
129. Smith MH, Denninghoff KR, Lompado A, Woodruff JB, Hillman LW, *Minimizing the influence of fundus pigmentation on retinal vessel oximetry measurements.* Proc. SPIE, 2001. **4245**.
130. Smith G, Atchison D, *The Eye and Visual Optical Instruments.* Cambride University Press, 1997.
131. Levin RE, *Recommended Practice for Photobiological Safety for Lamps and Lamp Systems - General Requirements.* American National Standards Institute, 2005. **RP-27.1-05**.
132. Boyd RW, *Radiometry and the Detection of Optical Radiation.* John Wiley & Sons, Inc., 1983.
133. Hecht E, *Optics.* Addison Wesley, 1997.
134. Born M, Wolf E, *Principles of Optics.* Cambride University Press, 1999.
135. *http://electron9.phys.utk.edu/optics421/modules/m3/Stops.htm.*
136. Fisher LD, Van Belle G, *Biostatistics: A Methodology for the Health Sciences.* John Wiley & Sons, Inc., 1993.

137. Streekstra GJ, Hoekstra AG, Nijhof E-J, Heethaar RM, *Light scattering by red blood cells in ektacytometry: Fraunhofer versus anomalous diffraction.* Applied Optics, 1993. **32**(13): p. 2266-2272.
138. Nilsson AMK, Alsholm P, Karlsson A, Andersson-Engels S, *T-matrix computations of light scattering by red blood cells.* Applied Optics, 1998. **37**(13): p. 2735-2748.
139. Borovoi AG, Naats EI, Oppel UG, *Scattering of light by a red blood cell.* Journal of Biomedical Optics, 1998. **3**(3): p. 364-372.
140. Shvalov AN, Soini JT, Chernyshev AV, Tarasov PA, Soini E, Maltsev VP, *Light-scattering properties of individual erythrocytes.* Applied Optics, 1999. **38**(1): p. 230-235.
141. Eremina E, Eremin Y, Wriedt T, *Analysis of light scattering by erythrocyte based on discrete sources method.* Optics Communications, 2004. **244**: p. 15-23.
142. Karlsson A, He J, Swartling J, Andersson-Engels S, *Numerical simulations of light scattering by red blood cells.* IEEE Transactions on Biomedical Engineering, 2005. **52**(1): p. 13-18.
143. Zohdi TI, Kuypers FA, *Modelling and rapid simulation of multiple red blood cell light scattering.* Journal of the Royal Society Interface, 2006. **3**: p. 823-831.
144. Reynolds L, Johnson C, Ishimaru A, *Diffuse reflectance from a finite blood medium: applications to the modeling of fiber optic catheters.* Applied Optics, 1976. **15**(9): p. 2059-2067.
145. Steinke JM, Shepherd AP, *Comparison of Mie theory and the light scattering of red blood cells.* Applied Optics, 1998. **27**(9): p. 4027-4033.
146. Hammer M, Schweitzer D, Michel B, Thamm E, Kolb A, *Single scattering by red blood cells.* Applied Optics, 1998. **37**(31): p. 7410-7418.
147. Twersky V, *Absorption and multiple scattering by biological suspensions.* Journal of the Optical Society of America, 1970. **60**(8): p. 1084-1092.
148. Flock ST, Wilson BC, Patterson MS, *Total attenuation coefficient and scattering phase function of tissues and phantom materials at 633 nm.* Medical Physics, 1987. **14**: p. 835-841.

149. Yaroslavsky AN, Yaroslavsky IV, Goldbach T, Swarzmaier H-J, *The optical properties of blood in the near infrared spectral range.* Proc. SPIE, 1996. **2678**: p. 314-324.

150. Hammer M, Yaroslavsky AN, Schweitzer D, *A scattering phase function for blood with physiological haematocrit.* Physics in Medicine and Biology, 2001. **46**: p. 65-69.

151. Meinke M, Muller G, Helfmann J, Friebel M, *Optical properties of platelets and blood plasma and their influence on the optical behavior of whole blood in the visible to near infrared wavelength range.* Journal of Biomedical Optics, 2007. **12**(1): p. 014024-014032.

152. Faber DJ, Aalders MCG, Mik EG, Hooper BA, van Gemert MJC, van Leeuwen TG, *Oxygen saturation-dependent absorption and scattering of blood.* Physical Review Letters, 2004. **93**(2).

153. Kocsis L, Herman P, Eke A, *The modified Beer–Lambert law revisited.* Physics in Medicine and Biology, 2006. **51**.

APPENDIX A: SPECTROSCOPY PRINCIPLES

Introduction

This document reviews the calculations in the spectroscopy measurements using the retinal oximetry device Ocean Optics spectrometer in single pass and double pass configurations, as well as the Olis Cary 14 spectrophotometer. The light paths involved in each setup and the calculations of the transmission spectrum will be reviewed. The calculations for the single pass configuration described here are the same as the experiments in Article I referred to as transmitted signal plus small angle forward scatter.

Device Single Pass Spectroscopy

The light paths involved in the single pass spectroscopy configuration are similar to a standard transmission spectroscopy experiment (figure A.1).

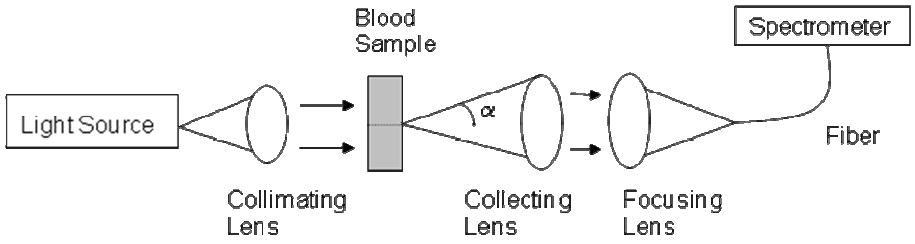

Figure A.1: Schematic diagram of experimental setup in single pass

The measured transmitted signal will depend on the spectrum of all the optical elements in the light paths and can be expressed as

(A-1)

$$Sample_{sin\,gle}(\lambda) = L(\lambda) \cdot O_1(\lambda) \cdot H(\lambda) \cdot Cuv(\lambda) \cdot Blood(\lambda) \cdot O_2(\lambda) \cdot F(\lambda) \cdot D(\lambda) + I_N(\lambda)$$

where $Sample_{single}(\lambda)$ is the measured transmitted signal of a blood sample, $L(\lambda)$ is the output spectrum of the light source, $O_1(\lambda)$ is the spectral transmission of the optical elements preceding the sample, $H(\lambda)$ is the spectral transmission of the cuvette holder, $Cuv(\lambda)$ is the spectral transmission of the cuvette (optical cell), $Blood(\lambda)$ is the spectral transmission of the blood sample, $O_2(\lambda)$ is the spectral transmission of the optical elements succeeding the sample, $F(\lambda)$ is the spectral transmission of the collection fiber, $D(\lambda)$ is the spectral response of the detector and $I_N(\lambda)$ is the noise in the system. To isolate the transmission spectrum of the blood sample, we must divide by a reference. A de-ionized (DI) water filled cuvette is placed in the holder for the measurement of the reference spectrum expressed as

(A-2)

$$Reference(\lambda) = L(\lambda) \cdot O_1(\lambda) \cdot H(\lambda) \cdot Cuv(\lambda) \cdot Water(\lambda) \cdot O_2(\lambda) \cdot F(\lambda) \cdot D(\lambda) + I_N(\lambda)$$

where $Water(\lambda)$ is the transmission spectrum of DI water. Correcting for noise and dividing the 2 equations gives

(A-3) $$T_{blood-single}(\lambda) = \frac{Sample(\lambda) - I_N(\lambda)}{Reference(\lambda) - I_N(\lambda)} = \frac{Blood(\lambda)}{Water(\lambda)}$$

where $T_{blood}(\lambda)$ is the calculated transmittance of the blood sample. We can see from equation (A-3) that to isolate the transmittance spectrum of blood we need to multiply by the transmittance of DI water. The reason we insert DI water into the reference cuvette instead of keeping it empty is to match the reflections of light at the cuvette interfaces.

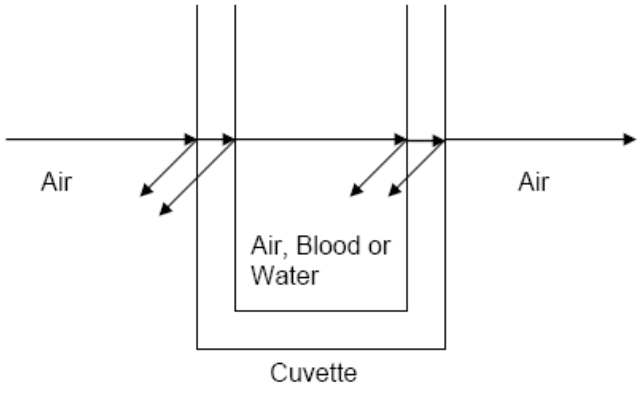

Figure A.2: Reflections at different cuvette interfaces

The amount of reflection at each interface is determined by the difference in refractive index of the medium on both sides of the interface (equation (A-4)).

(A-4) $$R(\lambda) = \left(\frac{n_2(\lambda) - n_1(\lambda)}{n_2(\lambda) + n_1(\lambda)} \right)^2$$

where $n_1(\lambda)$ and $n_2(\lambda)$ are the refractive indices of the mediums of the interface and $R(\lambda)$ is the reflectance. Blood has a refractive index of approximately 1.383 at 590 nm [1] while water has a refractive index of 1.333 at 590 nm [2]. The difference of total reflectance between a blood filled cuvette and a DI water filled cuvette is 0.4%, while the difference between a blood filled cuvette and an empty cuvette is 7.7%. Inserting DI water in the reference cuvette reduces the reflectance error by 7.3%. Since the transmittance of water is over 99.9% in the wavelength range considered for oximetry [3], the effects of water were neglected.

Device Double Pass Spectroscopy

In the double pass experimental setup, the light paths involved can increase the complexity of the spectroscopy calculations if not properly taken into account (figure A.3)

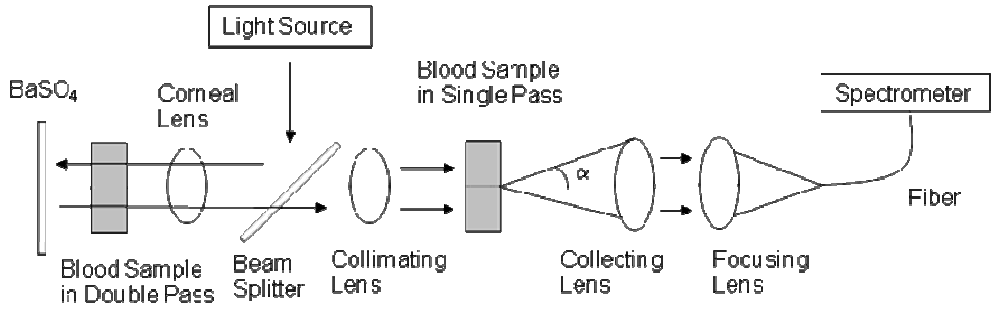

Figure A.3: Schematic diagram of double pass spectroscopy measurements

The challenge faced in any double pass systems is the reflections that are captured in the transmitted signal and can affect the transmission spectrum of the measured sample. An

easy way to avoid this problem is to tilt the cuvette slightly so that the optical system does not capture the unwanted reflections. When the cuvette is tilted, the sample transmission spectrum reduces to an equation similar to (A-1) and the transmittance is given by

$$\text{(A-5)}\quad T_{blood-double}(\lambda)=\frac{Sample(\lambda)-I_N(\lambda)}{Reference(\lambda)-I_N(\lambda)}=\frac{Blood(\lambda)\cdot Blood(\lambda)}{Water(\lambda)\cdot Water(\lambda)}$$

Device Transmission Spectrum Calculations

The signal data from the Ocean Optics spectrometer is given every 0.3 nm from 339.71 nm to 1022.28 nm (step size varies with wavelength). Before calculating the transmittance, the signals are binned in 2 nm steps and then equations (A-3) and (A-5) are applied to the data. The absorbance is calculated by

$$\text{(A-6)}\quad A_{blood}(\lambda)=-log\left(T_{blood}(\lambda)\right)$$

and the results of (A-6) are then interpolated by the SigmaPlot function “interpolate” to match the haemoglobin extinction coefficients given by Phral [4].

Olis Cary 14 Spectroscopy

The Olis spectrophotometer is a scanning spectrometer that captures the sample and reference spectrum simultaneously. The advantage of such a system is that the light source intensity is exactly the same for the sample and reference spectrum, thus the light source intensity fluctuations do not affect the accuracy of the transmittance spectrum.

Since the sample and reference spectrum do not have the same light paths however, the difference in these light paths must be taken into account (figure A.4)

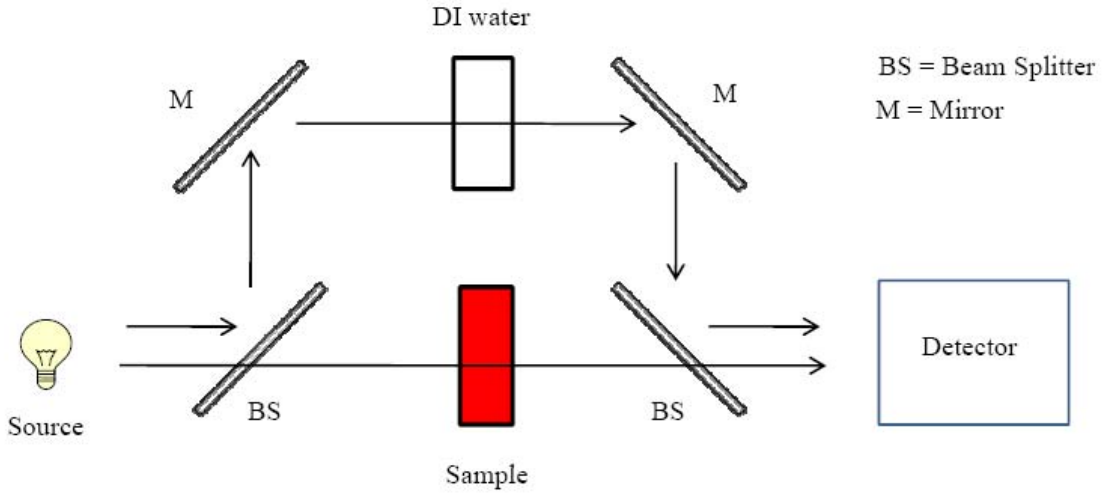

Figure A.4: Schematic diagram of light paths in Olis system

The measured spectra from the sample and reference arms are given by

(A-7) $Sample(\lambda) = L(\lambda) \cdot O_1(\lambda) \cdot H(\lambda) \cdot Cuv(\lambda) \cdot Blood(\lambda) \cdot O_2(\lambda) \cdot D_1(\lambda) + I_N(\lambda)$

(A-8) $Reference(\lambda) = L(\lambda) \cdot O_3(\lambda) \cdot H(\lambda) \cdot Cuv(\lambda) \cdot O_4(\lambda) \cdot D_2(\lambda) + I_N(\lambda)$

where $O_1(\lambda)$, $O_2(\lambda)$, $O_3(\lambda)$ and $O_4(\lambda)$ are the spectral transmission of the different light paths and $D_1(\lambda)$ and $D_2(\lambda)$ are the respective detector responses for the different measurement areas of the detector depending on the light paths. Dividing equation (A-7) by (A-8) gives

(A-9) $$T_{blood}(\lambda) = \frac{Sample(\lambda) - I_N(\lambda)}{Reference(\lambda) - I_N(\lambda)} = Blood(\lambda) \cdot \frac{O_1(\lambda) \cdot O_2(\lambda) \cdot D_1(\lambda)}{O_3(\lambda) \cdot O_4(\lambda) \cdot D_2(\lambda)}$$

where we define the Beam Ratio as

(A-10) $$BR(\lambda) = \frac{O_1(\lambda) \cdot O_2(\lambda) \cdot D_1(\lambda)}{O_3(\lambda) \cdot O_4(\lambda) \cdot D_2(\lambda)}$$

The Beam Ratio is found by acquiring a sample and reference spectrum with no sample in the sample path. The transmittance of blood is then obtained by dividing (A-9) by (A-10). For the same reasons as in the Ocean Optics measurement, a DI filled cuvette is included in the reference path.

References

1. Li H, Lin L, Xie S, *Refractive index of human blood with different types in the visible and near-infrared ranges.* Laser-Tissue Interaction XI: Photochemical, Photothermal and Photomechanical, 2000. 3914
2. Fernandez-Prini R, Dooley RB, *Release on the refractive index of ordinary water substance as a function of wavelength, temperature and pressue.* The International Association for the Properties of Water and Steam, 1997.
3. Pope RM, Fry ES, *Absorption spectrum (380-700 nm) of pure water II. Integrating cavity measurements.* Applied Optics, 1997, 36(33): p. 8710-8723.
4. Prahl S, *http://omlc.ogi.edu/spectra/hemoglobin/index.html*

APPENDIX B: RESEARCH ETHICS APPLICATION 1

NOTE: ALL DOCUMENTATION MUST BE TYPE WRITTEN.

Use the "TAB" key to move between fields.

1. PROTOCOL TITLE

A Pilot Study to Evaluate Optical Spectral Fitting as a Method for Detecting Oxygen Saturation in Whole Blood in a Healthy Population.

2. PRIMARY INVESTIGATOR FOR MULTICENTRE TRIALS

Last Name		First Name	
Title/Position		Department & Location (or full mailing address)	
Tel.			
Email		Fax	

3. PRINCIPAL INVESTIGATOR AT THE OTTAWA HOSPITAL

If the Principal Investigator does not hold an academic appointment, indicate who the responsible investigator will be.
Investigators must complete the *Tri-Council Policy Statement On-lineTutorial* and submit a copy of their certificate to The tutorial can be found at:

Last Name	Munger	First Name	Rejean
Title/Position		Tel.	
		Fax	
Dept/Unit & Location (full mailing address)		Email	
Division/ Portfolio		Signature:	

4. CO-INVESTIGATORS AT THE OTTAWA HOSPITAL

Last Name	LeBlanc	First Name	Serge
Title/Position		Tel.	
		Fax	
Dept/Unit & Location (full mailing address)		Email	
Division/ Portfolio		Signature:	

Last Name	Atanya	First Name	Monica
Title/Position		Tel.	
		Fax	
Dept/Unit & Location (full mailing address)		Email	
Division/ Portfolio		Signature:	

Last Name	Dollin	First Name	Michael
Title/Position		Tel.	
		Fax	
Dept/Unit & Location (full mailing address)		Email	
Division/ Portfolio		Signature:	

Last Name		First Name	
Title/Position		Tel.	( ) - ext.
		Fax	( ) -
Dept/Unit & Location (full mailing address)		Email	
Division/ Portfolio		Signature:	

Last Name		First Name	
Title/Position		Tel.	( ) - ext.
		Fax	( ) -
Dept/Unit & Location (full mailing address)		Email	
Division/ Portfolio		Signature:	

If you need more space an additional form for co-investigators is available on the website.

5. APPROVAL BY INVESTIGATOR'S DEPARTMENT/DIVISION HEAD/ CLINICAL MANAGER/CHIEF (THIS SHOULD NOT BE THE PRINCIPAL INVESTIGATOR AND/OR CO-INVESTIGATOR)

Hospital and university division and department administrators are responsible for academic activities within their unit, and may provide guidance and support to investigators. The purpose of this signature section is to ensure that administrators are aware of research activities and the impact of these activities.

- ☐ The study answers a reasonable scientific/clinical question and is consistent with hospital/faculty policies and mission.
- ☐ The study resources (budget, space, support staff) are adequate to support the study.
- ☐ The local investigators are qualified to perform the study.
- ☐ There are an adequate number of research participants suitable to be approached for enrolment for this study. This population is not already over-subscribed in clinical research.

I have reviewed this application and agree it should be submitted for ethics approval.

Name	Dr. S. Gilberg	Contact Number : ext.
Title/Position		Signature
Dept/Unit & Location (full mailing address)		
Date		

6. REVIEW TYPE

Please indicate whether you are requesting full or expedited review. (Please see our website www.ohri.ca/ohreb for more information on what qualifies for expedited review.)

☐	Full Review
☒	Expedited Review

7. STUDY TYPE

Describe the Research Project by checking as many of the following as apply:
Study Type:

☒	Investigator driven and sponsored by OHRI
☒	Experimental Research/Clinical Trial
☐	Interventional Research
☐	Non-Interventional Research
☐	Observational Research
☒	Pilot
☐	Sequel to previously approved project **(Protocol #: _____)**
☐	Genetic Research (Addendum 1 must be included with completed application)

☐	Program Evaluation						
☐	New therapeutic method						
☐	Medical Device Research Please attach a letter from sponsor indicating Health Canada application/approval. This is mandatory prior to final REB approval.						
	☐ **Health Canada Application/Approval** is attached (insert as next page)						
	☐ **Health Canada Application/Approval** will be forwarded.						
Location of the Study:							
☒	Single Centre Trial			☐	Multicentre Trial		
Study Design:							
☐	Randomized, controlled trial						
☐	Phase I	☐	Phase II	☐	Phase III	☐	Phase IV
☐	Open Label	☐	Single Blinded	☐	Double Blinded (or more)		
☐	Case-Control study						
☐	Cohort study						
☐	Interview, survey or questionnaire, observation						
☒	Database Research ☒ New ☐ Existing						
☐	Chart Review						
☐	Compassionate Use						
☐	N of 1 Study						
☐	Quality Assurance						
Drug Study: ☐ **Yes** ☒ **No**							
☐	Involves unusually elevated doses of available drugs						
☐	Involves anticipated high incidence of toxicity						
☐	Drug being used for currently approved indication						
☐	Approved Drug being used for a non-approved indication Please attach a letter from sponsor indicating Health Canada application/approval. This is mandatory prior to final REB approval.						
	☐ **Health Canada Application/Approval** is attached (insert as next page)						
	☐ **Health Canada Application/Approval** will be forwarded.						
☐	Investigational non-approved drug: Please attach a letter from sponsor indicating Health Canada application/approval. This is mandatory prior to final REB approval.						
	☐ **Health Canada Application/Approval** is attached (insert as next page)						
	☐ **Health Canada Application/Approval** will be forwarded.						

8. PURPOSE AND OBJECTIVES

Please state clearly the hypothesis to be tested, in lay terms.

Blood oxygen saturation levels are typically measured in a clinical environment by a pulse oximeter, a CO oximeter or a blood gas analyzer. Both the pulse oximeter and the CO oximeter, which is considered the gold standard in oxygen saturation measurements, take advantage of the different light absorption properties of oxygenated and de-oxygenated hemoglobin to measure the oxygen content in blood. Since oxyhemoglobin and de-oxyhemoglobin absorb light differently, by measuring the ratio of light absorption in blood at different wavelengths, the percentages of oxyhemoglobin and de-oxyhemoglobin in blood can be determined. A pulse oximeter uses the ratio of 2 wavelengths to determine oxygen saturation in blood while a CO oximeter can use up to 17 wavelengths to measure oxygen in blood. In Dr. Munger's visual optics laboratory at the Eye Institute, we have developed a model, based on the same operating principles as the CO oximeter, which utilizes the full spectrum of light for the visible and near infrared range to measure oxygen content in blood. In theory, using the full spectrum of light instead of only a few wavelengths will improve the accuracy of the blood oxygen saturation measurements. The proposed model fits the optical spectral response of blood to a theoretical absorption model based on the spectral absorption of oxyhemoglobin and de-oxyhemoglobin.

The purpose of this pilot study is to evaluate the proposed optical spectral fitting model as a method for detecting oxygen saturation in whole blood in a healthy population. In this pilot study, optical spectroscopy will be performed on blood samples taken from a control group of normal, healthy individuals. The samples will be analyzed using the optical spectral fitting model in order to determine oxygen saturation levels in the blood. The results will be compared to CO oximeter measurements taken on the same samples.

The research hypothesis for this pilot study is that the proposed optical spectral fitting model can be used to extract oxygen saturation levels from whole blood samples. This pilot study will be used to validate this hypothesis in normal, healthy controls.

Provide the rationale for the study.

For most tissues in the human body, oxygen plays an essential role in its normal function. Therefore, measuring oxygen saturation levels in blood is a critical component of the standard care of a patient. Oximetry measurements not only give information on oxygen consumption and supply, but it also provides information on the metabolic activity of a tissue or organ, oxygen being a key component of metabolic activity. Since oxygen plays such a critical role in the body's normal function, it is imperative that the instruments and methods developed to measure oxygen content in blood be accurate both in normal healthy blood and in diseased blood as well.

Recently, a new model was developed in Dr. Munger's visual optics laboratory at the Eye Institute to calculate oxygen saturation in blood samples. This model is based on the same operating principles as the current clinical instruments used to measure oxygen (pulse oximeter and CO oximeter). In theory, this model should be more accurate than current methods used for oxygen saturation measurements. However, this model was tested on a sample population of end stage renal disease patients undergoing hemodialysis from a study that is currently under way (**REB approved: protocol number 2005233-01H**), and the results of the oxygen saturation measurements did not match the values obtained from a CO oximeter. We believe there are two possible explanations for this result. Either the proposed model isn't complete and is unable to accurately measure oxygen saturation levels in blood, or, there may be something happening in the blood chemistry during hemodialysis that is affecting our ability to accurately measure oxygen. It is therefore important to test the proposed model on a normal healthy population to see if it can accurately measure oxygen saturation levels in these blood samples. Should the result of our investigation find that indeed the model is able to predict oxygen levels in healthy normal blood, but not in hemodialysis patients, this would mean that the current oxygen saturation measurements taken on these patients is most likely inaccurate. The standard care protocol of hemodialysis patients would therefore need to be reviewed and modified and a new accurate method of determining oxygen saturation levels in these patients would need to be developed.

In addition to the hemodialysis study, the visual optics lab is also conducting a study on patients with retinal degenerative diseases (**REB approved: protocol number 2009164-01H**). The proposed model to measure oxygen saturation levels will be used to measure oxygen content on the retinal tissue and vessels. A validation of this model is therefore necessary for this study as well.

STUDY DURATION	Start Date : **30/11/2009** DD/MM/YYYY	End Date : **30/11/2010** DD/MM/YYYY

9. RECRUITMENT

Describe how these research participants will be identified and recruited. **(Only members of the participant's health care team should contact patients at the Ottawa Hospital.)**

In addition, please ensure you address the following:

- If initial contact is by letter or if an **advertisement** is to be used, attach a copy.
- How will the researcher ensure that there are no breaches of patient **privacy**?
- How will the possibility of **coercion**, duress or undue incentive be avoided or minimized?

A total of 10 healthy, normal volunteers as a control group will be recruited for this pilot study. The control group will be chosen from the staff at the Eye institute at the General Campus. Control research participants will be recruited from the staff and students of the Eye Institute with no affiliation with either of the applicants. Recruitment will be done through a general email to the Eye Institute mailing list. (Email included in package) The email will be distributed by an Eye Institute Administrative Assistant. Copies of the email will also be left on a table at departmental assemblies such as Grand Rounds and Research Rounds and an anoucement will be made that anyone who whishes to learn more abou the study can pick up a copy of the email. This will prevent any feeling of coercion in regards to participating in the study. Voluntary participation without the fear of repercussions will also be stressed.
The identified controls will be approached for voluntary consent, the time to be scheduled by Dr. Rejean Munger. A consent form has been designed and will be accompanied by an explanation of the amount of blood to be collected and the purpose of the research (consent form attached). Consent forms will be held in the strictest confidence by Dr. Rejean Munger according to standard clinical trial practices. In this pilot study, no records bearing the names of the participants will leave the Ottawa Hospital. All blood samples sent for analysis will be coded with a study number only.

Are recruitment incentives provided? ☐ Yes ☒ No
If yes, please describe what they are, and when they will be provided.

Are controls involved? ☒ Yes ☐ No
Does the study include subjects in a control group? ☐ Yes ☒ No
If controls are involved, if their selection and/or recruitment differ from the above, provide details.

Oxygen saturation levels determined by the CO oximeter will be compared to the data obtained with the optical spectral fitting model. Therefore the controls are the blood samples that will be analyzed using CO oximeter (the gold standard).

Does the research include research participants who may not be competent to give informed consent? ☐ Yes ☒ No If yes, justify and explain how consent will be obtained and from whom.

- Number of Centres recruiting globally: **1 (University of Ottawa Eye Institute)**

  ☒ National Study – Country **1**

  ☐ International Study – Country

- Total number of research participants being recruited at all centres globally: **10**

  - Number of research participants to be recruited at each Ottawa Hospital campus:

☐ Civic	☒ General	☐ Riverside	☐ Other
	10		

Provide the rationale for the selected sample size and the methodology used to calculate the sample size:

This sample size is sufficiently small to minimize the burden on the healthy, control population and clinical staff while providing a sufficient sampling to demonstrate proof-of-principle of the optical spectroscopy model with a reasonably broad cross-section of the control population.
The sample size also ensures that the required measurements will be completed in a timely manner (extraction, preparation, measurement and disposal of a given sample within the same day), thereby circumventing issues of sample storage and handling.
This sample size is large enough for a positive test of our research hypotheses, and will allow a broader research study to be conducted in the future with statistical analyses based on a large sample size.

10. DESCRIPTION OF POPULATION

Inclusion Criteria - Who is being recruited and what are the criteria for their selection?

The healthy controls will be chosen from the population of staff at the Eye Institute of the General Campus. Healthy controls will be recruited via email sent by administrative staff, excluding those with any known medication condtions or history, those known or suspected to have hepatitis B or C, or other active infections.

Calls for volunteers will continue until 10 candidates are identified that satisfy the following inclusion criteria:

a. Normal, healthy individual, free of disease who is a staff member at the Eye Institute of the General Campus.

Note: up to but no more than 2 participants will be scheduled at the time by the study coordinator, to allow sufficient time facilitating blood extraction and analyses for the pilot study.

Exclusion Criteria - What research participants are excluded from participation?

Those with any known medical condition, those suspected of having active infections as stated above, and those who do not give consent. These guidelines will also be part of the exclusion criteria:

a. No participant in the group has or is suspected of having hepatitis B, C or any other active infection.
b. Participants must not have eaten one hour prior to blood sample being drawn.
c. Participants must not have experienced rigorous exercise or activity at least one hour prior to sample being drawn.
d. Participants must not have consumed alcohol at least 8 hours prior to sample being drawn

NB: please note that parts a, b, c and d are included to limit any effects in our results.

11. DESCRIPTION OF METHODS AND PROCEDURES
If additional space is required, insert one additional page)

Summary of Methods and Procedures. **Please include a summary of the following**:

- any specific manipulations;
- type, quantity, and route of administration of drugs and radiation; operations; tests; use of medical devices that are prototype or altered from those in clinical use;
- type, and number of interviews or questionnaires; are the questionnaires validated, reliable and have they been pilot tested?
- Are procedures/treatments standard practice or new, what is the risk level?

(Flow diagrams and point form discussion are encouraged and should be appended separately.)

The participants who have responded positively to the request for volunteer will be approached for voluntary consent, the time to be scheduled by Dr. Rejean Munger. They will be taken to a room in the Eye Institute where Dr. Munger will read the consent form to them and the amount of blood to be drawn and purpose of the research will be clearly explained.

Once consent has been given by the participant, the nurse or phlebotomist will draw three blood samples of 3 ml each by venipuncture. Standard practice and precautions of blood draw will be used at all times. Blood samples will be labeled by the nurse of phlebotomist and given to Monica Atanya to bring to the Visual Optics Lab for measurement.

Please refer to the attached research protocol for more details.

12. RISKS

Describe the discomfort or risks that participants may incur as a result of their participation in this research. Also note the following:

- particular risks associated with each procedure, drug, test or other aspect of the protocol.
- delineate, when appropriate, what risks relate to standard care,
- what risks relate to participation in the study.
- quantify risks where possible by providing percentages, or by describing as rare, common, etc.

As this pilot study involves human subjects and the handling of blood, a certain level of risk is inherent. Several measures are incorporated into the research protocol to mitigate this risk. First, qualified Eye Insitute staff members (see staff list) will be performing the clinical portion of the pilot study. Participant contact and consent will be managed by a member of the study staff, and blood extraction will be conducted by qualified Eye Insitute staff members. Transfer and disposal of the blood samples will be handled by Monica Atanya, who has been trained to properly handle blood samples. The patient sample will be chosen to exclude those known or suspected to have hepatitis B or C or active infections, and the Eye Institute staff members will follow universal precaution guidelines for the handling of blood samples.

To minimize participants' impact, a small amount of blood (3 samples of about 3ml each, since only 2ml is needed for each optical measurement) will be extracted by venipuncture one time only. The 3ml required for this study will be collected in 3 separate tubes containing an anti-clotting agent.

Will the management of the participant's condition be prolonged or delayed as a result of the research? ☐ Yes ☒ No
If yes, explain, specifying any risks associated with prolongation or delay.

Are there any standard therapies, diagnostic procedures or information to be withheld from participants for the purpose of the study? ☐ Yes ☒ No
If yes, explain, specifying the risks and benefits to the participants and justify.

Are there stopping rules for the study? **(This does not apply to individual patient withdrawal, but to the study as a whole)** ☐ Yes ☒ No
If yes, please describe.

Is there a data safety monitoring board in place? ☐ Yes ☒ No
If yes, describe the composition of the board.

What procedures in this protocol are additional to those required for **routine** patient care? **(Include the Impact Sheet with applicable attachments for all procedures which are attributable to this study)**

Study is performed using healthy normal research participants. All procedures in this protocol are additional to those required for routine patient care.

Additional to routine patient care, extra equipment (consumables) and staff (research nurse time) is required.

Is a placebo used? ☐ Yes ☒ No
If yes, please justify:

13. POSSIBLE BENEFITS

Describe any possible benefits to the participant as a result of their participation in this research.

As this is a preliminary study there are no direct benefits to the participant. However, research participants may benefit from having their blood saturation levels measured. If abnormality is detected they will be informed of the findings. Indirectly, long-term benefits to patients are possible as a result of the research. Benefits would be in the form of better management of the patient condition.

14. CONFIDENTIALITY

It is the policy of the OHREB that no records with the patient's name leave the Ottawa Hospital.

How will data be protected against breaches in security/privacy? **Be sure to include the following information:**

☒ If the information will be housed in a database, will it be password protected?
Any study information that is housed in a database will be password protected.
☒ Confirm that an independent study number will be assigned to each subject record.
Upon agreeing to be part of this study and after obtaining the signed Informed Consent Form (ICF), participants will be assigned a unique study number, which will be used as the identifier from this point forward.
☒ What information will be collected? (A 'Case Report Form' may be provided with these details). No identifying information should be used such as hospital unique number, OHIP #, etc. if any identifying information is required, justification must be provided.
No identifying information will be collected in the study database, only the study data as described in the Method section.
☒ Date of birth is also considered a personal identifier. Confirm that you are not using date of birth. If it is required, clarify whether month and year of birth will suffice? If you require full date of birth, justification must be provided.
Only month and year of birth will be used.
☒ Indicate how the master list linking the subject to the independent study number will be maintained and safeguarded, and confirm that it will be stored separately and securely.
A Study File and/or Study Database will be created where all Personal Health Information (PHI) will be de-

identified and only the unique study number will appear. Any link between the patient's identifying information and unique study number (Master list) will be kept in a locked office and/or password protected database.

☒ Indicate how data containing Personal Health Information (PHI) will be protected against breaches of privacy. (i.e. locked cabinets? password protected?)

Utmost subject confidentiality will be assured. PHI will be kept in a locked office and/or password protected database.

☒ Indicate who will have access to the study data, and which organizations and/or individuals will have access to PHI for audit purposes. Add the OHREB and Ottawa Health Research Institute (OHRI) to the list of possible reviewers.

Only the study personnel directly involved in the study will have access to the study data. The Ottawa Hospital Research Ethics Board (OHREB) and Ottawa Hospital Research Institute (OHRI) may review study information under the supervision of the PI in the event of an audit.

☒ Confirm that no PHI will be leaving the Ottawa Hospital.

PHI that is not coded will not leave the Ottawa Hospital.

☒ Indicate how long information will be kept after the close of the study? (**25 years** for investigational drug and device studies regulated by Health Canada as outlined in Health Canada's Food and Drug Regulations, Division 5 – Drugs for Clinical Trials Involving Human Subjects, Section C.05.012. For all other studies, records must be kept by the investigator for **15 years**.)

The study records will be kept for a minimum period of 15 years after termination of the study.

☒ Indicate how paper and electronic data will be destroyed once the storage date has expired (shredded? deleted?)

When the storage date has expired paper study documents will be disposed of in confidential waste or shredded. Electronic data will remain password protected.

Names of study participants will be withheld by Dr. Rejean Munger. Optical Spectroscopy testing will be performed on the blood samples at the Principal Investigator's laboratory at the Eye Institute with numbers identifying the samples, corresponding to a single-blinded experimental design.

Optical Spectroscopy data fitted with the Optical Spectral Model will be compared to standard blood test results, again with names removed from the results. Participant information will be held at the Visual Optics laboratory according to standard clinical trial protocol. Only authorized personnel from the Visual Optics laboratory will have access.

15. BUDGET

Has this research been funded? ☒ **YES** ☐ **NO**	
☒ **If <u>YES</u> provide the:** Name of the Agency/Sponsor: **University Medical Research Funds (UMRF)** Amount of funding received: **$ 2,000.00**	☐ **If <u>NO</u> complete the following:** Has funding been applied for: ☐ **YES** ☐ **NO** Name of the Agency/Sponsor: Amount of funding applied for**: $** Date submitted: DD/MM/YYYY
If no funding has been applied for, how will the research be supported? If the study was peer-reviewed, please provide the name of the individual or agency that completed the review. UMRF	
Does the industry-sponsored budget contain appropriate overhead? ☐ A Clinical Trial Agreement has been forwarded to the Contracts Officer ☐ A Clinical Trial Agreement is attached to the OHREB application Have you included a budget summary for the protocol? **(If this is not included, approval of protocol will be delayed. Details on the disbursement of any excess funds received for this study should also be provided.)**	☐ **YES** ☐ **NO** ☒ **N/A** ☒ **YES** ☐ **NO** ☐ **N/A**
Does the REB review fee apply to this study? ☐ A cheque is enclosed ☐ An invoice request is enclosed ☐ A transfer request is enclosed **(All industry sponsored research projects are subject to a $3,000.00 administration fee, and any cooperative group studies that are funded in excess of $3,000.00 per patient.)**	☐ **YES** ☒ **NO** ☐ **N/A**
POTENTIAL CONFLICTS OF INTEREST Please indicate if you have a conflict of interest or separate financial agreements with the sponsor of this study. If yes, please explain.	☐ **YES** ☐ **NO** ☒ **N/A**

16. STAFFING

What staffing will be required? All staff should be listed and this list maintained during the course of the study. Staff must complete the *Tri-Council Policy Statement On-lineTutorial* and submit a copy of their certificate to Hillary Falconer. It can be found at www.pre.ethics.gc.ca

This includes research nurses, research co-ordinators, etc. Research nurses should provide a copy of their Nursing Certificate for the current year, to the Research Services Office if this has not already been done for another study.

Name & Role in Study	Already Employed?	Full-time vs. Part-time	Office/Laboratory Location and Telephone Number If new office or laboratory space is required, the Space Planning & Management section of the Departmental Impact form must be signed and submitted
1. Dr. Rejean Munger Senior Scientist	☒ YES	☒ FT	
	☐ NO	☐ PT	
3. Monica Atanya; perform Optical Spectroscopy measurements on sealed blood samples	☒ YES	☒ FT	
	☐ NO	☐ PT	
4. Serge Emile LeBlanc; perform Optical Spectroscopy measurements on sealed blood samples	☒ YES	☒ FT	
	☐ NO	☐ PT	
2. Gail Kayuk Phlebotomist	☒ YES	☐ FT	
	☐ NO	☒ PT	
5. Nancy Whyte Study Nurse	☒ YES	☐ FT	
	☐ NO	☒ PT	

In the space below please provide:

a) a list of their qualifications:

Dr. Rejean Munger, Senior Scientist, Monica Atanya, B.Sc. Serge Emile LeBlanc, B.Sc. Gail Kayuk, Phlebotomist, Nancy Whyte, RN.

b) a list of the duties to be performed, including delegated/sanctioned medical acts and acts performed under the Regulated Health Professions Act if this has not already been done for another study:

Dr. Rejean Munger will be responsible for the informed consent form process and storage of ICFs. Gail Kayuk and Nancy Whyte will be responsible for the blood collection and handling. These staff members are under the supervision of Dr. W.B. Jackson (see signature below). Monica Atanya will be responsible for blood manipulation and Serge Emile LeBlanc will be responsible for spectral measurements and data analysis.

DEPARTMENTAL IMPACT

Protocol Title:

A Pilot Study to Evaluate Optical Spectral Fitting as a Method for Detecting Oxygen Saturation in Whole Blood in a Healthy Population.

Does the protocol require use of Hospital and/or OHRI resources (equipment, staff, space) over and above those normally required in the standard care of a patient?

Equipment	☒ **YES**	☐ **NO**
Staff	☒ **YES**	☐ **NO**
Space	☐ **YES**	☒ **NO**

Will hospitalization or outpatient visits be required beyond what is required for standard care?0

Outpatient Visits	☐ **YES**	☒ **NO**
Hospitalization	☐ **YES**	☒ **NO**

Indicate impacts associated with this Protocol, by Department:
IF YES is indicated, a signature of an individual authorized to sign for the department must be obtained. (Please see our website for a list of contact names http://www.ohri.ca/ohreb***/)***

			Signature:
Nursing/Phlebotomist	☒ **YES**	☐ **NO**	
Emergency Department	☐ **YES**	☒ **NO**	Please submit Clinical Director's Acknowledgment www.ohri.ca/ohreb/forms.htm
Health Records (See Appendix A)	☐ **YES**	☒ **NO**	Please submit signed Health Records form. www.ohri.ca/ohreb/forms.htm
Laboratory Services	☐ **YES**	☒ **NO**	Please submit signed Lab Impact form. www.ohri.ca/ohreb/forms.htm
Radioisotopes (See Appendix B)	☐ **YES**	☒ **NO**	Please submit Radiation Safety form. www.ohri.ca/ohreb/forms.htm
Diagnostic Imaging (See Appendix B and C)	☐ **YES**	☒ **NO**	Please submit signed Diagnostic Imaging form. www.ohri.ca/ohreb/forms.htm
Pharmacy	☐ **YES**	☒ **NO**	Please submit signed Pharmacy form www.ohri.ca/ohreb/forms.htm
Nutrition And Food Services	☐ **YES**	☒ **NO**	
Opthalmology	☐ **YES**	☒ **NO**	Please submit signed Opthalmology form www.ohri.ca/ohreb/forms.htm
Space Planning & Management	☐ **YES**	☒ **NO**	
Clinical Investigation Unit	☐ **YES**	☒ **NO**	
Cardiopulmonary Services	☐ **YES**	☒ **NO**	

APPENDIX C: INFORMATION CONSENT FORM 1

Protocol Title:	**A Pilot Study to Evaluate Optical Spectral Fitting as a Method for Detecting Oxygen Saturation in Whole Blood in a Healthy Population.**
Principal Investigator:	**Dr. Rejean Munger**
Co-Investigators:	**Serge Emile LeBlanc**
	Monica Atanya

Managed by the University of Ottawa Eye Institute- Clinical Trials Group

INTRODUCTION:
We are asking you to take part in a research study at the Ottawa Hospital. Taking part in this study is completely voluntary. The study is described below. This description tells you about the purpose, additional tests, and risks/discomforts, which you might experience. You should take the time to read this information sheet and discuss any questions you have about your potential participation in this study with the person who explains it to you.

PURPOSE OF THE STUDY:
You are being asked to participate in this research study because you have been identified as a normal, healthy individual, free of disease. The purpose of this pilot study is to evaluate a new optical spectral fitting model as a method for detecting oxygen saturation in whole blood. The status of your blood (using a sample of whole blood) will be analyzed using this novel technique developed at the University of Ottawa Eye Institute. Your blood status will form part of a representative control group of normal, healthy individuals. If this study proves successful, it could help develop a more accurate method of measuring oxygen content in blood.

We are planning on enrolling approximately 10 healthy, normal volunteers as a control group in the research study at the Eye Institute of the General Campus.

STUDY PROCEDURES:
We are asking your permission to draw a total of 3 tubes of blood (approximately 2 teaspoons) at the time scheduled by the study coordinator (this will be at approximately 8am). The drawing of the sample will be done one time only, and will require approximately 10 minutes of your time **Please follow the 3 steps below before coming in for the blood sample draw on your scheduled date and time**.

A) You must not have eaten one hour prior to blood sample being drawn.

B) You must not have experienced rigorous exercise or activity at least one hour prior to sample being drawn.

C) You must not have consumed alcohol at least 8 hours prior to sample being drawn.

NB: please note that these steps are taken to make sure that the blood sample results are not altered.

One blood sample will be sent for blood gas analysis and CO oximetry measurements while the remaining two will be taken to the Visual Optics Laboratory located at the Eye Institute of the General Campus for spectral analysis. The results of the analysis will be compared to clinical oxygen measurements.

RISKS OF PARTICIPATION:
There are no additional risks involved with having this procedure completed, aside from those involved in standard clinical practices for drawing blood. Risks associated with having blood drawn are slight but may include: excessive bleeding, fainting or feeling light-headed, hematoma (blood accumulating under the skin) and infection (a slight risk any time the skin is broken) Every effort will be made to minimize the potential for risk.

BENEFITS OF PARTICIPATION

As this is a preliminary study there are no direct benefits to you. However, you may benefit from having your blood saturation levels measured. If an abnormality is detected, you will be informed of the findings. Indirectly, long-term benefits to patients are possible as a result of the research. Benefits would be in the form of better management of the patient condition.

VOLUNTARY PARTICIPATION:
Your participation in this study is completely voluntary.

CONFIDENTIALITY:
All names of volunteers for the study and study-related information about you will be kept confidential. Representatives of the Ottawa Hospital Research Ethics Board (OHREB), as well as the Ottawa Hospital Research Institute (OHRI), may review your relevant study records for audit purposes. You will not be identifiable in any publications or presentations resulting from this study. No identifiable information will leave the Ottawa Hospital. All blood samples sent to the Visual Optics Laboratory will be coded with a unique study number and your month and year of birth.

The link between your name and the independent study number will only be accessible by the study staff. The link and study files will be stored separately and securely. Both files will be kept for a period of 15 years after the study has been completed. All paper records will be stored in a locked file and/or office. All electronic records will be stored on a hospital server and protected by a user password, again only accessible by the study staff. At the end of the retention period, all paper records will be disposed of in confidential waste or shredded, and all electronic records may be kept or deleted.

QUESTIONS:
If you have any questions about the study, you may contact the following study staff:
Dr. Rejean Munger, Ophthalmology.

The Ottawa Hospital Research Ethics Board (OHREB) has reviewed this protocol. The OHREB considers the ethical aspects of all research studies involving human subjects at The Ottawa Hospital. If you have any questions about your rights as a research subject, you may contact the Chairperson of the Ottawa Hospital Research Ethics Board.

Consent Form

A Pilot Study to Evaluate Optical Spectral Fitting as a Method for Detecting Oxygen Saturation in Whole Blood in a Healthy Population

Consent to Participate in Research

I understand that I am being asked to participate in a research study about oxygen saturation measurements in blood. This study has been explained to me by the study staff.

I have read this 4-page Patient Information Sheet and Consent Form (or have had this document read to me). All my questions have been answered to my satisfaction. If I decide at a later stage in the study that I would like to withdraw my consent, I may do so at any time.

I voluntarily agree to participate in this study.

A copy of the signed Information Sheet and Consent Form will be provided to me.

Signatures

_____
Participant's Name (Please Print)

_____ _____
Participant's Signature Date

Investigator Statement (or Person Explaining the Consent)
I have carefully explained to the research participant the nature of the above research study. To the best of my knowledge, the research participant signing this consent form understands the nature, demands, risks and benefits involved in participating in this study. I acknowledge my responsibility for the care and well being of the above research participant, to respect the rights and wishes of the research participant, and to conduct the study according to applicable Good Clinical Practice guidelines and regulations.

_____
Name of Investigator/Delegate (Please Print)

_____ _____
Signature of Investigator/Delegate Date

APPENDIX D: RESEARCH ETHICS APPLICATION

NOTE: ALL DOCUMENTATION MUST BE TYPE WRITTEN.
Use the "TAB" key to move between fields.

1. PROTOCOL TITLE

Evaluation of a fundus camera equipped with light spectroscopy as a non-invasive tool for measuring retinal oxygen tension in normal and diseased populations

2. PRIMARY INVESTIGATOR FOR MULTICENTRE TRIALS

Last Name		First Name	
Title/Position		Department & Location	
Tel.			
Email		Fax	

3. PRINCIPAL INVESTIGATOR AT THE OTTAWA HOSPITAL

If the Principal Investigator does not hold an academic appointment, indicate who the responsible investigator will be.

Last Name	Munger	First Name	Rejean
Title/Position		Tel.	
		Fax	
Dept/Unit & Location		Email	
Division/ Portfolio		Signature:	

4. CO-INVESTIGATORS AT THE OTTAWA HOSPITAL

Last Name	Hurley	First Name	Bernard
Title/Position		Tel.	
		Fax	
Dept/Unit & Location		Email	
Division/ Portfolio		Signature:	

Last Name	LeBlanc	First Name	Serge
Title/Position		Tel.	
		Fax	
Dept/Unit & Location		Email	
Division/ Portfolio		Signature:	

Last Name	Dollin	First Name	Michael
Title/Position		Tel.	
		Fax	
Dept/Unit & Location		Email	
Division/ Portfolio		Signature:	

Last Name		First Name	
Title/Position		Tel.	( ) - ext.
		Fax	( ) -
Dept/Unit & Location		Email	
Division/ Portfolio		Signature:	

Last Name		First Name	
Title/Position		Tel.	( ) - ext.
		Fax	( ) -
Dept/Unit & Location		Email	
Division/ Portfolio		Signature:	

If you need more space an additional form for co-investigators is available on the website.

5. APPROVAL BY INVESTIGATOR'S DEPARTMENT/DIVISION HEAD/ CLINICAL MANAGER/CHIEF (THIS SHOULD NOT BE THE PRINCIPAL INVESTIGATOR AND/OR CO-INVESTIGATOR)

Hospital and university division and department administrators are responsible for academic activities within their unit, and may provide guidance and support to investigators. The purpose of this signature section is to ensure that administrators are aware of research activities and the impact of these activities.

- ☐ The study answers a reasonable scientific/clinical question and is consistent with hospital/faculty policies and mission.
- ☐ The study resources (budget, space, support staff) are adequate to support the study.
- ☐ The local investigators are qualified to perform the study.
- ☐ There are an adequate number of research participants suitable to be approached for enrolment for this study. This population is not already over-subscribed in clinical research.

I have reviewed this application and agree it should be submitted for ethics approval.

Name	Dr. S. Gilberg	Contact Number :	ext.
Title/Position		Signature	
Dept/Unit & Location			
Date			

6. REVIEW TYPE

Please indicate whether you are requesting full or expedited review. (Please see our website www.ohri.ca/ohreb for more information on what qualifies for expedited review.)

☐	Full Review
☒	Expedited Review

7. STUDY TYPE

Describe the Research Project by checking as many of the following as apply:

Study Type:

☐	Investigator driven and sponsored by OHRI
☒	Experimental Research/Clinical Trial
☐	Observational Research
☒	Pilot
☐	Sequel to previously approved project **(Protocol #: _____)**
☐	Genetic Research (Addendum 1 must be included with completed application)
☐	Program Evaluation
☐	New therapeutic method
☒	Medical Device Research (The medical device used in this study is a research instrument not used for clinical purposes at this point, and has no commercial value in this form. The technology created in this study will be used to develop an instrument that will one day be used in the clinic) Please attach a letter from sponsor indicating Health Canada application/approval. This is mandatory prior to final REB approval.
	☐ **Health Canada Application/Approval** is attached (insert as next page)
	☐ **Health Canada Application/Approval** will be forwarded.

Location of the Study:

☒	Single Centre Trial	☐	Multicentre Trial

Study Design:

☐	Randomized, controlled trial						
☐	Phase I	☐	Phase II	☐	Phase III	☐	Phase IV
☐	Open Label	☐	Single Blinded	☐	Double Blinded (or more)		
☐	Case-Control study						
☐	Cohort study						
☐	Interview, survey or questionnaire, observation						
☒	Chart Review						
☐	Compassionate Use						
☐	N of 1 Study						
☐	Quality Assurance						

Drug Study: ☐ **Yes** ☒ **No**

☐	Involves unusually elevated doses of available drugs

☐	Involves anticipated high incidence of toxicity
☐	Drug being used for currently approved indication
☐	Approved Drug being used for a non-approved indication Please attach a letter from sponsor indicating Health Canada application/approval. This is mandatory prior to final REB approval.
	☐ **Health Canada Application/Approval** is attached (insert as next page)
	☐ **Health Canada Application/Approval** will be forwarded.
☐	Investigational non-approved drug: Please attach a letter from sponsor indicating Health Canada application/approval. This is mandatory prior to final REB approval.
	☐ **Health Canada Application/Approval** is attached (insert as next page)
	☐ **Health Canada Application/Approval** will be forwarded.

8. PURPOSE AND OBJECTIVES

Please state clearly the hypothesis to be tested, in lay terms.

Purpose:

The purpose of this pilot study will be to evaluate the clinical value of light spectroscopy mounted onto a fundus camera (herein referred to as Fundus Spectroscopy) as a useful, non-invasive, optical technique for measuring and tracking retinal oxygen tension in normal and diseased retinas.

Objectives:

(1) To measure variations in retinal oxygen tension in healthy individuals (Control Group) in order to establish oxygen tension measurement resolution.

(2) To measure retinal oxygen tension in a clinical population before and after treatment (intravitreal injections) to demonstrate that the effect size (change in oxygen tension) is within the resolution of the device and, if measured, changes correlate with clinical measurements.

a. To measure retinal oxygen tension in diabetic patients diagnosed with macular edema. To measure retinal oxygen tension in previously healthy patients diagnosed with retinal vein occlusion and secondary macular edema.

b. To compare agreement between our Fundus Spectroscopy measurements and standard definitions of ischemic vs. non-ischemic retinal vein occlusions such as Fluorescein Angiography (FA), Optical Coherence Tomography (OCT), and Multifocal Electroretinography (mf-ERG).

Provide the rationale for the study.

As with most tissues in the body, oxygen is essential for normal retinal function. It is well recognized that retinal hypoxia plays a critical role in many disorders of the retina, such as diabetic retinopathy and retinal vein occlusions. Given the prevalence of these disorders and their impact on visual function, accurate tools for monitoring retinal oxygen tension in normal and diseased states would be of benefit, and would permit a more complete understanding of the specific role of oxygen in healthy and unhealthy retinas.

To date, several techniques for measuring retinal oxygen tension have been studied, ranging from the use of phosphorescent dye or magnetic resonance imaging, to oxygen microelectrodes for mapping out oxygen gradients within the retina. Although currently available techniques are generally accurate at higher oxygen tensions, they typically fail when retinal oxygen tension falls to below 80%. Moreover, reliable non-invasive techniques are lacking.

In this study, we would like to evaluate the use of light spectroscopy mounted onto a fundus camera (fundus spectroscopy) as a useful non-invasive optical technique for measuring retinal oxygen tension. This represents a novel approach compared to existing spectroscopic methods of measuring oxygen tension in the retina. In standard spectroscopic oxymetry, such as pulse-oxymetry, the absorption of light in the blood is measured at specific wavelengths. The ratio of light absorption at these wavelengths determines the oxygen tension in the blood. With this approach, full spectrum absorption of the blood will be measured in specific targeted areas of the retina. Because the blood vessels of the retina aren't the only absorbers of light in the eye, an absorption model of the eye has been developed to compensate for the change in the absorption spectrum of the blood vessels due to the other absorbing elements (e.g. crystalline lens, aqueous humor). The proof of principle of this technique has been demonstrated by Faubert et al. 2008. It has been shown to be accurate to as high as +/- 1% oxygen tension measurements. This device is currently under development in Dr. Munger's laboratory.

This study would consist of a step 1 validation of the measurement technique in healthy individuals under different levels of oxygen stress. Upon validation and implementation of this technique, the clinical benefits will be demonstrated for patients suffering from conditions that result in significant changes in retinal oxygen tension, such as retinal vein occlusion and diabetic retinopathy with macular edema. Important future applications of this tool would be early detection of sub-clinical retinal hypoxia in patients at risk, monitoring disease progression, and evaluating treatment.

STUDY DURATION	Start Date: **01 / 03 /2009** DD/MM/YYYY	End Date: **01 /03/2011** DD/MM/YYYY

9. RECRUITMENT

Describe how these research participants will be identified and recruited. **(Only members of the participant's health care team should contact patients at the Ottawa Hospital.)**

In addition, please ensure you address the following:

- If initial contact is by letter or if an **advertisement** is to be used, attach a copy.
- How will the researcher ensure that there are no breaches of patient **privacy**?
- How will the possibility of **coercion**, duress or undue incentive be avoided or minimized?

A total of 15 research subjects will be recruited for this study.

Control Group (n=5)
Five research subjects with normal ocular exams will be recruited as the Control Group (see below).

Experimental Group (n=10)
The remaining 10 research subjects will be chosen among patients previously followed by or newly referred to Dr. B. Hurley for either diabetic macular edema or retinal vein occlusion and secondary macular edema. Patients who will be receiving treatment for their condition in the form of an intravitreal injection of an anti-VEGF agent (e.g. Lucentis) by Dr. Hurley, as per his usual standard of care will also be included.

After OHREB approval has been obtained, all patients to be seen at the University of Ottawa Eye Institute during the above specified study duration will be identified by Dr. Hurley, following screening of their medical records. At their scheduled visit, a candidate patient who fulfills the study's inclusion/exclusion criteria (see below) will be approached by a member of the primary circle of care. The purpose of this study, requirements of the patient, potential risks and benefits will be explained to the patient, and a consent form will be presented for signature.

All information will be held in the strictest confidence by the study staff. Patients will specifically be told, as well it will be stated in the consent form, that their decision to participate in the study or not will in no way affect the care they receive from Dr. Hurley, nor will it influence the type of treatment they are offered for their condition.

Are recruitment incentives provided? ☐ Yes ☒ No
If yes, please describe.

Are controls involved? ☒ Yes ☐ No
Does the study include subjects in a control group? ☒ Yes ☐ No
If controls are involved, if their selection and/or recruitment differs from the above, provide details.

The Control Group will consist of 5 patients with healthy eyes and normal ocular exams recruited to participate in the study. The Control Group can include anyone from the normal population who hasn't had any previously diagnosed ocular condition.

Does the research include research participants who may not be competent to give informed consent? ☐ Yes ☒ No If yes, justify and explain how consent will be obtained and from whom.

- Number of Centres recruiting globally: **1; TOH – General, UofO Eye Institute**

  ☒ National Study – Country **Canada**

  ☐ International Study – Country

- Total number of research participants being recruited at all centres globally: **15**

  - Number of research participants to be recruited at each Ottawa Hospital campus:

☐ Civic	☒ General	☐ Riverside	☐ Other
	15		

Provide the rationale for the selected sample size and the methodology used to calculate the sample size:

This sample size is sufficiently small to minimize the burden on the patient population and clinical staff while providing a sufficient sampling to demonstrate unequivocal proof-of-principle of our non-invasive monitoring technique. This sample size also ensures that the required measurements will be completed in a timely manner.

This is a pilot study. Our expected effect size for patients is of the order of 5% oxygen saturation. The accuracy of the technique is believed to have a standard deviation of 2% or less. For a power of 0.95, we thus require at least 6 patients (t-test). Because of our uncertainty in the device accuracy, response of patients to treatment and confounding factors, we will recruit 10 patients. A large number is not justified until this pilot study demonstrates some value to the technique.

10. DESCRIPTION OF POPULATION

Inclusion Criteria - Who is being recruited and what are the criteria for their selection?

Control Group (n=5)

Inclusion criteria: Adults with normal ocular exams.

Experimental Group (n=10)

For the patients with diabetic macular edema:

Inclusion criteria: Diabetic patients diagnosed with diabetic macular edema, deemed by their retina specialist (Dr. Hurley) as candidates for intervention in the form of intravitreal injections (e.g. Lucentis).

For the patients with retinal vein occlusion and secondary macular edema:

Inclusion criteria: Patients with branch or central retinal vein occlusion and secondary macular edema, deemed by their retina specialist (Dr. B. Hurley) as candidates for intervention in the form of intravitreal injections (e.g. Lucentis).

Exclusion Criteria - What research participants are excluded from participation?

Control Group (n=5)

Exclusion criteria: Patients with retinal disease, any significant ocular media opacity including advanced cataract, any systemic vascular disease, including diabetes and hypertension.

Experimental Group (n=10)

For the patients with diabetic macular edema:

Exclusion criteria: Patients with diabetic retinopathy and other concurrent retinal disease, significant ocular media opacity including advanced cataract or vitreous hemorrhage, or having received retinal laser in the past.

For the patients with retinal vein occlusion and secondary macular edema:

Exclusion criteria: Patients with other concurrent retinal disease, significant ocular media opacity including advanced cataract or vitreous haemorrhage.

11. DESCRIPTION OF METHODS AND PROCEDURES
If additional space is required, insert one additional page)

Summary of Methods and Procedures. **Please include a summary of the following**:

- any specific manipulations;
- type, quantity, and route of administration of drugs and radiation; operations; tests; use of medical devices that are prototype or altered from those in clinical use;
- type, and number of interviews or questionnaires; are the questionnaires validated, reliable and have they been pilot tested?
- Are procedures/treatments standard practice or new, what is the risk level?

(Flow diagrams and point form discussion are encouraged and should be appended separately.)

The measurement of retinal oxygen tension using our device, Fundus Spectroscopy, is new and is thus not currently part of standard practice. However, it is non-invasive and poses no risk or harm to the patient (see below).

Once a patient has agreed to participate in the study and signed the consent form, they will be brought to the Eye Institute Visual Optics Lab, where the Ph.D. candidate (Serge LeBlanc) in Dr. Munger's lab will guide him or her to the instrument and place their head in the appropriate measurement position. A final review of the procedure will be explained to the patient. Testing will require dilated pupils, which, in the case of the patients in the experimental group, will have already been performed for the regular exam in Dr. Hurley's clinic. Patients in the control group will have their eyes dilated by Dr. Dollin prior to being brought to the Visual Optics Lab.

Retinal oxygen tension will then be measured in all patients after stimulating the retina by shining light onto it at 2 intensities (10, 100 cd/M2 using a tungsten lamp) and 3 exposure times (0.5s. 5.0s and 50s) to create various metabolic activity rates in the retina. There will be a 5 minute rest between tests.

The patients in the experimental group will have received Fluorescein Angiography (FA) and Optical Coherence Tomography (OCT) scans as part of their routine work-up by their retina specialist (Dr. B. Hurley). Copies of these will be obtained by us for the purpose of analysis from the patient's medical record at the time of their visit.

Multifocal Electroretinograms (mf-ERGs) will also be performed on the experimental group patients and data will be collected for analysis. For this test, subjects will have their eyes dilated and anesthetized with drops. A microconductive fiber (thinner than a human hair) will be placed on the white part of each eye. This fiber records the electroretinal signal. A reference electrode will be placed on the wrist. The test takes approximately 8 minutes to complete on each eye. During this time the patient is sitting comfortably looking into an instrument that is projecting a changing pattern of black and white hexagons.

Patients will then receive their intravitreal injection by Dr. Hurley, independent of us or this study.

As Dr. Hurley's normal standard of care dictates, patients will return to see him in follow-up at 4-6 weeks, at which time the investigations will be repeated.

12. RISKS

Describe the discomfort or risks that participants may incur as a result of their participation in this research. Also note the following:

- particular risks associated with each procedure, drug, test or other aspect of the protocol.
- delineate, when appropriate, what risks relate to standard care,
- what risks relate to participation in the study.
- quantify risks where possible by providing percentages, or by describing as rare, common, etc.

This study will use non-invasive measurements and will pose no risk to the participants, nor will they alter the standard treatment of patients in any way. Moreover, light intensity levels and exposure times will not exceed those encountered during every day fundus camera measurements and are well below acceptable limits as determined by ANSI/IESNA RP-27.1-05 "Recommended Practice for Photobiological Safety for Lamps and Lamp Systems"; please refer to Appendix A.

There is some risk associated with dilating the pupils such as angle closure glaucoma; however, this is a routine procedure.

Will the management of the participant's condition be prolonged or delayed as a result of the research? ☐ Yes ☒ No
If yes, explain, specifying any risks associated with prolongation or delay.

Are there any standard therapies, diagnostic procedures or information to be withheld from participants for the purpose of the study? ☐ Yes ☒ No
If yes, explain, specifying the risks and benefits to the participants and justify.

Are there stopping rules for the study? **(This does not apply to individual patient withdrawal, but to the study as a whole)** ☐ Yes ☒ No
If yes, please describe.

Is there a data safety monitoring board in place? ☐ Yes ☒ No
If yes, describe the composition of the board.

What procedures in this protocol are additional to those required for **routine** patient care? **(Include the Impact Sheet with applicable attachments for all procedures which are attributable to this study)**

1- Fundus Spectroscopy: The actual device being evaluated in this study would represent an additional non-invasive investigation not currently required as routine patient care.

2- Multifocal Electroretinogram (mf-ERG) is not typically a component of the routine work-up of patients with diabetic macular edema or retinal vein occlusion. Thus, this would represent an "additional" investigation. However, it is non-invasive, relatively quick to perform and would not prolong or delay the management of a patient's condition in any significant way. With regards to the purpose of our study, it would yield important functional information about a patient's retina, which would complement the anatomic information provided by the optical coherence scans, both of which we would like to correlate with measurements of retinal oxygen tension by our device.

Patients with diabetic macular edema or retinal vein occlusion would normally receive Fluorescein Angiography (FA) and Optical Coherence Tomography (OCT) scans as part of their regular evaluation by their retina specialist (Dr. B. Hurley). Thus, these would not represent investigations that would be considered "additional" to routine care.

Is a placebo used? ☐ Yes ☒ No
If yes, please justify:

13. POSSIBLE BENEFITS

Describe any possible benefits to the participant as a result of their participation in this research.

As this is a preliminary study to evaluate our device there are no foreseeable direct benefits to the study participants. However, the analysis of the study data may indicate our device to be a useful, non-invasive, optical technique for measuring and tracking retinal oxygen tension in normal and diseased retinas. Important future applications of this tool would be early detection of sub-clinical retinal hypoxia in patients at risk, monitoring disease progression, and evaluating treatment.

14. CONFIDENTIALITY

How will data be protected against breaches in security/privacy? If the information will be housed in a database, will it be password protected? There should not be any patient identifiers such as hospital unique number, OHIP #, etc. (An independent study number should be assigned to each patient, and the link between the patient and the study number housed separately and securely) Will there be written documentation kept? If so, how long will the information be kept? Where? Who will have access? **It is the policy of the OHREB that no records with the patient's name leave the Ottawa Hospital. For all drug studies, records must be kept by the investigator for a period of 25 years as outlined in Health Canada's Food and Drug Regulations, Division 5 – Drugs for Clinical Trials Involving Human Subjects, Section C.05.012. For all other studies, records must be kept by the investigator for a period of 15 years.**

- Upon agreeing to be part of this study and after obtaining the signed Informed Consent Form (ICF), subjects will be assigned a unique study number., which will be used as the identifier from this point forward
- A Study File and/or Study Database will be created where all Personal Health Information (PHI) will be de-identified and only the unique study number will appear.
- Utmost subject confidentiality will be assured. Any link between the patient's identifying information and unique study number (Master list) will be kept in a locked office and/or password protected database and only the study personnel directly involved in the study will have access to this information
- All database will be password protected. No records with patient health information will leave the Ottawa Hospital
- The OHRI, and OHREB may review study information under the supervision of the PI in the event of an audit
- The study records will be kept for a minimum period of 15 years after termination of the study at which time paper copies will be shredded and database may be deleted.

15. BUDGET

Has this research been funded? ☐ **YES** ☒ **NO**	
☐ **If YES provide the:**	☒ **If NO complete the following:**
Name of the Agency/Sponsor:	Has funding been applied for: ☒ **YES** ☐ **NO**
Amount of funding received: **$**	Name of the Agency/Sponsor: **UOMRF**
	Amount of funding applied for**: $ 5500**
	Date submitted: **25/ 01 / 2009** DD/MM/YYYY
If no funding has been applied for, how will the research be supported? Using existing equipment in the testing laboratory and existing personnel. The tests are expected to be completed within one day, resulting in minimum impact upon the lab. The results of the testing will be utilized to apply for peer-reviewed funding to further the research. If the study was peer-reviewed, please provide the name of the individual or agency that completed the review.	
Does the industry-sponsored budget contain appropriate overhead? ☐ A Clinical Trial Agreement has been forwarded to the Contracts Officer ☐ A Clinical Trial Agreement is attached to the OHREB application Have you included a budget summary for the protocol? **(If this is not included, approval of protocol will be delayed. Details on the disbursement of any excess funds received for this study should also be provided.)**	☐ **YES** ☐ **NO** ☒ **N/A** ☒ **YES** ☐ **NO** ☐ **N/A**
Does the REB review fee apply to this study? ☐ A cheque is enclosed ☐ An invoice request is enclosed ☐ A transfer request is enclosed **(All industry sponsored research projects are subject to a $2,000.00 administration fee, and any cooperative group studies that are funded in excess of $3000 per patient.)**	☐ **YES** ☒ **NO** ☐ **N/A**

AMOUNT OF FUNDS REQUIRED

Professional Salaries	880$
Equipment - Optics (lens and motor)	3000$
Multifocal Electroretinogram (mfERG)	1620$ ($81.00 x10 patients x 2 tests)
TOTAL$	**5500$**

POTENTIAL CONFLICTS OF INTEREST Please indicate if you have a conflict of interest or separate financial agreements with the sponsor of this study. If yes, please explain.	☐ **YES** ☐ **NO** ☒ **N/A**

16. STAFFING

What staffing will be required? All staff should be listed and this list maintained during the course of the study.

This includes research nurses, research co-ordinators, etc. Research nurses should provide a copy of their Nursing Certificate for the current year, to the Research Services Office if this has not already been done for another study.

	Name & Role in Study	**Already Employed?**	**Full-time vs. Part-time**	**Office/Laboratory Location and Telephone Number** **If <u>new office or laboratory space</u> is required, the Space Planning & Management section of the Departmental Impact form must be signed and submitted**
1.		☐ **YES** ☐ **NO**	☐ **FT** ☐ **PT**	**Campus:** **Office/Lab #**
2.		☐ **YES** ☐ **NO**	☐ **FT** ☐ **PT**	**Campus:** **Office/Lab #**
3.		☐ **YES** ☐ **NO**	☐ **FT** ☐ **PT**	**Campus:** **Office/Lab #**
4.		☐ **YES** ☐ **NO**	☐ **FT** ☐ **PT**	**Campus:** **Office/Lab #** ( ) - **x.**
5.		☐ **YES** ☐ **NO**	☐ **FT** ☐ **PT**	**Campus:** **Office/Lab #** ( ) - **x.**

In the space below please provide:

a) a list of their qualifications:

b) a list of the duties to be performed, including delegated/sanctioned medical acts and acts performed under the Regulated Health Professions Act if this has not already been done for another study:

DEPARTMENTAL IMPACT

Protocol Title:

Evaluation of a fundus camera equipped with light spectroscopy as a non-invasive tool for measuring retinal oxygen tension in normal and diseased populations

Does the protocol require use Hospital and/or OHRI resources (equipment, staff, space) over and above those normally required in the standard care of a patient?

Equipment	☒ **YES**	☐ **NO**
Staff	☒ **YES**	☐ **NO**
Space	☐ **YES**	☒ **NO**

Will hospitalization or outpatient visits be required beyond what is required for standard care?

Outpatient Visits	☐ **YES**	☒ **NO**
Hospitalization	☐ **YES**	☒ **NO**

Indicate impacts associated with this Protocol, by Department:
IF YES is indicated, a signature of an individual authorized to sign for the department must be obtained. (Please see our website for a list of contact names http://www.ohri.ca/ohreb***/)***

			Signature:
Nursing	☐ **YES**	☒ **NO**	
Emergency Department	☐ **YES**	☒ **NO**	
Health Records (See Appendix A)	☐ **YES**	☒ **NO**	Please submit signed Health Records form. www.ohri.ca/ohreb/forms.htm
Laboratory Services	☐ **YES**	☒ **NO**	Please submit signed Lab Impact form. www.ohri.ca/ohreb/forms.htm
Radioisotopes (See Appendix B)	☐ **YES**	☒ **NO**	Please submit Radiation Safety form. www.ohri.ca/ohreb/forms.htm
Diagnostic Imaging (See Appendix B and C)	☐ **YES**	☒ **NO**	Please submit signed Diagnostic Imaging form. www.ohri.ca/ohreb/forms.htm
Pharmacy	☐ **YES**	☒ **NO**	Please submit signed Pharmacy form www.ohri.ca/ohreb/forms.htm
Nutrition And Food Services	☐ **YES**	☒ **NO**	
Space Planning & Management	☐ **YES**	☒ **NO**	
Clinical Investigation Unit	☐ **YES**	☒ **NO**	
Cardiopulmonary Services	☐ **YES**	☒ **NO**	
Others: Ophthalmology	☒ **YES**	☐ **NO**	Signature:

APPENDIX E: INFORMATION CONSENT FORM 2

Protocol Title:	**A pilot study to determine the clinical value of a fundus camera equipped with light spectroscopy as a non-invasive tool for measuring retinal oxygen tension**
Principal Investigator:	**Dr. Réjean Munger**
Co-Investigators:	**Dr. Bernard Hurley** **Dr. Michael Dollin** **Serge LeBlanc**

Managed by the University of Ottawa Eye Institute- Clinical Trials Group

Consent Form presented to patient on _____ at _____
DD/MMM/YY Time

INTRODUCTION:
We are asking you to take part in a research study at the University of Ottawa Eye Institute because you have either normal vision or are being treated for an ocular condition, specifically macular edema or retinal vein occlusion. Macular edema is associated with an increase in fluid in the retina (the nerve layer that lines the back of the eye) producing swelling and thickening of the retina. A retinal vein occlusion is a blockage in the blood vessels on the retina. Taking part in this study is completely voluntary. The quality of care you will receive will not be affected by your decision to participate or not. The study is described below. This description tells you about the purpose, additional tests, and risks/discomforts, which you might experience. You should take the time to read this Patient Information Sheet and Consent Form and discuss any questions you have about your potential participation in this study with the person who explains it to you. You can also discuss this decision with your family, friends, and your health-care team.

PURPOSE OF THE STUDY:
The purpose of this study is to determine if it is possible to get new information from the eye using a novel technique called Fundus Spectroscopy, which was developed at the University of Ottawa Eye Institute. It is a non-invasive (will not touch or penetrate your eye) tool used to take pictures of the back of your eye and measure oxygen tension in your retina. If this technique

proves successful, it could, in the long term, result in a method to predict and monitor ocular disease simply by taking an image of the back of the eye.

We are planning on enrolling a total of 15 research participant for this study. Five patients with normal ocular exams will be recruited as the Control Group, and ten patients with macular edema or retinal vein occlusions will be recruited from Dr. B. Hurley's clinic as the Experimental Group.

STUDY PROCEDURES:
We are asking your permission to perform additional tests for this study and to collect your study data for possible publication.

ADDITIONAL TESTS TO BE PERFORMED FOR THIS STUDY:

1. Fundus Spectroscopy

This non-invasive instrument takes images of the back of your eye. The procedure is performed at the Eye Institute Visual Optics Laboratory and should not take more than 15 minutes to complete. Your eyes will be dilated and your head placed in the appropriate measurement position. Retinal oxygen tension will then be measured in all research participants (both the Control and the Experimental Group) after stimulating the retina by shining light onto it at 2 intensities (10, 100 cd/M2 using a tungsten lamp) and 3 exposure times (0.5s. 5.0s and 50s) to create various metabolic activity rates in the retina. There will be a 5 minute rest between tests. The light intensity levels are well below danger levels and will not be too uncomfortable.

2. Multifocal Electroretinography (mf-ERG) on the Veris System:

Only patients being treated for an ocular condition by Dr. Hurley (Experimental Group) will need to perform this test. Multifocal electroretinography (mf-ERG) provides an accurate measurement of the change of the functioning of the central region of the retina, a region that is thickened in macular edema. Your eyes will be dilated and anesthetized with drops. This may cause slight stinging. A microconductive fiber (thinner than a human hair) will be placed on the white part of each eye. This fiber records electrical signals from your retina. A reference electrode will be placed on the surface of your wrist. The test takes approximately 8 minutes to complete on each eye. During this time you will be sitting comfortably looking into an instrument that is projecting a changing pattern of black and white hexagons. There are frequent rest periods to allow you to blink your eyes and remain comfortable.

COLLECTION OF DATA:
In addition to collecting study data from above-mentioned tests, we are asking permission to collect addition data from your Fluorescein Angiography (FA) and Optical Coherence

Tomography (OCT) scans, only if they were obtained as part of standard care (Experimental Group). These tests will not be performed unless required as part of you routine work-up.

STUDY DURATION:
If you are a patient and part of the Experimental Group, both the Fundus Spectroscopy and mf-ERG testing will be done during your initial scheduled visit at the University of Ottawa Eye Institute and then again at your regular follow up visit (~4-6 weeks). If you are a control subject with normal vision, and therefore part of the Control Group, you will be asked to come in for two study visits at approximately 4-6 weeks apart and only the Fundus Spectroscopy test will be done.

RISKS of PARTICIPATION:
There are no potential risks involved with having the non-invasive Fundus Spectroscopy procedure completed. The light intensity levels sent to the back of your eye are below 10% of levels that could cause damage to your eye.

There is some risk associated with dilating the pupils such as angle closure glaucoma; however, this is a routine procedure that you will have already had done during your clinic visits.

There are no significant risks or discomfort associated with Multifocal Electroretinography. It is a standard clinical test that is used routinely to test patients with various types of retinal dysfunction. There is some minor stinging when eye drops are placed in the eyes but this is extremely brief and only causes some minor tearing.

BENEFITS of PARTICIPATION:
There may be no direct benefit to you as a result of participating in this research study. However, a potential benefit may be the development of a non-invasive method to better manage patients with various eye conditions in the future.

ALTERNATIVE TREATMENT AVAILABLE

If you are part of the Experimental Group and have macular edema or retinal vein occlusion, you do not have to participate in this study to receive treatment for your ocular condition. Fundus Spectroscopy is not considered an alternative treatment to the regular standard of care, but an additional test that accompanies your regular standard of care. Your doctor will discuss your standard of care treatment with you.

WITHDRAWAL FROM THE STUDY

You have the right to withdraw from the study at any time without any impact to your current and future care at the Ottawa Hospital. Should you decide to withdraw your consent, we will not collect any new data from this point forward. However, you may not be able to withdraw your coded data if it has already been collected and used in a publication or presentation,

COMPENSATION

In the event of a research-related injury or illness, you will be provided with appropriate medical treatment/care. You are not waiving your legal rights by agreeing to participate in this study. The study doctor and the hospital still have their legal and professional responsibilities.

STUDY COSTS

You will not be paid to participate in this research study.

CONFIDENTIALITY

All personal health information will be kept confidential, unless release is required by law. Representatives of government regulators such as Health Canada, or the Food and Drug Administration (U.S.A.), representatives of the Ottawa Hospital Research Ethics Board, as well as the Ottawa Health Research Institute, may review your original medical records under the supervision of study staff for audit purposes.

You will not be identifiable in any publications or presentations resulting from this study. No identifying information will leave the Ottawa Hospital. All information which leaves the hospital will be coded with an independent study number.

The link between your name and the independent study number will only be accessible by the study staff. The link and study files will be stored separately and securely. Both files will be kept for a period of 15 years after the study has been completed. All paper records will be stored in a locked file and/or office. All electronic records will be stored on a hospital server and protected by a user password, again only accessible by the study staff. At the end of the retention period, all paper records will be disposed of in confidential waste or shredded, and all electronic records will be deleted.

VOLUNTARY PARTICIPATION

Your participation in this study is voluntary. If you choose not to participate, your decision will not affect the care you receive at this Institution at this time, or in the future. You will not have any penalty or loss of benefits to which you are otherwise entitled to.

NEW INFORMATION ABOUT THE STUDY

You will be told of any new findings during the study that may affect your willingness to continue to participate in this study. You may be asked to sign a new consent form.

QUESTIONS

If you have any questions about the study, you may contact the following study staff:
Dr. Rejean Munger, Principal Investigator
Dr. Bernard Hurley, Ophthalmologist
Dr. Michael Dollin, PGY2 Resident

The Ottawa Hospital Research Ethics Board (OHREB) has reviewed this protocol. The OHREB considers the ethical aspects of all research studies involving human subjects at The Ottawa Hospital. If you have any questions about your rights as a research subject, you may contact the Chairperson of the Ottawa Hospital Research Ethics Board.

Consent Form

A pilot study to determine the clinical value of a fundus camera equipped with light spectroscopy as a non-invasive tool for measuring retinal oxygen tension

Consent to Participate in Research

I understand that I am being asked to participate in a research study about retinal oxygen tension. This study has been explained to me by the study staff.

I have read this 6-page Patient Information Sheet and Consent Form (or have had this document read to me). All my questions have been answered to my satisfaction. If I decide at a later stage in the study that I would like to withdraw my consent, I may do so at any time.

I voluntarily agree to participate in this study.

A copy of the signed Information Sheet and Consent Form will be provided to me.

Signatures

_____
Participant's Name (Please Print)

_____ _____
Participant's Signature Date

Investigator Statement (or Person Explaining the Consent)
I have carefully explained to the research participant the nature of the above research study. To the best of my knowledge, the research participant signing this consent form understands the nature, demands, risks and benefits involved in participating in this study. I acknowledge my responsibility for the care and well being of the above research participant, to respect the rights and wishes of the research participant, and to conduct the study according to applicable Good Clinical Practice guidelines and regulations.

_____
Name of Investigator/Delegate (Please Print)

_____
Signature of Investigator/Delegate

Consent process completed on _____ at _____
DD/MMM/YY Time